Characterizing cochlear neural degeneration using frequency-following responses

Märcher-Rørsted, Jonatan

Publication date:
2022

Document Version
Publisher's PDF, also known as Version of record

CONTRIBUTIONS TO
HEARING RESEARCH

Volume 57

Jonatan Märcher-Rørsted

Characterizing cochlear neural degeneration using frequency-following responses

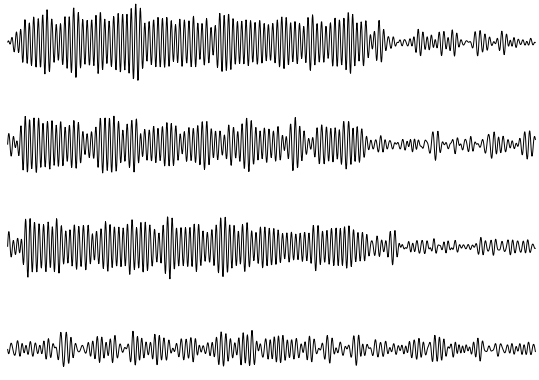

DTU Health Tech
Department of Health Technology

Characterizing cochlear neural degeneration using frequency-following responses

PhD thesis by
Jonatan Märcher-Rørsted

Technical University of Denmark

2022

This PhD dissertation is the result of a research project carried out at the Hearing Systems Group, Department of Health Technology, Technical University of Denmark.

The project was supported by the Novo Nordisk Foundation synergy grant NNF-17OC0027872 (UHeal).

Supervisors

Professor Torsten Dau
Associate Professor Jens Hjortkjær
Post-Doc. Gerard Encina-Llamas
Hearing Systems Group
Department of Health Technology
Technical University of Denmark
Kgs. Lyngby, Denmark

Abstract

Our communication in social settings relies on our ability to accurately capture the acoustic environment through our sense of hearing. Hearing loss affects this ability, with detrimental consequences for many aspects of social life. Clinical hearing loss is in its most common age-related form defined as a loss of sensitivity, but not all hearing difficulties are necessarily captured by traditional clinical audiological assessment of sensitivity. Recent evidence suggests that neural losses at the level of the inner ear, the cochlea, can be caused by aging and noise exposure without affecting threshold sensitivity. Specifically, it has been shown that the amount of functional auditory nerve fibers (ANF) in the cochlea declines progressively throughout life. Such neural loss is argued to precede the loss of sensory cells in the cochlea and may exist before hearing loss is detected in the hearing clinic. Yet, the consequence of ANF loss on our ability to communicate in everyday life is still debated and robust in-vivo diagnostic measures are missing.

The work presented investigates electrophysiological frequency-following responses (FFR) as a potential measure of cochlear neural degeneration. FFRs are neurophonic potentials that phase-lock to the periodicity of an acoustic stimulus and can be recorded using scalp electroencephalography (EEG). It has previously been shown that the FFR to pure tones below 1 kHz is reduced with advancing age, and it has been argued that this reduction arises from age-related deficits in the auditory brainstem where the FFR originates. In this thesis, we challenged this hypothesis, and investigated the low-frequency FFR as a correlate of peripheral ANF loss in humans.

In the first study, we confirmed previously reported age-related reductions of the FFR by using frequency sweeps and pure tones in older normal-hearing listeners. The experimental results were compared to computer simulations of auditory nerve (AN) activity to the same stimuli informed by human histopathology. The simulations suggested that age-related ANF loss across cochlear frequency reduces the phase-locked population AN response in a manner consistent with the observed FFR reductions. Simulations also indicated that loss of outer hair cells had no detrimental effect on the synchronized AN response. In a second study, we further explored the relation between FFRs and AN integrity in a large cohort of aging listeners. The FFR was here compared to the wave-I of the auditory brainstem response (ABR), which reflects synchronized AN activity evoked by click sounds. We found strong reductions on the ABR

wave-I amplitude with increasing age, and the reductions were correlated with the FFR reductions. In the third study, we further compared the effect of age on brainstem FFRs with neurophonic potentials arising from the AN by using recording electrodes placed on the tympanic membrane. The electrocochleography recordings again suggested an age-related reduction of neurophonic responses to low-frequency tones at the level of the AN. In a fourth study, we investigated the causal effect of ANF loss on the FFR by examining the effect of noise-induced ANF loss on the FFR using an animal (chinchilla) model of temporary threshold shift. Results again suggested that ANF loss reduces the population neurophonic response of the AN, but the relation to central FFRs was inconclusive from the data.

Together, the work presented in this thesis supports a relationship between age-related ANF loss and the brainstem FFR to low-frequency pure tones. As a result, the FFR might constitute valuable potential tool for diagnosing cochlear neural degeneration in humans.

Resumé

Kommunikation i sociale sammenhænge afhænger i høj grad af vores evne til præcist at kunne afkode vores akustiske omgivelser ved hjælp af høresansen. Høretab påvirker denne evne hvilket har skadelige konsekvenser for mange aspekter af vores sociale liv. Klinisk høretab er defineret som et tab af sensitivitet, men ikke alle hørevanskeligheder er nødvendigvis afspejlet i de audiologiske mål for sensitivitet, der normalt anvendes klinisk. Det er i stigende grad tydeligt at neurale skader i det indre øre fremkommer ved almindelig aldring og ved støjeksponering, men disse neurale skader kan forekomme uden at påvirke høretærskler. Specifikt er det blevet vist, at mængden af funktionelle fibre i hørenerven formindskes progressivt igennem hele livet. Et sådant neuralt tab menes at kunne gå forud for et tab af sensoriske celler i de indre øre og kan derfor eksistere før et høretab registreres i klinisk sammenhæng. Konsekvensen af hørenervetab for eksempelvis taleopfattelse debatteres og robuste in-vivo diagnostiske mål for sådanne nerveskader mangler.

Det her fremførte arbejde undersøger elektrofysiologiske frekvens-følgende potentialer (frequency-following responses, FFR) som et potentielt mål for nervedegeneration i cochlea. FFR er neurofoniske potentialer som følger perioden af en akustisk stimulus og som kan optages ved brug af elektroenncephalografi (EEG). Aldersbetinget reduktion af FFR til toner under 1 kHz er tidligere blevet påvist, og man har ment at disse reduktioner afspejler aldersbetinget ændringer i den auditive hjernestamme hvor FFRet opstår. I denne afhandling udfordrer vi denne hypotese, og undersøger den alternative mulighed at det lavfrekvente FFR kan afspejle perifært hørenervetab.

I det første studie, fandt vi, i overenstemmelse med tidligere studier, en aldersrelateret reduktion af FFR ved brug af frekvens-sweeps og toner i ældre normalthørende lyttere. De eksperimentelle resultater blev sammenholdt med simuleringer af hørenerveaktivitet informeret af histopatologidata i respons til tilsvarende stimuli. Simuleringerne indikerede at tab af hørenerver reducerer det faselåste respons på tværs af nerven i overenstemmelse med de eksperimentelt observerede FFR optagelser. Simuleringerne indikerede også at tab af ydre hårceller ikke reducerer det synkroniseret hørenerverespons på tværs af fibre. I næste studie udforskede vi yderligere sammenhængen mellem FFR og hørenervens status i en stor kohorte af forsøgspersoner. FFR blev her sammenlignet med bølge-I af det auditive hjernestamme respons (ABR), som afspejler isoleret hørenerveaktivitet udløst af korte kliklyde. Her fandt vi stærkt reducerede bølge-I amplituder med stigende alder og denne reduktion var korreleret

med reduktionen i FFR. I et tredje studie sammenlignede vi aldersbetingede ændringer i hjernestamme-FFRet med tilsvarende neurofoniske potentialer fra hørenerven ved brug af elektroder placeret på trommehinden. Disse elektrocochleografiske målinger viste som ventet en aldersrelateret reduktion af det neurofoniske respons til lavfrekvente toner fra hørenerven. I et fjerde studie undersøgte vi den kausale effekt af hørenervetab på FFR ved hjælp af en dyremodel af midlertidigt tærskel skift (temporary threshold shift) med støjinduceret selektivt hørenervetab. Resultater fra dette studie pegede igen på at hørenervetab reducerer det neurofoniske populationsrespons fra hørenerven, men relationen til det hjernestemmegenererede FFR kunne ikke fastslås ud fra disse data.

Det præsenterede arbejde støtter hypotesen om en sammenhæng mellem aldersrelateret hørenervetab og det hjernestammegenerede FFR til lavfrekvente toner. Dette kunne pege på FFR som et muligt diagnostisk værktøj til undersøgelse af hørenervetab i mennesker.

Acknowledgments

Completion of this work would not have been possible without the help of many colleagues, funding sources, friends, and family. Although this period of time has been hard work, it has also been a lot of fun. This would not have been possible without the constant support from a number of people which I would like to acknowledge.

First, I would like to thank my supervisors, Torsten Dau, Jens Hjortkjær and Gerard Encina-Llamas for supervision of the highest quality. Torsten, it has been a pleasure (and still is) to discuss topics, both of scientific and personal character with you. I have great respect for your outstanding leadership, and appreciate your contribution to this specific work. I would like to especially thank you for the numerous iterations of feedback you have provided these last few intense weeks. Jens, this all started as a small special-project a number of years ago, which has now grown into a very fruitful and productive scientific collaboration. It is truly inspiring to work with you, and I hope we can continue to pursue new ideas together in future projects. Gerard, thank you for many interesting and inspiring discussions throughout this project. You always seem to have the argument or the paper I am looking for. Also, I would especially like to thank you for your contribution to modeling aspects of this work.

A big thanks goes out to all my wonderful colleagues at hearing systems. It has been a pleasure to work here. A Special acknowledgement goes out to my office mates, Nicolai, Mihaela, Chiara and Mie. Thank you for providing a relaxed and open atmosphere in office 128.

I would like to acknowledge and thank everyone who was involved in the Uncovering Hidden Hearing Loss (UHEAL) project. Our weekly meetings have pushed me to present my work to a panel of specialists countless times, and I feel privileged to have been part of such a great synergetic collaborations. In this connection, I would especially like to thank Søren Fuglsang for numerous discussions, mentorship, and for always having a skeptical mindset. I must also thank Charlotte Sørensen for her excellent effort and dedication in the data collection involved in the UHEAL project, and Sam Watson for assistance with piloting and initial data collection. I would also like to thank Charles M. Liberman and Pei-Zhe Wu for sharing their histopathological data. Thank you to Novo Nordisk Fonden for making this collaboration and great project possible.

Next, I would like to thank everyone from the Center for Hørelse og Balance

(CHBC) involved with the electrocochleographic recordings. In particular, I would like to thank Dr. Michael Bille, Dr. Jesper Yde and Dr. Per Caye. Without your contribution, this part of the project would not have been possible. A special thanks goes out to Miguel Temboury Gutierrez for a great collaboration and work on the ECochG project.

I was lucky enough to be able to spend a few months at Purdue University. In connection to this I would like to express my gratitude towards Michael Heinz. It was a privilege to be able to work with you. I look forward to future discussions and collaborations. I would also like to thank everyone I had the honor of working with at Purdue department for Speech Language and Hearing Science. It was truly impressive and inspiring to witness the level of dedication you all have to your work and to research in general. I would also like to thank William Demant Fonden, Augustinus Fonden and Knud Højgaards Fond for making this external stay possible.

To everyone who volunteered to be a test subject in one or many of my experiments. Without your contribution, this work would not be possible. Thanks!

Last but not least, I would like to thank my friends and family. Thanks to everyone from Ahlefeldtsgade and Sigurdsgade. Thank you E-L for always being a constant inspiration and amazing partner. I am proud of our accomplishments together, especially in these last hopeless and tough months. Finally, thank you Lars, Mette, Emil and Sally for all the support and encouragement.

Related publications

Journal papers

- Märcher-Rørsted, J., Encina-Llamas, G., Dau, T., Liberman, M.C., Wu, P., & Hjortkjær, J. (**2022**). "Age-related reduction in frequency-following responses as a potential marker of cochlear neural degeneration.", Hearing Research 414 . 10.1016/j.heares.2021.108411.

- Märcher-Rørsted, J., Encina-Llamas, G., Fuglsang, S. A., Watson S.D., Sørensen C., Seibner H.R., Liberman, M.C., Dau, T. & Hjortkjær J., (**In preparation**). "On the relationship between measures of age-related cochlear neuropathy in humans."

- Märcher-Rørsted, J. & Temboury-Gutierrez, M., Bille, M., Yde, J.B., Encina-Llamas, G., Hjortkjær, J. & Dau, T. , (**In preparation**). ''Electrocochleographic frequency following responses as a potential marker of age-related peripheral degeneration."

- Märcher-Rørsted, J.,Hjortkjær, J., Encina-Llamas, G., Dau, T. , & Heinz M., (**In preparation**). "Interactions between peripheral and central measures of temporal coding in a chinchilla model of noise-induced cochlear synaptopathy."

Conference papers

- Märcher-Rørsted, J., Temboury-Gutierrez, M., Encina-Llamas, G., Hjortkjær, J., Dau, T. **(2022)**. "Age-related reduction in frequency-following responses as a potential marker of cochlear neural degeneration."
  19th International Symposium on Hearing

Published abstracts

- Märcher-Rørsted, J.,Hjortkjær, J., Encina-Llamas G.,Dau, T.**(2019)**. "Age-dependent changes in frequency-following responses as a potential marker of cochlear synaptopathy in humans.",
  ARCHES (Audiological Research Cores in Europe)

- Märcher-Rørsted, J.,Hjortkjær, J., Encina-Llamas G.,Dau, T.**(2019)**. "Age-dependent changes in frequency-following responses as a potential marker of cochlear synaptopathy in humans.",
  International Symposium on Auditory and Audiological Research

- Märcher-Rørsted, J., Encina-Llamas G.,Dau, T., Liberman, M.C., Hjortkjær, J. **(2021)**. "Age-related reduction in frequency-following responses as a potential marker of cochlear neural degeneration.",
  Association for Research in Otolaryngology

- Märcher-Rørsted, J. & Temboury Gutiérrez, M., Hjortkjær, J., Encina-Llamas, G., Dau, T. **(2021)** "Investigating peripheral contributions to the frequency following response using electrocochleography.",
  International Symposium on Auditory and Audiological Research

- Märcher-Rørsted, J., Hjortkjær, J. , Encina-Llamas, G., Dau, T., Heinz, M.G. **(2022)** "Interactions between peripheral and central measures of temporal coding in a chinchilla model of noise-induced cochlear synaptopathy.",
  Association for Research in Otolaryngology

Additional contributions

- Hjortkjær, J., Märcher-Rørsted, J., Fuglsang, S. A. & Dau, T. (**2020**). “Cortical oscillations and entrainment in speech processing during working memory load.”, European Journal of Neuroscience 51. 10.1111/ejn.13855

- Fuglsang, S. A., Märcher-Rørsted, J., Dau, T. & Hjortkjær, J. (**2020**), ”Effects of sensorineural hearing loss on cortical synchronization to competing speech during selective attention.”, Journal of neuroscience 40. 10.1523/jneurosci.1936-19.2020

Contents

1 General introduction

Our ability to communicate in social settings relies heavily on our sense of hearing. Hearing loss can greatly diminish our ability to discriminate speech from background sounds in everyday acoustic scenarios, and can therefore be detrimental for communication in everyday life. The number of individuals with hearing loss in the population is rising due to increasing exposure to industrial and recreational noise (Saeed and Ramsden, 1994) and demographical shifts. In addition, an increasing amount of patients seek audiological help despite being found to have clinically normal hearing sensitivity (Hind et al., 2011). Although diagnosis and treatments of hearing deficits have progressed, there are still multiple aspects of cochlea degeneration which are not fully understood. Understanding how specific pathologies in the cochlea develop, and how they affect the processing of sound along the auditory pathway, as well as perception, is essential for the treatment and diagnosis of this growing body of patients.

1.1 Hearing loss and peripheral neural degeneration

Sensorineural hearing loss (SNHL) defines the loss of sensitivity to pure tones due to a degeneration in the cochlea, the auditory nerve, or in the central auditory nervous system. SNHL is the most common form of hearing loss in aging humans. Clinical diagnosis of SNHL relies heavily on the pure-tone audiogram, which examines the listeners ability to detect low-level sounds in quiet at various frequencies. Although the audiogram is an efficient way to characterize frequency-specific sensitivity loss, there may be damages in the cochlea which are not captured by a listeners' ability to detect a tone in quiet. Suprathreshold deficits typically also accompany hearing loss. Conversely, listeners with normal or near-normal hearing thresholds sometimes report listening difficulties in complex acoustic environments. In lack of diagnosis, this latter condition is commonly referred to as hidden hearing loss (HHL, Schaette and McAlpine (2011)). Yet, potential cochlear deficits underlying this condition

is a matter of heated debate (e.g., Bharadwaj et al. (2019, 2014), Bramhall et al. (2019), Grinn et al. (2017), Guest et al. (2017a), Liberman et al. (2016), Paul et al. (2017), Plack et al. (2014), Prendergast et al. (2019), Schaette and McAlpine (2011), and Shehabi et al. (2022)).

The main cochlear damage behind reduced sensitivity to sound has conventionally been asscociated with the loss of outer hair cells (OHC), the amplifiers in cochlear transduction (Ryan and Dallos, 1975). It is well known that the loss of auditory nerve fibers (ANF) has only little impact on audiometric thresholds as long as the outer hair cells are intact (Schuknecht and Woellner, 1955a). More recently, it has been found that prolonged noise exposure can cause the ribbon synapses connecting the cochlear inner hair cells (IHC) and the auditory nerve (AN) to rupture and disconnect while leaving the hair cells intact; a concept referred to as cochlear synaptopathy (CS) (Furman et al., 2013; Kujawa and Liberman, 2009; Lin et al., 2011b; Parthasarathy and Kujawa, 2018; Shaheen et al., 2015; Valero et al., 2017; Valero et al., 2016). Deafferentation between the sensory cell and the AN ultimately leads to a degeneration of the peripheral axon of the AN (Jensen et al., 2015; Kujawa and Liberman, 2015; Liberman and Liberman, 2015). A reduced number of functioning ANFs has been shown to be associated with decreased electrophysiological measures reflecting AN activity, such as the suprathreshold ($>$ 100 dB) wave-I amplitude of the auditory brainstem response (ABR), without affecting threshold sensitivity. Importantly, ANF loss can exist without significant damage to other cochlea structures such as the OHCs. Apart from the acute effects of noise exposure, progressive peripheral neural loss also occurs with natural aging. Animal studies have shown that the percentage of surviving synaptic ribbons (and thereby the number of functional ANFs) decreases with the age of an animal (Kujawa, 2006; Parthasarathy and Kujawa, 2018; Sergeyenko et al., 2013).

Recent histopathology in human temporal bones has confirmed advancing deafferentation in aging humans (Wu et al., 2020). By using microdissection and immunostaining techniques, it was possible to evaluate the percentage of cell survival as a function of age for both sensory cells (i.e., OHC and IHC), spiral ganglion cells (SGC), as well as peripheral axons of ANFs. The data indicates that different cell types have different robustness to advancing age. In contrast to IHCs and SGCs, ANFs appear to be more vulnerable to age-related degeneration. The histopathological data indicates that, at 60 years of age, an average approximate loss of 60-70 % of peripheral axons can be expected, whereas IHC

and SGC showed up to 90 % of cell survival relative to newborns. In contrast to age-induced OHC dysfunction, which usually affects more basal regions of the cochlea (presbycusis), age-related ANF loss was found throughout the cochlear partition. This suggests that age-related neuronal loss is a relatively broadband phenomenon. Wide-spread ANF loss may thus exceed damage to other cochlear structures but this damage is not well captured by current audiological evaluation strategies. Inevitably, the functional consequences of ANF loss are unclear. In light of this, a re-evaluation of the standard measures of cochlear health is needed. Developing diagnostics that are sensitive to cochlear pathologies beyond what is captured by current audiological measures is essential for our understanding of the underlying mechanisms with hearing impairment, and their consequences for auditory processing.

Despite its persistence, consequences of ANF loss for auditory processing and perception are still debated. While some studies claim a connection between suprathreshold ABR wave-I amplitudes and speech-in-noise performance (Grant et al., 2020; Liberman et al., 2016), others have failed to find such evidence (Grinn et al., 2017; Guest et al., 2017a; Prendergast et al., 2019). A growing amount of conflicting research results has led to a debate about whether ANF loss influences auditory perception in humans (Bramhall et al., 2019). However, it is possible that diagnostic measures of ANF loss are not sensitive enough to accurately capture the pathology. Without reliable measures of the cochlear pathology in humans, inferences about perceptual consequences are difficult to draw.

1.2 Diagnostic measures of auditory nerve-fiber loss

Efforts in developing diagnostic measures of ANF loss have primarily been focused on electrophysiological paradigms. Investigations have been centered around evoked responses to acoustic stimuli, which can be recorded using electroencephalography (EEG) by placing recording electrodes on the scalp of the listener. The most established measure is arguably the ABR, which is widely used in clinical settings and in auditory neuroscientific research. The ABR, which is typically evoked by simple transient stimuli (e.g. a click or chirp), consists of a series of peaks and valleys, each considered to reflect neural activity from distinct auditory sources along the ascending pathway (Picton et al., 1974). The first positive deflection (wave-I) is considered to arise from population-level

neural activity in the AN, whereas later waves reflect synchronous activity in the cochlear nucleus (i.e. waves II and III) and from the auditory brainstem and midbrain (i.e. wave-V). The unique latencies associated with different neural generators thus allow for the examination of deficits along the auditory pathway.

A reduced number of functioning ANFs in CS models has been demonstrated to reduce wave-I of the ABR to high-level sounds (Furman et al., 2013; Kujawa and Liberman, 2009; Parthasarathy and Kujawa, 2018; Sergeyenko et al., 2013; Shaheen et al., 2015; Valero et al., 2017; Valero et al., 2016), while the responses at threshold remain relatively normal. In animal studies, electrodes placed sub-dermally make it is possible to measure wave-I responses reliably already at threshold level. However, for human scalp recordings, wave-I is typically only detectable at high sound pressure levels ($>$ 80 dB), and requires a high number of repetitions. Although ABR wave-I has been established as a measure of AN health in animal models, it is difficult to measure in clinical settings in humans (Beattie, 1988; Lauter and Loomis, 1988). Wave-I can be difficult to identify by the clinician, especially in older and/or hearing-impaired people (e.g. Garrett and Verhulst (2019)), which makes this measure suboptimal for clinically relevant patient groups.

Steady-state responses constitute a group of measurements obtained with sustained and typically periodic stimuli. The frequency-following response (FFR) refers to the electrophysiological response to periodic stimuli, typically the frequency of the fine-structure of an acoustic stimulus (e.g. the carrier frequency of a pure tone or fundamental frequency of speech), but can also refer to responses to other periodic sounds, such as an amplitude modulated (AM) tones or noises. Accordingly, responses entrained to the envelope of a stimulus can be distinguished from those following the sound's fine structure, and are typically referred to as the envelope-following response (EFR). In this thesis, the term FFR is used to refer specifically to responses to the carrier frequency of the stimulus.

Steady-state responses have also been considered in the search for processing deficits associated with ANF loss. Synaptopathy-inducing noise exposure may not necessarily affect the precision of phase-locked firing in individual surviving ANFs (Suthakar and Liberman, 2021), and yet phase-locked population responses in the ascending auditory pathway may be reduced with a lower number of surviving ANFs (Parthasarathy and Kujawa, 2018; Shaheen et al., 2015). Given that sustained responses rely on large populations of fibers

synchronously firing to the rate of the stimulus, steady-state responses may more directly reflect the consequence of ANF loss on temporal processing than responses to transient sounds.

1.3 The frequency-following response

This thesis investigated the FFR to the carrier frequency of pure tones as a potential marker for cochlear neural degeneration in humans. In auditory research, the FFR has typically been examined in relation to speech vowels or pure tones. Although it is easy to record, the generation and origin of the scalp FFR is complex (Gardi et al., 1979). While the AN has been shown to follow (i.e. phase-lock) to stimuli with frequencies in the range of 1000s of cycles per second (Dynes and Delgutte, 1992; Johnson, 1980), the ascending auditory pathway demonstrates a low-pass characteristic. When examining neural generators at the level of the brainstem (e.g. the inferior colliculus), phase-locking occurs up to around 1 kHz (Bidelman, 2018; Liu et al., 2006), and is most prominent in the range of 100s of Hz. Cortical neurons typically only phase-lock consistently to very slow (<20 Hz) fluctuations in the stimulus (Kowalski et al., 1996; Miller et al., 2002). It is therefore often assumed that lower stimulation frequencies increases the contribution of later stages in the auditory pathway. In the present work, we focused on FFRs to pure tones of mid-frequency tones (200-1000 Hz), which are assumed to be dominated by brainstem neural generators (Smith et al., 1975; Worden and Marsh, 1968).

Previous work has established age-related changes in mid-frequency sustained responses, showing decreased FFR or EFR amplitudes with advancing age (Anderson et al., 2012; Bidelman et al., 2014; Garrett and Verhulst, 2019; Marmel et al., 2013; Skoe et al., 2015). This decrease has also been observed in older listeners with normal or near-normal hearing thresholds (Carcagno and Plack, 2020; Clinard and Cotter, 2015; Clinard and Tremblay, 2013; Clinard et al., 2010; Mamo et al., 2016; Presacco et al., 2019; Roque et al., 2019; Vasilkov et al., 2021). Reduced FFR amplitudes at these frequencies in aging humans have therefore been attributed to central deficits in the auditory system (Frisina and Frisina, 1997; Pichora-Fuller et al., 2007). However, it is possible that peripheral deficits in the cochlea could, at least partly, be driving this age-related decrease. If peripheral integrity is a prerequisite for intact central phase locking, the FFR may in turn be sensitive to peripheral loss that does not affect audiometric

thresholds, even for FFRs generated in the auditory brainstem.

The generation of the scalp FFR is thought to require synchronous activity in a large population ANFs, and is therefore only measurable at high sound pressure levels where sufficient amounts of off-frequency basal fibers are contributing to the response (Dau, 2003). Although it is known that the existence of the scalp FFR may be limited by the peripheral neural response, the scalp FFR to mid-frequency pure tones in humans is mainly generated by brainstem auditory nuclei, with the inferior colliculus as the main contributor. It has been shown that the response is hierarchical, and disrupting spike generation in the auditory nerve or cochlear nucleus (e.g. by neurotoxic chemicals) can abolish the scalp FFR (Henry, 1995; Snyder and Schreiner, 1984). Although the response is complex to understand, the interplay between different generators in the auditory system may be clinically relevant for hearing disorders not readily diagnosed by classical audiological tests. Reduced FFR amplitudes at the scalp may represent neural deficits already at the level of the auditory periphery. This thesis examined the possibility of the FFR being sensitive to peripheral neural integrity. If the loss of ANF is reflected in the scalp FFR , it may present clinical relevance in the search for reliable and robust diagnostics of ANF loss.

1.4 Overview of the thesis

This thesis examines the FFR as a potential marker of age-related neural degeneration in the cochlea though a series of electrophysiological experiments and simulation-based computational modeling.

In chapter 2, we examine the effect of age on the brainstem generated FFR. The study combines FFR experiments in older and younger clinically normal-hearing listeners with computational AN modeling. FFR responses to pure tones at fixed frequencies as well as to frequency sweeps are recorded to examine previously reported age-related reductions in FFR amplitudes. To investigate the possibility of a peripheral component driving this age-related decrease, we simulate the phase-locked AN activity potentially driving the FFR with a computational model of the AN. Histopathological data from human temporal bones are used to inform the model of age-related loss of AN fibers and hair cells.

In chapter 3, we examine the potential relationship between the AP component of the ABR and the FFR in a large cohort of listeners between 18 and

76 years of age with normal audiometric thresholds ($\leq$ 40 dB hearing level) up to 4 kHz. We hypothesized that an age-related reduction suprathreshold AP amplitudes as a signature of AN loss would be correlated with a reduction in the amplitude of the brainstem generated FFR. We collected additional clinical measures, such as OAEs and MEMRs, to further characterize cochlear health and potentially dissociate neurodegeneration from other age-related cochlear deficits.

In chapter 4, we attempt to dissociate the peripheral part of the phase locked response to pure tone stimulation from the more central (brainstem) activity. We hypothesized that an age-related reduction in the brainstem FFR would be associated with a reduction in the neurophonic response from the AN. To do so, we used electrocochleography (ECochG) with electrodes positioned on the tympanic membrane to isolate the auditory nerve neurophonic (ANN) response in young and older human listeners with normal hearing thresholds. The ECochG recordings are compared to simultaneously recorded FFRs in the classical scalp EEG montage with the same pure tone stimulation. We also record click-evoked ECochG responses to investigate potential age-related reductions in the AN-generated compound action potential.

In the studies reported in chapters 2, 3, and 4, the FFR is investigated as a measure of cochlear neural degeneration in healthy aging humans. However, neural degeneration in clinically normal-hearing humans can co-occur with other age-related auditory deficits. Since the status of the cochlea is only indirectly inferred, it is difficult to conclude that neural degeneration specifically and causally reduces the FFR. Therefore, in chapter 5, we examine the effect of noise-induced auditory nerve loss on the FFR using a chinchilla model of temporary threshold shift. To attempt to isolate peripheral activity from central activity, we record electrophysiological and electrocochleographic responses simultaneously using different montaging techniques.

Finally, chapter 6 presents a summary of the main findings of this work, and discusses implications and perspectives for future investigations in this exciting field of research.

2

Age-related reduction in frequency-following responses as a potential marker of cochlear neural degeneration[a]

Abstract

Healthy aging may be associated with neural degeneration in the cochlea even before clinical hearing loss emerges. Reduction in frequency-following responses (FFRs) to tonal carriers in older clinically normal-hearing listeners has previously been reported, and has been argued to reflect an age-dependent decline in temporal processing in the central auditory system. Alternatively, age-dependent loss of auditory nerve fibers (ANFs) may have little effect on audiometric sensitivity and yet compromise the precision of neural phase-locking relying on joint activity across populations of fibers. This peripheral loss may, in turn, contribute to reduced neural synchrony in the brainstem as reflected in the FFR. Here, we combined human electrophysiology and auditory nerve (AN) modeling to investigate whether age-related changes in the FFR would be consistent with peripheral neural degeneration. FFRs elicited by pure tones and frequency sweeps at carrier frequencies between 200 and 1200 Hz were obtained in older (ages 48–76) and younger (ages 20–30) listeners, both groups having clinically normal audiometric thresholds up to 6 kHz. The same stimuli were presented to a computational model of the AN in which age-related

[a] This chapter is based on Märcher-Rørsted, J., Encina-Llamas, G., Dau, T., Liberman, M.C., Wu, P., & Hjortkjær, J. (**2022**). "Age-related reduction in frequency-following responses as a potential marker of cochlear neural degeneration.", Hearing Research 414 . 10.1016/j.heares.2021.108411.

loss of hair cells or ANFs was modelled using human histopathological data. In the older human listeners, the measured FFRs to both sweeps and pure tones were found to be reduced across the carrier frequencies examined. These FFR reductions were consistent with model simulations of age-related ANF loss. In model simulations, the phase-locked response produced by the population of remaining fibers decreased proportionally with increasing loss of the ANFs. Basal-turn loss of inner hair cells also reduced synchronous activity at lower frequencies, albeit to a lesser degree. Model simulations of age-related threshold elevation further indicated that outer hair cell dysfunction had no negative effect on phase-locked AN responses. These results are consistent with a peripheral source of the FFR reductions observed in older normal-hearing listeners, and indicate that FFRs at lower carrier frequencies may potentially be a sensitive marker of peripheral neural degeneration.

2.1 Introduction

Aging is often accompanied by listening difficulties in noisy situations, even when audiometric thresholds indicate normal hearing (Humes, 2005). Such difficulties could be due to age-related declines in temporal processing arising at different levels of the auditory system. A number of studies have reported an age-related reduction in frequency-following responses (FFRs) to pure tones (Marmel et al., 2013) or vowels (Anderson et al., 2012; Bidelman et al., 2014; Skoe et al., 2015), also in older listeners with clinically normal audiometric thresholds (Clinard and Cotter, 2015; Clinard and Tremblay, 2013; Clinard et al., 2010; Mamo et al., 2016; Presacco et al., 2019; Roque et al., 2019). Reduced FFRs in older listeners without loss of audiometric sensitivity have been argued to reflect a decline in neural synchrony arising in the central auditory system (Anderson et al., 2012; Clinard and Cotter, 2015; Walton, 2010). Such central desynchronization has been hypothesized to cause temporal processing deficits and underlie declines in speech perception in older listeners, even in the absence of peripheral dysfunction assessed through audiometric thresholds (Frisina and Frisina, 1997; Pichora-Fuller et al., 2007). However, normal audiograms do not preclude a peripheral source of age-related changes in the FFR. In particular, an age-dependent degeneration of auditory nerve (AN) fibers

may have little effect on audiometric thresholds (Kujawa and Liberman, 2009; Schuknecht and Woellner, 1955b; Wu et al., 2020) and yet may reduce precise population-level neural phase-locking as reflected in the FFR. The current study investigates this possibility.

FFRs are neurophonic potentials generated by periodic or near periodic auditory stimuli. The FFR reflects sustained neural activity integrated over a population of neural elements. It is often phase-locked to the individual cycles of the stimulus waveform and/or the envelope of the periodic stimuli[b]. Scalp-recorded FFRs are considered to be predominantly produced by synchronous neural activity in the rostral brainstem and midbrain (Krishnan, 2006; Marsh et al., 1974; Smith et al., 1975; Worden and Marsh, 1968). While the main generator of the scalp-recorded FFR is not peripheral (Sohmer et al., 1977), temporal coding of spectral information is first represented by neural phase-locking across populations of auditory nerve (AN) fibers (Reale and Geisler, 1980; Sachs et al., 1983; Young and Sachs, 1979). The auditory nerve neurophonic (ANN) response is the mass potential correlate of phase-locked neural activity across AN fibers recorded near the cochlea, which can be dissociated from the cochlear microphonic (CM) response produced by hair cell activity (Fontenot et al., 2017; Snyder and Schreiner, 1984; Verschooten and Joris, 2014). The ANN shows properties that reflect neural coding not present in the CM, such as rectification and adaptation (e.g., Verschooten and Joris (2014)), and these response properties are also present in the scalp FFR (Snyder and Schreiner, 1985). Damage to AN fiber terminals or a suppressed spike generation in the AN abolish both the ANN and the scalp FFR (Fontenot et al., 2017; Henry, 1995; Snyder and Schreiner, 1984). Intact phase-locked activity across populations of AN fibers is thus a prerequisite for the generation of the FFR. While ANF loss diminishes or eliminates the FFR, more systematic studies of the effects of AN neuropathy on scalp FFRs are missing. It is therefore unclear whether response properties of a pathological ANN are inherited at the brainstem as reflected by the FFR.

In the present study, we propose that age-related reductions in the FFR could, at least in part, reflect the age-dependent neural degeneration in the cochlea. Synapses between inner hair cells (IHC) and AN fibers, and eventually the fibers themselves, degenerate progressively with age (Keithley et al., 1989;

[b] Here, the term FFR is used to refer to the response to pure tones or tonal sweeps, as distinct from envelope-following responses (EFRs) in the case of amplitude modulated stimuli.

Sergeyenko et al., 2013). Exposure to noise accelerates this age-related cochlear synaptopathy (CS) (Fernandez et al., 2015). Recent histopathological examinations of 'normal-aging' human temporal bones have indicated an age-related AN peripheral axon loss across the cochlea (Wu et al., 2019) that typically exceeds age-related degeneration of hair cells. Such primary neural degeneration challenges the conventional understanding that outer hair cells (OHC) represent the primary and most vulnerable element in age-related hearing loss. AN fiber loss can occur without affecting audiometric thresholds, as long as the OHCs are intact (Schuknecht and Woellner, 1955b).

Importantly, the degeneration of AN fibers in the aging human cochlea occurs across the cochlear partition (Fu et al., 2019; Gleich et al., 2016; Viana et al., 2015; Wu et al., 2020). A wide-spread neural loss across characteristic frequency (CF) regions in the cochlea would be expected to reduce phase-locking by AN fiber populations at both higher and lower carrier frequencies (Henry, 1995). Assuming that the frequency-specific response properties are preserved in the scalp-recorded FFR, the FFR would be reduced at both higher and lower carrier-tone frequencies due to fewer contributing fibers. An age-dependent decline in temporal resolution, on the other hand, should predominantly limit phase-locking at higher carrier frequencies, and thus mainly reduce FFRs at higher stimulation rates (Anderson et al., 2012; Frisina and Frisina, 1997). Previous results are unclear as to whether an age-dependent reduction in the FFR to tonal carriers is broadly distributed across stimulation frequency. Clinard et al. (2010) reported a correlation between age and FFR amplitudes to tone frequencies around 1000 Hz, but not to lower frequency tones around 500 Hz. Using tonal frequency sweeps, Clinard and Cotter (2015) reported reduced FFRs also at lower frequencies in older listeners with normal audiometric thresholds up to 4 kHz, and also reported weaker FFRs for faster sweep rates. The authors concluded that the results reflect an age-related decline of phase-locking specific to stimuli with dynamic frequency content such as tonal sweeps. Age-dependent reductions in FFRs elicited by vowel sounds that also have dynamic frequency content (Anderson et al., 2012; Clinard and Tremblay, 2013; Presacco et al., 2019; Roque et al., 2019) may support this view. Yet, it remains unclear whether age-group effects would also be observed for tonal stimuli at lower frequencies.

Using both pure-tone stimuli and frequency sweeps, the current study investigated FFRs at different stimulation frequencies in young and older listeners with clinically normal audiograms up to 6 kHz. We hypothesized that age-related

peripheral neural degeneration across the cochlea would be consistent with reduced FFR amplitudes across a range of stimulation frequencies. In addition to FFRs, we measured middle-ear muscle reflexes (MEMRs) and audiometric thresholds at extended high frequencies, each of which have been proposed to be sensitive to cochlear neuro-degeneration (Bharadwaj et al., 2019; Liberman et al., 2016; Valero et al., 2016). To investigate the effects of nerve fiber loss on phase-locked responses at the level of the AN, we used a computational model of the AN (Bruce et al., 2018). Histological data from a recent human otopathologic study (Wu et al., 2020) were included to simulate the effects on the phase-locked population response. Specifically, we asked if ANF loss simulates a change in FFR that is qualitatively consistent with changes in the observed far-field FFR in aging listeners. The model was also used to dissociate the effects of neural loss from OHC damage based on age-specific threshold curves.

2.2 Materials and Methods

2.2.1 Participants

Twenty-five subjects participated in the study. The participants were recruited based on standard audiometric pure-tone sensitivity profiles ($\leq$ 20 dB hearing level (HL) from 125 Hz to 6 kHz) in our patient database, and grouped by age. To ensure the validity of the audiometric data from the database, all participants took part in a clinical evaluation of their hearing status on the day of the experiment. This included audiogram measurements using Sennheiser HAD300 earphones (air conduction thresholds at audiometric frequencies 0.25, 0.5, 1, 2, 3, 4, 6 and 8 kHz, as well as for extended high-frequencies at 10, 11.25, 14 and 16 kHz), the examination of middle- and outer-ear functionality via wide-band tympanography, and otoscopy. One of the twenty-five participants was found to have slightly elevated thresholds at 3 kHz (35 dB HL) and 6 kHz (40 dB HL) and was therefore excluded from the analyses, resulting in a young group (n = 12, 5 males, mean age 24.8 +/- 3.38) and an older group (n = 12, 4 males, mean age 63.3 +/- 8.91; age difference: $t(22) = -14.01$, $p < 0.001$). All subjects provided written informed consent to participate. The experiment was approved by the Science Ethics Committee for the Capital region of Denmark (protocol H-16,036,391) and was conducted in accordance with the Declaration of Helsinki.

2.2.2 Distortion product otoacoustic emissions (DPOAEs)

It is possible that OHC dysfunction can confound potential differences in FFR between young and older listeners. As a physiological indicator of OHC status, distortion product otoacoustic emissions (DPOAE) were measured, both as a function of frequency (2- 8 kHz at 64 dB sound pressure level (SPL)) and level (40-70 dB SPL at 4 kHz). Both negative and positive middle-ear pressure can impact the quality of DPOAE recordings (Sun, 2012). To compensate for this, we pressurized the ear to correct for middle-ear pressure while measuring DPOAEs. DPOAE measures were conducted in both ears of all participants using the Interacoustics Titan system and standardized protocols. DPOAEs were measured using two pure tones, known as primaries (F1 and F2) with a ratio of 1.22 (F2/F1). For the level dependent DPOAEs at 4 kHz, the level difference between the two primary tones was kept constant (F2 = F1- 10 dB) while F1 was varied in level from 40 to 70 dB SPL in steps of 10 dB. Level dependent distortion products were considered significant if their amplitude exceeded -15 dB SPL. For the frequency dependent DPOAEs, the levels of the two tones were fixed (F1 = 65 dB SPL, and F2 = 55 dB SPL) while the frequency of F2 was varied (2, 3, 4, 5, 6 and 8 kHz). Cubic distortion products (2F1- F2) were recorded. Frequency dependent distortion products were considered significant if their amplitude exceeded -10 dB SPL.

2.2.3 Middle-ear muscle reflex (MEMR)

The middle-ear muscle reflex (MEMR) was measured to indicate the status of efferent neural feedback which has also been proposed to indicate potential degeneration in the auditory nerve (Bharadwaj et al., 2019; Valero et al., 2016). A custom assay was implemented according to a recent study (Mepani et al., 2019), using the Titan system. The protocol consisted of click-noise-click sequences, presented to the right ear. The click response of the ear canal was measured before and after 500 ms white noise elicitors (0.5–2 kHz) at levels of 75–105 dB SPL, using a 5 dB step size. The probe click was presented at 100 dB SPL, calibrated to the peak-to-peak voltage of a 100 dB SPL 1 kHz tone. The noise elicitors had a 50 sample (2.3 ms) long onset and offset ramp defined by a 1st order Kaiser window function. The MEMR was assessed by comparing the frequency response of the first and second click for each of the noise elicitor levels. Growth-level functions for each participant were evaluated by taking

the absolute value of the frequency response differences summed across all frequencies. To investigate the sensitivity of the MEMR to different elicitor levels, a linear function was fitted to the MEMR responses. The estimated linear coefficient from the linear fit for each participant was used for the group based analysis. For one older participant, it was not possible to complete the MEMR measurement due to technical issues. Data from this participant were therefore excluded from this part of the analysis.

2.2.4 EEG

Experiment and Stimuli

FFRs were recorded with both amplitude modulated pure-tones and frequency sweeps. Pure-tone stimulation consisted of continuous tones at carrier frequencies of 326 Hz and 706 Hz, sinusoidally amplitude modulated at 4 Hz. Pure-tone sequences were presented to the right ear. A total of 8 conditions of 250-s each was measured in this part of the experiment. The conditions consisted of either high or low carrier frequencies (326 and 706 Hz), alternating polarities (condensation and rarefaction start phase), as well as with or without the presence of a contralateral threshold equalizing noise (TEN) masker at a signal-to-noise ratio (SNR) of 5 dB relative to the pure-tone stimulus. Contralateral noise was presented to investigate effects of efferent feedback on the FFR. The presentation order of the conditions was randomized for each participant. Next, the participants listened to 1800 repetitions of pure-tone frequency sweeps. The stimuli consisted of 0.6 s long up-down cosine frequency-modulated sweeps ranging from 0.2 to 1.2 kHz presented continuously. The average absolute frequency change rate was of 3333 Hz/s. Due to the sinusoidal modulator, the frequency change rate was not constant across the frequency range. The onset polarity was positive and sweeps were presented in a continuous manner. The sweep stimuli were presented monaurally to the right ear for all participants. The TEN was presented to the left ear. Both pure-tone and sweep stimuli were presented via metal-shielded ER-3 insert earphones (Etymotic Research) at 85 dB HL for all conditions, synthesized at a sampling rate of 48 kHz. Preliminary measurements using dummy head recordings were conducted to ensure the absence of electrical artefacts. For the sweep and pure-tone stimuli, the level was adjusted using frequency dependent filters according to equal-loudness level contours as described in ISO 226:2003. The frequency response of the

sound reproduction chain (i.e., soundcard and earphones) was linearized by means of the inverse impulse response of the earphones.

Data acquisition

EEG data were continuously recorded using the BioSemi ActiveTwo system. EEG was recorded from gold-foil tiptrode electrodes inside left and right ear canals, as well as from 8 pin-type scalp electrodes (CMS, DRL, Cz, FCz, Fz, Fpz, P9 and P10). The sample rate was 16,384 Hz. The participants were asked to lie down on a bed in a doubled-walled sound treated electromagnetically shielded booth, keeping their eyes closed. Otoscopy was performed directly before insertion of the tiptrodes, ensuring correct insertion. No preparation of the ear canals was performed.

EEG pre-processing

All EEG data were segmented into trials from 0.1 s preceding the onset of each stimulation cycle, to 0.8 s after. Line noise (50 Hz) was removed using notch filters centered around 50 Hz and the corresponding harmonics (100, 150 etc.) up to 1 kHz. The data were bandpass filtered between 80 Hz and 2 kHz using a windowed sinc type I linear phase finite impulse response filter. The data were re-referenced to the response of the right tiptrode.

Sweep FFR analysis

Frequency sweeps were evaluated as a combination of both horizontal and vertical montages, by using potentials from the vertex (Cz) and the left tiptrode, referenced to the right tiptrode. In this way, sources from the lower as well as higher brainstem could contribute to the FFR to sweeps (Bidelman, 2018). Trials of 600 ms (corresponding to one cosine sweep cycle) were first examined for artefacts, rejecting any trials where EEG activity exceeded +/- 40 mV. Clean trials were then weighted by the inverse of their variance and averaged (John et al., 2001). On average, 3.1 % +/- 4.9 % of trials were rejected for this part of the analysis, leaving, on average, 1744 trials for each participant. Time frequency representations of the neural response were calculated using a discrete Gabor transform for real-signals using two-sample second-order Gaussian filters. To investigate potential differences between older and younger listeners across the entire stimulus frequency range, a stimulus-response cross-correlation

analysis was performed on the average time series for each listener. This was done over the entire time course of the stimulus. To identify potential frequency dependent differences across listener groups, the instantaneous FFR over sweep frequency was calculated in the spectrotemporal domain. Time-frequency bins containing the stimulus were identified and the FFR magnitude across frequency was extracted.

Pure-tone FFR analysis

To evaluate the neural synchronization of the response to the tonal carrier frequency of the amplitude modulated stimuli, horizontal and vertical montages were combined using potentials from the vertex (Cz) and the left tiptrode, referenced to the right tiptrode. Trials of 0.5-s were first examined for artefacts, rejecting trials where EEG activity exceeded +/- 40 mV. On average, 1.0 % +/- 2.2 % of trials were rejected. Trials of negative polarities were multiplied by -1 to enhance the FFR response ((C-R)/2) (Kraus and Skoe, 2010). Clean trials were then averaged and weighted by the inverse of their variance, and concatenated to create 1-s long segments (corresponding to 2 trials of 0.5 s). FFR magnitudes were evaluated on the averaged response for each condition, and for each participant separately. The spectral magnitude at the carrier frequency (326 Hz or 706 Hz) was evaluated, and compared to the surrounding noise floor (+/- 20 Hz) using an F-statistic test (Dobie and Wilson, 1996). The SNR (F-ratio) was calculated as the power in the FFR frequency bin divided by the average of the surrounding noise floor power. Side bands from the amplitude modulation were disregarded as part of the noise floor (+/- 4 Hz around the carrier frequency). The probability (p) of the FFR power being different from the noise was assed as 1-F, where F represents the cumulative distribution of the power ratio. FFR measurements were considered statistically significant if $p \leq 0.01$ ($\alpha = 0.01$). Non-significant FFR responses were excluded from statistical analysis.

To compare the data with those from previous studies, the FFR was also analyzed using other metrics. A stimulus-response cross-correlation analysis was performed as in Clinard et al. (2010) and Marmel et al. (2013), whereby average responses were cross-correlated with a down-sampled version of the stimulus to match the EEG sample rate. The cross-correlation coefficient was chosen as the maximum value of the cross-correlation function within a time window of +/-15 ms from t = 0.

Auditory nerve Modeling

A humanized phenomenological model of the AN (Bruce et al., 2018) was used to investigate the consequences of hair-cell and neural loss with advancing age on FFRs at the level of the nerve. The input to the model is an instantaneous pressure waveform of the stimulus and the output is a series of AN spike times. The model consists of a middle-ear filter, a nonlinear basilar membrane filtering stage mimicking OHC gain, IHC transduction, adaptation at the IHC-AN synapse, and generation of the instantaneous discharge rate. The model was implemented to simulate the whole AN population response, as in Encina-Llamas et al. (2021). In short, 32,000 AN fibers, distributed non-uniformly across 300 CFs ranging from 125 Hz to 20 kHz, were computed in each simulation. For each CF, a distribution of respectively 61, 23 and 16 of high-, medium-, and low-SR fibers, was used (Liberman, 1978).

Histopathological data from 120 human temporal bones (Wu et al., 2020) were used to simulate plausible age-related degeneration of hair cells and ANFs in humans. The histological data consisted of microscopic analyses of hair cells, ANFs and strial tissue in 120 human inner ears. The specimens ranged in age from 0 to 104 years. Mean loss profiles of IHCs, and ANFs were evaluated in three age groups (1–50, 50–75 year and 75–100 years of age) across discrete cochlear segments (CFs 170 Hz, 300 Hz, 700 Hz, 1.8 kHz, and 7.5 kHz for ANFs, and 144 Hz, 275 Hz, 488 Hz, 832 Hz, 1391 Hz, 2297 Hz, 3767 Hz, 6150 Hz, 10,016 Hz, and 16,285 Hz for IHCs). For each CF, loss of ANFs was implemented by removing the number of fibers corresponding to the percentage loss, agnostic to fiber type (Suthakar and Liberman, 2021). In histopathological counting, IHC loss indicates loss of the whole cell (in contrast to IHC dysfunction). IHC loss was simulated by removing all ANFs connected to the missing IHC. It was then assumed that the sur-viving IHCs were functionally intact (i.e. the 'cihc' parameter in the model by Bruce et al. (2018) was not modified).

Directly linking OHC loss from the histopathological data to the model parameter that controls the OHC gain ('cohc' in Bruce et al. (2018)) is challenging. Instead, OHC gain loss was simulated based on audiometric thresholds by means of the MATLAB function *fitaudiogram2* implemented by Zilany et al. (2009). This adjusts the AN model thresholds to account for the audiometric threshold elevations. This was first done for standard clinical frequencies (<8 kHz) for the histopathological data of Wu et al. (2020). In addition, age-normal

audiometric profiles (Rodríguez Valiente et al., 2014), also including extended high frequencies (0.125 to 20 kHz), were also simulated. This dataset is based on 635 'normal-aging' listeners between 5 and 90 years of age, grouped in 6 age groups (20-29, 30-39, 40-49, 50-59, 60-69 and 70-90 years). The mean threshold curves for each age group were used.

The same sweep stimulus and amplitude modulated pure-tone stimuli as used in the FFR experiments were used in the model simulations. The gross AN response was obtained by summing the output spike trains from each CF in the frequency domain. This avoided potential phase interaction effects induced by non-uniform nerve fiber loss across frequency, which were highly non-linear and difficult to interpret. Specifically, the 300 CFs were divided into 10 cochlear regions (CR) and the same spectral analysis was performed per CR as performed on the FFR data. Although it is known that phase interactions between basal and apical neural generator are important when interpreting transient evoked auditory brain stem responses (ABR) (Abdala and Folsom, 1995), it is still unknown to which degree these interactions influence the response to sustained frequency-dynamic stimuli, such as the sweep stimulus used in this study. It has been argued that the FFR is predominately generated by basal fibers (Dau, 2003), which might argue for only including basal fibers in the model output. Including only basal AN fibers in the model simulations led to very similar results (not shown) to the results obtained after disregarding the phase. However, due to the low-frequency content of the stimulus, and missing knowledge about the model's ability to represent phase information with complex stimuli, it was decided to include low-frequency fibers, but to disregard any phase interactions between basal and apical cochlear channels. To quantify effects of OHC dysfunction, IHC deafferentation and ANF loss, the outputs of the impaired models were normalized to the output of the 'healthy' AN model.

Statistical tests

Non-parametric permutation tests were used to examine differences between groups. To test for statistical group differences in the FFR amplitudes at different sweep frequencies, the p-values across frequency were corrected by means of false discovery rate (Benjamini and Hochberg, 1995). All statistical tests were considered significant at $p < 0.05$. Permutation tests were conducted with 100,000 permutations, unless otherwise stated.

2.3 Results

2.3.1 Hearing thresholds and OAEs

We recruited younger and older listeners from our database to have normal hearing as defined by their audiometric thresholds at standard clinical frequencies up to 6 kHz. Figure 2.1A) shows the measured group-averaged threshold functions (right ear) for the younger (solid black) and the older (solid red) listener groups. All listeners were confirmed to have audiometric thresholds ≤ 20 dB HL up to 6 kHz. At 8 kHz, the older listeners had thresholds ≤ 35 dB HL. Despite normal or near-normal audiometric thresholds in the clinical range, the older listeners had significantly higher thresholds above 8 kHz compared to the younger listeners (pure-tone average of all frequencies from 10 kHz to 16 kHz: $t(22) = -11.2396, p < 0.001$). Also at frequencies ≤ 6 kHz, the young group had significantly lower mean thresholds compared to the older group (pure-tone average from 125 to 6000 Hz: $t(22) = -4.0814, p < 0.001$), although both were within the normal range. There were no differences in thresholds in the frequency range of the tonal stimuli (200-1200 Hz) used in the EEG study (pure tone average from 125 to 2000 Hz: $t(22) = -1.9225, p = 0.0784$). Cubic

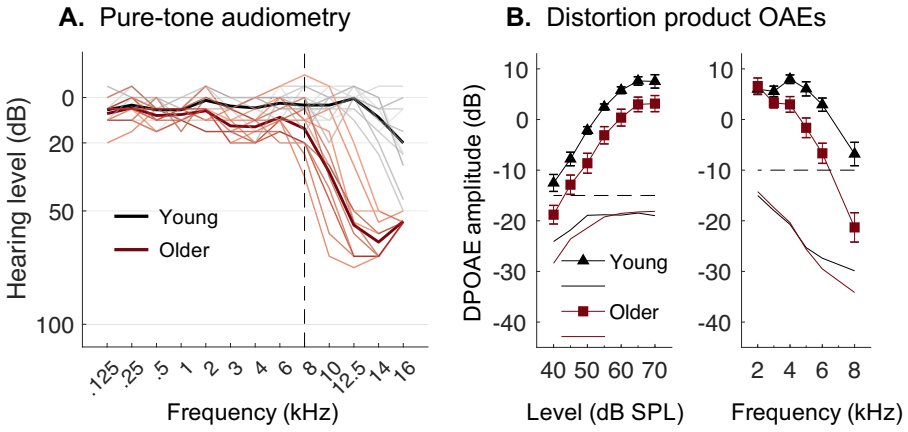

Figure 2.1: **A**) Pure-tone audiograms from 125 Hz to 16 kHz. Individual threshold function are plotted as thin black (young) and red (older) lines. **B**) DPOAEs at 4 kHz for levels 40 to 70 dB SPL (left), and DPOAE grams at 64 dB SPL for frequencies 2, 3, 4, 5, 6 and 8 kHz (right). Solid lines without markers indicate the averaged noise floor. Dashed lines indicate threshold for significant responses above the noise floor. Error bars show standard error of the mean (SEM).

DPOAEs were measured as a correlate of OHC function. Figure 2.1B) shows the group-averaged DPOAEs obtained for F2 = 4 kHz as a function of F2 level

(left) and obtained for a fixed level (F1 = 65 dB SPL, F2 = 55 dB SPL) as a function of F2 frequency (right). On average, significant DPOAEs were obtained for levels above 40 dB SPL in the young listeners and above 45 dB SPL in the older listeners. When averaging across level, the older listeners showed lower DPOAE responses compared to the young listeners ($t(22) = 3.2201, p = 0.0042$), indicating reduced OHC function in the older listeners at this frequency (4 kHz). The DPOAE frequency functions (right) showed, on average, significant DPOAEs at all frequencies in the young group. For the older group, significant DPOAEs were obtained only up to 6 kHz, and the response amplitudes were smaller than those for the young group at frequencies at and above 4 kHz, indicating decreased OHC function at the higher frequencies. Statistical analysis showed no difference between the groups at frequencies below 4 kHz (Bonferroni corrected $p < 0.0083$: 2 kHz: $t(22) = 2.4156, p = 0.7628$, 3 kHz: $t(22) = -0.3090, p = 0.1452$, 4 kHz: $t(22) = 1.5003, p = 0.0129$). For frequencies above 4 kHz, the older listeners showed reduced DPOAE responses compared to the young group (Bonferroni corrected $p < 0.0083$: 5 kHz: $t(22) = 3.0789, p = 0.0030$, 6 kHz: $t(22) = 3.8611, p = 0.0006$, 8 kHz: $t(22) = 3.7450, p = 0.0012$), consistent with elevated audiometric thresholds at higher frequencies in the older group.

2.3.2 Effects of age on MEMR sensitivity

Figure 2.2 shows the MEMR results obtained in the two listener groups for different levels of the wide-band noise elicitor. Figure 2.2A) shows the group average MEMR as a function of frequency for the younger group (left) and the older group (right).

The responses represent the change in absorbance in the ear canal after the pre-sentation of the noise elicitor. Different colors indicate the results for the different noise elicitor levels (between 75 and 105 dB SPL). The younger listeners showed larger MEMR responses than the older listeners at higher noise elicitor levels. This is also reflected in the left panel of figure 2.2B) which shows the sum of absolute change in absorbance as a function of level, averaged across frequency, for the younger listeners (triangles) and the older listeners (squares). The right panel of figure 2.2B) shows the slope of the linear functions fitted to level growth functions of the two listener groups. The younger listeners showed significantly steeper slopes than the older listeners ($t(21) = 2.7330, p = 0.0118$), indicating a reduced strength of the MEMR at higher elicitor levels in the older group. However, even though the MEMR values were larger among the younger

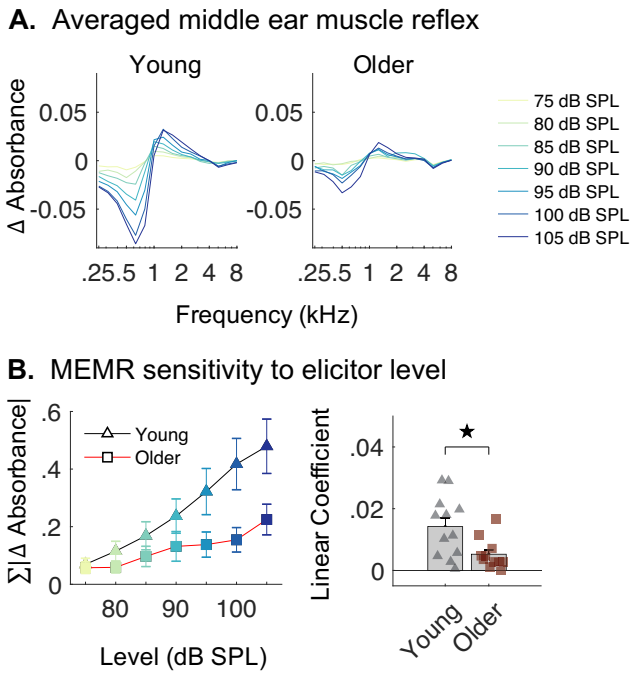

Figure 2.2: **A**) Mean MEMR responses for levels 75-105 dB SPL for young and older participants. **B**) Sum of absolute change in absorbance over frequency for levels 75-105 dB SPL for young and older participants (left), and the slope of the linear fit of the growth level function for each participant (right). Error bars show SEM. $\star$ =p < 0.05, $\star\star$ =p < 0.01, $\star\star\star$=p < 0.001.

listeners, a large variability between the individual participants was found, consistent with results from previous work (Guest et al., 2019).

2.3.3 Effects of age on frequency sweep FFRs

To investigate effects of age on phase-locked neural activity across a range of frequencies, we first considered FFRs to continuous frequency sweeps. Figure 2.3A) shows the spectrogram of the cosine sweep stimulus, sweeping continuously between 200 Hz and 1200 Hz. Figure 2.3B) shows the average FFR responses to the sweep stimulus for the young (left) and the older (right) listeners. As a global similarity metric across frequency and time, the cross-correlation between the time-domain EEG response and the sweep stimulus was computed. Figure 2.3C) shows the cross-correlation coefficient for the young (triangles) and the older listeners (squares). The analysis suggests a significantly reduced response to the sweep stimulus in the older listeners ($t(22) = 3.0526, p = 0.0063$). To quantify the differences in the FFR between the groups at the different frequencies in the

sweep, the FFR spectral amplitudes were extracted and subjected to statistical permutation tests (see Methods). Repeated measures across frequencies was

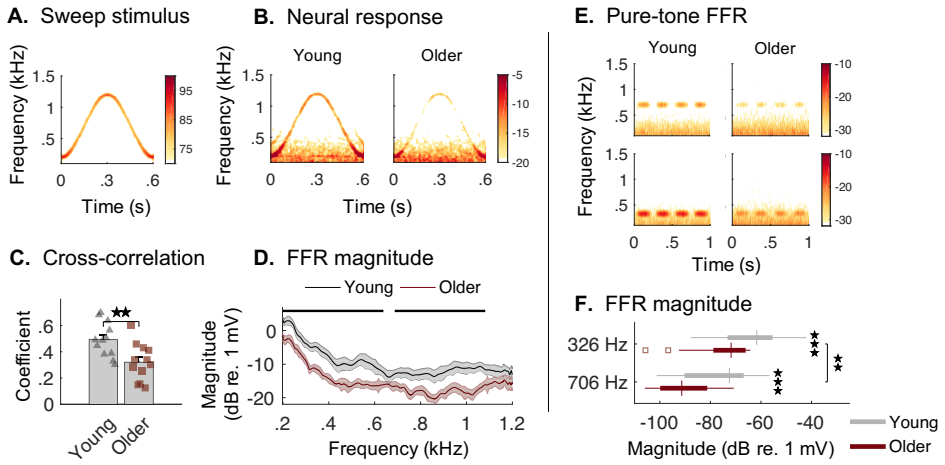

Figure 2.3: FFR results. A) Spectrogram representation of the sinusoidal sweep stimulus. Color bar indicates presented sound pressure level (dB). **B**) Spectrograms of FFR responses to the sweep stimulus in the young (left) and older (right) listener groups. Color bars indicate EEG magnitude (dB re. 1 mV). **C**) Average cross-correlation coefficients in young and older listeners. **D**) FFR magnitudes at time-frequency bins of the sweep stimulation for young and older listeners. Shaded error bars represent ± 1 SEM. Solid black lines above the curves indicate significant differences between listener groups after false discovery rate correction. **E**) Spectrograms of FFR responses to pure-tones at 706 Hz (top) and 326 Hz (bottom) for young (left) and older (right) listeners. **F**) Box plot of FFR magnitudes for 326 Hz and 706 Hz pure-tone stimuli for young and older listeners. Unfilled squares indicates non-significant data points compared to the noise floor. Error bars show SEM. $\star$ =p < 0.05, $\star\star$ =p < 0.01, $\star\star\star$=p < 0.001.

accounted for using false discovery rate. Figure 2.3D) shows the FFR amplitudes as a function of frequency for both listener groups. The FFR amplitudes were consistently smaller in amplitude across frequency in the older listeners than in the younger listeners. Frequency regions with significantly reduced FFR responses in the older group (black lines in figure 2.3D) were identified both at lower (200-600 Hz) and higher frequencies (700–1100 Hz).

2.3.4 Effects of age on pure-tone FFRs

The FFR responses to the sweep stimuli indicated reduced neural phase-locking in the older listeners at both lower and higher frequencies. Age-related changes could relate to the dynamic nature of the sweep stimulation (Clinard and Cotter, 2015). We therefore investigated FFR responses to pure tones separately at a lower (326 Hz) and a middle frequency (706 Hz) in the two listener groups.

Figure 2.3E) shows spectrograms of the group averaged EEG responses to the 706 Hz tone (top panels) and the 326 Hz tone (bottom panels) for the two listener groups. The FFR responses were quantified in terms of the spectral amplitudes at the stimulation frequency. Figure 2.3F) shows group-based FFR amplitude boxplots for the young (gray bars) and the older listeners (red bars). All listeners showed significant responses to both stimuli, except for two of the older listeners where no significant FFR response could be obtained to the lower-frequency tone (unfilled squares). Compared to the young listeners, the older listeners showed significantly reduced FFR responses at both stimulation frequencies (ANOVA main effect of age: $F(1,44) = 17.3062, p < 0.001$). Additionally, the FFRs to the lower-frequency tone (326 Hz) were significantly larger than those to the higher-frequency tone in both listener groups (ANOVA, main effect of frequency: $F(1,44) = 9.0473, p = 0.0098$). No significant interactions between frequency and age were found. In agreement with these observations, the stimulus-response cross-correlation analysis showed similar effects of age and frequency (ANOVA main effect of age: $F(1,44) = 22.6711, p < 0.001$; main effect of frequency $F(1,44) = 11.7565, p = 0.0035$). Figure 2.4 shows the average time-domain FFR to both sweeps and pure-tone stimuli for both listener groups.

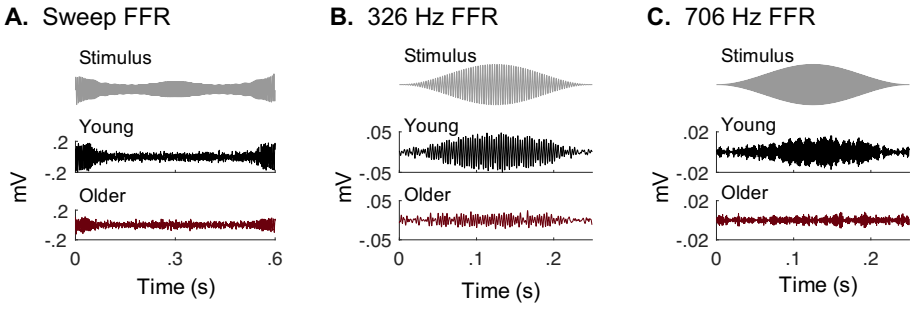

Figure 2.4: Grand average time-domain FFRs. Averaged FFR for **A**) sweep stimulus, **B**) 326 Hz pure-tone, and **C**) 706 Hz pure-tone. In all panels, stimuli are shown in gray, and averaged FFRs are shown in black for young and red for older listeners. Pure-tone FFRs (**B** and **C**) have been bandpass filtered ± 100 Hz around the stimulus frequency for visualization purposes.

To ensure that differences between the two groups were not a result of a different quality of the EEG recordings, we also calculated the SNR between the FFR and the surrounding noise floor. No differences between groups were found in terms of the noise floor level ($F(1,44) = 0.0043, p = 0.9475$). FFRs with and without the presence of the contralateral noise masker revealed no significant

difference in FFR amplitudes for young (Bonferroni corrected $p < 0.0125$: 326 Hz: $t(11) = 2.7668, p = 0.0231$, 706Hz: $t(11) = 1.9310, p = 0.0676$) or for older listeners (326 Hz: $t(11) = 1.1292, p = 0.3090$, 706 Hz: $t(11) = -1.9736, p = 0.0760$), suggesting no effect of efferent feedback on the FFR.

2.3.5 Auditory nerve modeling

We used a computational model of the auditory nerve (Bruce et al., 2018) to examine the effects of age-related hair-cell and AN degeneration. The modeling allowed us to dissociate effects of hair cell loss from neural degeneration on AN responses to the tone stimuli used in the current FFR experiments. We did not attempt to simulate the FFR generated in the central auditory brainstem (Dau, 2003; Rønne et al., 2012; Verhulst et al., 2018). Rather, assuming that the stimulus representation at the level of the nerve is a bottleneck for subsequent neural processing (Joris et al., 2004), we used the model to investigate whether age-related AN degeneration was qualitatively consistent with age effects observed in the FFR.

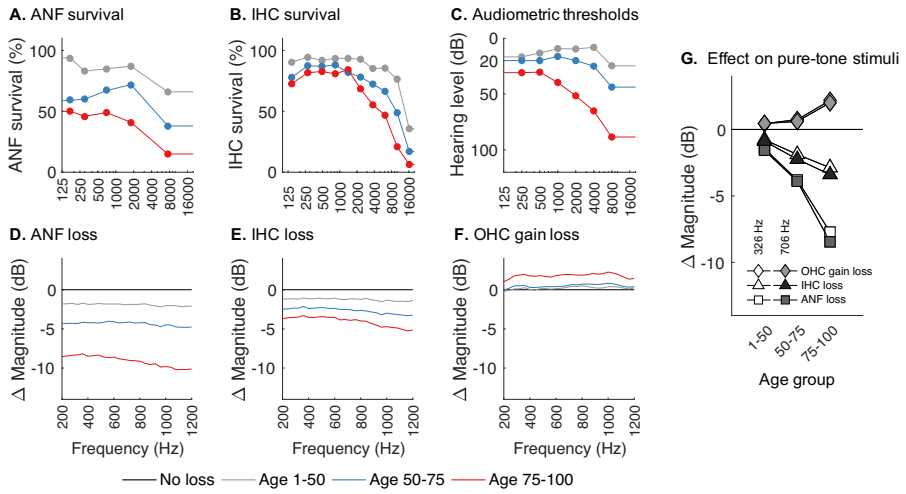

Figure 2.5: Model-generated AN frequency-following responses to the sweep and pure tone stimuli (**D**-**G**) for different levels cochlear degeneration (**A**-**B**) and hearing loss (**C**) in aging humans. **A**) Mean ANF survival from human temporal bone histopathology (Wu et al., 2020) for three age groups. Losses are expressed in % of survival as a function of cochlear frequency. **B**) Mean IHC survival. **C**) Mean audiometric thresholds, **D**) Effect of ANF loss on the change in AN response to the sweep relative to the unimpaired model. **E**) Effect of IHC loss on the AN response. **F**) Effect of OHC gain loss corresponding to audiometric threshold shifts on AN responses. **G**) Change in AN responses to pure tones at 326 Hz (white) and 705 Hz (shaded) with OHC gain loss (diamonds), IHC deafferentation (triangles) or ANF loss (squares).

To model age-related degeneration, we used histopathological data from human temporal bones that quantified hair-cell and ANF survival in aging humans (Wu et al., 2020). Figure 2.5A) and 2.5B) shows the mean ANF and IHC fractional survival for all 120 cases divided into three age groups, and figure 2.5C) shows their mean hearing loss. In the model, we separately removed ANFs or IHCs corresponding to the histological data for each age group and examined AN responses to the sweep stimuli used in the FFR experiments (see methods). Figure 2.5D) and 2.5E) shows the effect of age-related loss of ANFs and IHCs, respectively, on the change in magnitude of the summed phase-locked AN response relative to an intact 'unimpaired' model. ANF loss in older subjects was found to strongly reduce frequency-following AN activity. Importantly, the phase-locked AN response was uniformly reduced across frequency, consistent with the age effects observed in the FFR data. Noticeably, the reduction was substantial already in the 50–75 years age group where thresholds were relatively normal (Figure 2.5C) up to 4 kHz. However, IHC loss, although present mostly in the basal part of the cochlea, also led to a uniform reduction of the phase-locked AN response at lower frequencies, even though this effect was markedly smaller than for ANF loss.

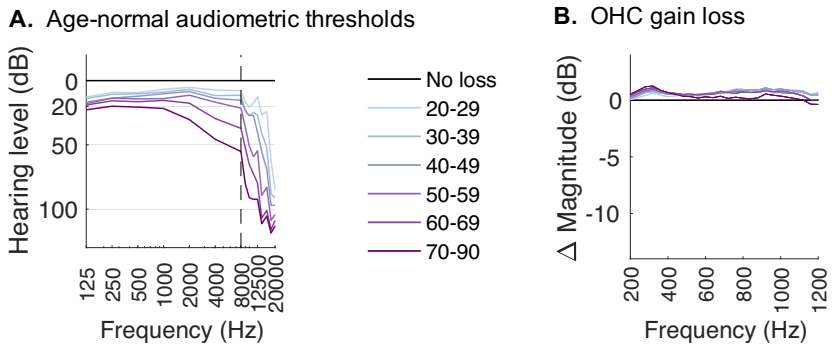

Figure 2.6: **A**) Age-normal sensitivity curves replotted from Rodríguez Valiente et al. (2014). Each curve represents the mean hearing threshold in dB HL for six different age groups. **B**) Relative magnitude change due to sensitivity loss attributed OHC gain loss in the sweep stimulus for the six mean age group sensitivity profiles seen in **A**).

OHC dysfunction cannot directly be modelled from the histology data, which quantifies only cell survival, because the relation between OHC loss and changes in the amplifier gain is not known. Instead, to examine the effects of OHC dysfunction we reduced the OHC gain, as implemented in Bruce et al. (2003), in proportion to the audiometric thresholds of the subjects (Figure 2.5C).

Loss of OHC gain did not reduce the phase-locked AN response to sweeps (Figure 2.5F). To further investigate age-related hearing loss, we used age-normal audiometric profiles from a large sample (Rodríguez Valiente et al., 2014) where narrower age groups were defined and audiometric frequencies up to 20 kHz were measured (Figure 2.6A). Again, in the framework of the model, even large degrees of OHC gain loss at high frequencies did not reduce the phase-locked AN response to the sweep stimulus (Figure 2.6B).

Simulated AN responses were also obtained using the two pure-tone stimuli used in the FFR experiment. Figure 2.5G) shows the change in magnitude of the simulated phase-locked AN response for each age group and for the different types of cochlear impairment. Again, the greatest reduction was observed with loss of ANFs (Figure 2.5G, squares), similar to the effects obtained for the sweep stimulus. The reduction was virtually identical at 326 Hz and 706 Hz, confirming a relatively broadband reduction as observed with the sweep stimulus. A small increase was found in the case of OHC dysfunction (Figure 2.5G, diamonds), most likely due to the loss of cochlear compressive gain.

2.4 Discussion

Consistent with previous work, our study confirmed that pure-tone FFRs are reduced in older human listeners with clinically normal hearing thresholds. We also found that this age-related reduction occurs across stimulus frequencies in the range examined (200–1200 Hz). Using model simulations, we found this reduction across frequencies to be qualitatively consistent with the pattern of age-related degeneration of ANFs suggested by human inner ear histopathology. Model simulations also indicated that OHC dysfunction, if present, would have little or no impact on the phase-locked population response at the level of the AN (cf. Encina-Llamas et al. (2021, 2019). If the AN neurophonic response is assumed to be a bottleneck on the downstream synchronous neural activity reflected in the FFR (Dau, 2003), then peripheral degeneration may contribute significantly to the response reduction seen in the experimental data. If the FFR is selectively sensitive to cochlear neural degeneration and not affected by OHC status, then this may also imply a clinical potential of the FFR, also in listeners with hearing loss. However, simulations also indicated that high-frequency loss of IHCs may reduce the amount of phase-locking at lower frequencies, albeit to a lesser degree.

In contrast to our findings, some previous studies reported reduced FFR amplitudes in normal-hearing older adults predominantly at higher frequencies (1000 Hz), but not at lower ones (500 Hz, Clinard et al. (2010) and Grose et al. (2017)). However, age-related reductions have also been observed previously at lower frequencies (≈400 Hz) with frequency sweeps as in the current study (Clinard and Cotter, 2015). Clinard and Cotter (2015) argued that this effect may be specific to dynamic frequency content (such as sweeps), reflecting degraded processing of time-varying spectral cues in the aging auditory system. Yet, in the current study, FFR responses to pure tones were found to be reduced also at lower frequencies (326 Hz). Consistent with this, reduced FFRs to the fundamental frequency (F0) of sustained vowel sounds, i.e. evoked by lower frequencies, have also been frequently reported (e.g., Anderson et al. (2012), Presacco et al. (2016a), and Roque et al. (2019)). Reduced FFR responses in older listeners with clinically normal audiograms have been argued to indicate a degradation of temporal processing originating in the central auditory system (Anderson et al., 2012; Clinard and Cotter, 2015; Clinard and Tremblay, 2013). However, hearing thresholds in the clinically normal range are not sufficient to rule out a peripheral origin of these FFR changes. Loss of AN fibers, by itself, has only a minor effect on audiometric thresholds (Schuknecht and Woellner, 1955b; Wu et al., 2020). In the current study, we included other measures that could indicate peripheral degeneration in our clinically normal-hearing listeners. Although the older subjects had clinically normal hearing at standard audiometric frequencies up to 6 kHz, thresholds at the extended high frequencies (> 8 kHz) were found to be distinctly elevated. Additionally, MEMR level-growth functions were significantly reduced in the older group. Elevated high-frequency thresholds and reduced MEMRs may indicate peripheral degeneration beyond what is indicated by the clinical audiogram (Bharadwaj et al., 2019; Liberman et al., 2016; Mepani et al., 2019; Valero et al., 2016). It is likely that most older listeners with clinically normal thresholds have high-frequency threshold loss similar to that seen here (Matthews et al., 1997). A peripheral source of the FFR reduction in older listeners cannot be excluded without other measures of peripheral function. Indeed, identifying older listeners with a peripheral hearing status matching that of young listeners may be challenging. A larger sample size than the one used here might further explore the relation between the FFR and measures of peripheral hearing status.

Direct evidence for effects of age-related AN degeneration on scalp-recorded

FFRs is missing. It is well-established that AN damage reduces the neurophonic response recorded close to the nerve (Choudhury et al., 2012; Fontenot et al., 2017; Henry, 1995; Snyder and Schreiner, 1984), but evidence about the consequences on scalp-recorded FFRs is sparse. Envelope-following responses (EFRs), on the other hand, have been used more extensively to examine the functional consequences of cochlear synaptopathy. Similar to FFR responses to tone carriers, the scalp-recorded EFR to amplitude modulated (AM) stimuli is thought to reflect population phase-locked activity which may be reduced by AN damage. In rodents, EFRs to modulation frequencies around 1 kHz are dominated by AN activity and are reduced with synaptopathy following noise exposure (Shaheen et al., 2015) or aging (Parthasarathy et al., 2014, 2018, 2016). The magnitude of EFR reductions around 1 kHz has been shown to predict the degree of ANF loss, i.e. the percentage of surviving fibers Shaheen et al. (2015), also before age-related loss of thresholds emerge (Parthasarathy et al., 2019; Parthasarathy and Kujawa, 2018). In humans, age-related EFR reductions have been observed at modulation frequencies around 120 Hz where the response is dominated by subcortical generators (Vasilkov et al., 2021). Human EFRs at lower modulation frequencies are increasingly dominated by cortical sources (Herdman et al., 2002), and lower modulation frequencies show minimal effects or are even enhanced with age (Goossens et al., 2016, 2018; Grose et al., 2009; Herrmann et al., 2017; Lai et al., 2017; Parthasarathy and Bartlett, 2012). This could be explained by the presence of a central gain enhancement mechanism that restores sound-evoked response levels after ANF loss but not precise temporal coding (Chambers et al., 2016; Herrmann et al., 2017; Parthasarathy et al., 2014). It is therefore unclear whether EFR enhancements at lower modulation frequencies occur because such gain mechanisms mostly affect slower neural activity or because of a stronger contribution from more central sources in the EFR (or a combination of both). It is, perhaps, less likely that FFR responses to temporal fine structure are similarly affected by central compensation mechanisms (Parthasarathy and Kujawa, 2018). More generally, it remains unclear whether the population responses to envelope and fine-structure are similarly limited by the number of contributing AN fibers (Joris and Smith, 2008).

It is important to highlight that the FFR represents a population response. Single AN fibers that survive degeneration in aged animals can retain intact coding of both temporal fine structure and envelope (Heeringa et al., 2020). Accordingly, in our model simulations, we simulated AN degeneration by remov-

ing a percentage of fibers while leaving the remaining fibers functionally intact. AN phase-locking computed from the summed activity across remaining fibers decreased as the number of AN fibers was reduced. However, the generation of a synchronous population response is most likely not the result of a simple summation at the level of the AN. Convergence of multiple AN fibers at their target synapse is known to enhance phase-locking to the fine-structure of low frequency tones (<1 kHz) in CN bushy neurons relative to the AN (Joris et al., 1994a,b). Such synchronization enhancement in the brainstem has been proposed to rely on a synaptic mechanism that requires coincident AN inputs for spike generation (Chanda and Xu-Friedman, 2010; Kuhlmann et al., 2002; Rothman and Young, 1996) which effectively reduces the variability in spike-timing in the AN (Joris and Smith, 2008; Xu-Friedman and Regehr, 2005). Importantly, synchronization strength at the postsynaptic output increases with the number of converging ANF inputs (Xu-Friedman and Regehr, 2005). The effects of ANF loss might therefore be particularly pronounced post-synaptically where a reduction in the ANF population size would reduce this synchrony enhancement occurring for low-frequency tones (<1 kHz). This is consistent with the age-related FFR reductions at lower frequencies (<1 kHz) observed in the current study. Since the FFR reflects phase-locking at the brainstem level, FFR reductions at lower frequencies may thus be the consequence of ANF loss observed post-synaptically. Yet, the model framework used in the current study does not incorporate synaptic mechanisms that account for any synchronization enhancement, and including these may yield a better estimation of the effects of ANF loss on synchronous activity at the brainstem level.

2.5 Conclusion

The current study offers a peripheral account of FFR reductions in older listeners. Recent human temporal bone histopathology indicates that AN fibers are vulnerable to aging and that cochlear neural degeneration may precede hearing threshold loss and typically exceeds the loss of sensory cells (Wu et al., 2019; Wu et al., 2020). Bearing this in mind, we reasoned that older listeners with normal thresholds would, on average, have a higher degree of ANF loss compared to young normal-hearing listeners. Reduced FFRs in older listeners is consistent with a reduced number of ANFs contributing to the population synchronous response. FFR reductions were observed across stimulation frequency (200–1200

Hz), as would be expected from a reduction in the number of ANFs, whereas a centrally induced age-dependent reduction in temporal precision (Frisina, 2001) would be expected to reduce responses more at higher frequencies (Clinard and Cotter, 2015; Clinard et al., 2010). Yet, without more direct evidence about the AN status in our older normal-hearing subjects, we cannot rule out that age-related changes occurring in the central auditory system also contribute significantly to the reduced FFR. It remains uncertain how AN degeneration translates to more central stages where the scalp recorded FFR is generated, and evidence about how central stages adapt to neural degeneration in the auditory periphery is critically missing. Yet, if AN degeneration is indeed sensitive to the response synchrony represented by the FFR, as we propose, then the FFR may provide valuable diagnostic information .

Acknowledgments

This work was supported by the Novo Nordisk Foundation synergy grant NNF-17OC0027872 (UHeal) and a grant from the National Institutes of Health (P50 DC015857).

3

On the relationship between potential measures of age-related cochlear neuropathy in humans [c]

Abstract

Healthy aging is thought to cause auditory nerve (AN) degeneration, and may be associated with auditory processing deficits beyond what is captured by the clinical audiogram. Although it is assumed that AN damage can lead to suprathreshold hearing deficits, reliable and robust diagnostics are missing. Traditionally, the integrity of the AN is examined using transient evoked potentials measured using electroencephalography. More specifically, the first wave of the auditory brainstem response (ABR), also known as the compound action potential (CAP or AP), has been used both in animal studies and in human studies as indirect measures of peripheral neural integrity. However, the AP component of the scalp ABR relies on high-level stimulation, and is often difficult to acquire within a reasonable time frame in most clinical settings. It is known that the amplitude of the brainstem frequency-following responses (FFR) elicited by tones decreases with age. The source of this decrease may reflect upstream consequences of age-related cochlear degeneration. In recent modelling work, we proposed that age-related loss of AN fibers can explain a reduction in synchronized population activity, but further experimental support for a peripheral source of age-related FFR reductions is missing. If the age-related reduction in the brainstem FFR is predominantly driven by AN loss, the FFR

[c] This chapter is based on Märcher-Rørsted, J., Encina-Llamas, G., Fuglsang, S. A., Watson S.D., Sørensen C., Seibner H.R., Liberman, M.C., Dau, T. & Hjortkjær J., (In preparation). “On the relationship between potential measures of age-related cochlear neuropathy in humans."

may demonstrate clinical potential as a diagnostic of peripheral neural loss. Here, we recruited a large cohort of listeners, across a wide age-span (18 to 77 years of age), with normal to near-normal hearing ($\leq$ 20 dB hearing level (HL) up to 2 kHz). We measured suprathreshold (115 dB peak-to-peak equivalent sound pressure level (SPL)) click-evoked ABRs and FFRs to 250-ms low-frequency (326 Hz) tones presented at 85 dB SPL. Additionally, we measured extended high-frequency audiometric thresholds (from 8 to 16 kHz), as well as the middle-ear muscle reflex, self-reported hearing status (SSQ12) and estimated life-span accumulated noise exposure. Loudness perception was measured using an adaptive categorical loudness scaling test (ACALOS), and cognitive performance was assessed using a reverse digit-span test. We observed correlated age-related reductions in pure-tone FFR and ABR wave-I amplitude in listeners with relatively normal audiometric thresholds. Later waves of the click-evoked ABR, in particular the brainstem generated ABR wave-V, did not show a similar age-related reduction. Adding age to the AP component in a linear model of the FFR explained additional variance in the FFRs between subjects, indicating that other aspects of aging may still contribute partially to the age-related decline in the FFR.

3.1 Introduction

Hearing loss among older listeners is a common problem in society (Lin et al., 2011a), usually defined as a loss of sensitivity to high-frequency pure tones. The progressive age-related loss of sensory cells in the cochlea (i.e., loss of outer- and inner hair cells, OHC and IHC, respectively) is thought to be the primary cause for such loss. Hair-cell loss, particularly OHC loss, is well captured in the pure-tone audiogram (Ryan and Dallos, 1975). However, older adults often have suprathreshold speech-in-noise deficits, even when pure-tone sensitivity at standard audiometric frequencies is normal (Hind et al., 2011; Schaette and McAlpine, 2011). Increasing evidence suggests that other age-related deficits at the level of the cochlea may influence perceptual difficulties in aging listeners beyond what is captured by the audiogram. Recent human histopathology has suggested that healthy aging implies a progressive loss of auditory nerve

fibers (ANF) which may supersede the loss of sensory cells (Wu et al., 2019; Wu et al., 2020). Consistently, animal models of cochlear synaptopathy indicate that AN synapses may be among the cochlear structures that are most vulnerable to noise exposure and aging (Kujawa and Liberman, 2009). It is well known that even extensive damage to AN fibers leaves little impact on audiometric thresholds (Schuknecht and Woellner, 1955b), but may, in turn, influence suprathreshold processing (Chambers et al., 2016; Lobarinas et al., 2013).

It is known that the amplitude of the brainstem frequency-following response (FFR) elicited by pure tones decreases with age. It has been argued that the source of this decrease may be attributed age-related desynchronization in the central auditory system where the FFR is thought to be mainly generated (Anderson et al., 2012; Snyder and Schreiner, 1984; Walton, 2010), but it is possible that downstream consequences of age-related peripheral (i.e., cochlear) neural degeneration also contributes. In recent modelling work, we proposed that age-related loss of ANF can explain a reduction of synchronized population activity (Märcher-Rørsted et al., 2022), but further experimental support for a peripheral source of an age-related FFR reductions is missing. If the age-related reduction in the brainstem FFR is predominantly driven by AN loss, then the reduction should correlate with other, more direct, measures of AN function, such as wave-I of the auditory brain stem response (ABR), reflecting synchronous AN population activity. If the FFR and action potential (AP) measures are equally sufficient in quantifying age-related peripheral loss, the FFR presents a clinical potential as it is more readily acquired and may reflect aspects of temporal processing which the ABR cannot assess. On the contrary, it may be the case that age-related changes of more central (i.e., retro-cochlear) origin may be driving the decrease in the FFR such that the FFR is more readily explained by age than by peripheral activity. Here, we explored this relation.

The relationship between neural loss at the level of the cochlea and perception is still unclear. The loss of ANFs has traditionally been investigated using transient acoustic stimulation in combination with electrophysiology. In particular, the AP component of the ABR wave-I is usually interpreted as a measure of synchronous activity at the level of the AN (Møller et al., 1988). Although the amplitude of the AP has been used to verify the degeneration of ANFs in animal models (Kujawa and Liberman, 2009; Sergeyenko et al., 2013), it still remains unclear whether this measure is sensitive to cochlear neural loss in humans, and whether reductions in the AP potential may influence auditory

processing. Previous studies have indicated a relationship between speech-in-noise performance and the amplitude of the AP component related to noise exposure (Liberman et al., 2016) and aging (Grant et al., 2020). However, other studies have not found such relationships, especially in connection to measures of life-span accumulated noise-exposure (Grinn et al., 2017; Guest et al., 2017b; Le Prell, 2019; Prendergast et al., 2019). Thus, it remains unclear whether behavioral measures are sensitive to AN loss, or whether the quantification of such loss is fragile (Bramhall et al., 2019).

Although early potentials of transient evoked responses are usually missing or decreased in older listeners (Carcagno and Plack, 2020; Garrett and Verhulst, 2019), transient evoked synchronous activity in the auditory brainstem and midbrain (i.e., wave-V, Møller and Jannetta (1982) is usually unchanged or compensated with increasing age (Carcagno and Plack, 2020; Rumschlag et al., 2022). On the contrary, sustained responses believed to arise from the same generator as wave-V (i.e., the brainstem), are reduced with age, even when audiometric thresholds are normal (Clinard et al., 2010; Mamo et al., 2016; Presacco et al., 2019; Roque et al., 2019). This may suggest that transient evoked responses do not capture central temporal processing deficits, otherwise seen with more periodic and sustained stimuli, like the pure-tone FFR. This could imply that transient and periodic stimuli are processed differently in the auditory brainstem, and may be relevant in understanding the consequences of peripheral loss on central temporal processing.

The current investigation focused on physiological and electrophysiological outcome measures, and their interrelation with age, noise exposure, and each other. We investigated signs of cochlear aging in healthy aging listeners with clinically normal or near-normal hearing. We expected that suprathreshold ABR wave-I as a measure of AN integrity should decrease with age, even in older listeners with relatively normal clinical thresholds. Moreover, we investigated the relationship between age-related effects on the ABR and FFRs evoked by low-frequency high-intensity pure tones. The middle-ear muscle reflex and extended high-frequency audiometry was also measured as other potential proxies for AN integrity. As additional controls for noise-exposure, we used two questionnaires designed to probe the extent of accumulated noise exposure over lifespan (NESI) as well as a self-reported hearing status questionnaire (SSQ12).

3.2 Materials and Methods

3.2.1 Participants

One hundred and sixteen subjects participated in the study. The subjects were recruited based on audiometric profiles and age from a subject database, as well as from recruitment advertisements. To confirm pre-existing audiometric thresholds, all participants took part in an audiological evaluation on the day of experimentation. This included audiogram measurements using both ER-3 insert earphones at octave frequencies between 0.25 to 8 kHz and Sennheiser HDA200 earphones at extended high-frequencies at 9, 10, 11.25, 12, 14 and 16 kHz. Outer- and middle-ear function was evaluated with otoscopy and wide-band tympanometry. A general screening by means of standardized questionnaires was performed to exclude subjects who suffered from neurological conditions or severe chronic tinnitus.

To ensure that the entire age range ($\geq$ 18 years of age) was represented in our cohort, we recruited participants in three groups: young normal-hearing subjects (n = 33, 13 male, mean age 22.1 $\pm$ 2.38), middle-aged normal-hearing subjects (n = 57, 25 male, mean age 39.8 $\pm$ 11.72), and older normal-hearing subjects (n = 14, 6 male, mean age 67.7 $\pm$ 5.18). Listeners were considered normal hearing if their audiometric thresholds were $\leq$ 20 dB HL from 0.5-2 kHz and $\leq$ 40 dB HL at 4 kHz, similar to Carcagno and Plack (2020). Listeners with asymmetric audiometric thresholds over 20 dB at any frequency between 0.25 and 4kHz were excluded from the study. After audiometric evaluation, the better hearing ear was chosen as the test ear for the following procedures. Additionally, a group of older subjects with sloping hearing loss was also recruited (n = 12), but results from hearing-impaired subjects are not included here. All subjects provided written informed consent to participate. The experiment was approved by the Science Ethics Committee for the Capital region of Denmark (protocol H-16.036.391), and was conducted in accordance with the Declaration of Helsinki.

3.2.2 Clinical hearing profiles

Transient-evoked otoacoustic emissions (TEOAEs)

As a physiological indicator of OHC function, we measured transient-evoked otoacoustic emissions (TEOAE) to clicks using the Interacoustics Titan system

and standardized protocols. Non-linear clicks were presented at a peak-to-peak equivalent (ppe) sound pressure level (SPL) of 83 dB at a presentation rate of 80/s for 120 s (9600 sweeps). OAE responses to the clicks were evaluated from 4 - 12.5 ms succeeding each click presentation. Recorded responses which exceeded a 55 dB SPL noise-floor level were rejected from further analysis. Fourier-transformed epochs were divided into 1-kHz wide non-overlapping frequency bands with center frequencies from 1 to 5 kHz, resulting in 5 bands of equal bandwidth. TEOAEs were evaluated as the average sound power in each frequency band (dB SPL). Frequency-band averaged responses were considered significantly different from the noise floor if the TEOAE amplitude exceeded 6 dB signal-to-noise ratio (SNR). TEOAEs were measured in the test ear only.

Middle-ear muscle reflex

The middle-ear muscle reflex (MEMR) was measured to evaluate the status of the efferent neural feedback similar to Märcher-Rørsted et al. (2022) and Mepani et al. (2019). Click-noise-click sequences were presented to the test ear while measuring the ear canal sound pressure, before and after a 500-ms white noise elicitor (0.5-2 kHz) at levels of 75-105 dB SPL in steps of 5 dB. The probe click was presented at 100 dB ppeSPL. Growth-level functions were computed for each participant by taking the absolute value of the frequency response differences between the pre- and post-elicitor click responses, summed across all frequencies. A linear function was fitted to the growth of change of the absorbed power, and the linear coefficient of the linear fit from each subject was used in the statistical analysis. For 12 of the participants, it was not possible to correctly position the probe, resulting in missing data for these subjects.

Noise-exposure questionnaires

Exposure to controlled amounts of noise has been shown to produce significant amounts of cochlear synaptopathy in a variety of animal models (e.g., Furman et al. (2013), Kujawa and Liberman (2009), Lin et al. (2011b), Valero et al. (2017), and Valero et al. (2016)). However, the accumulated noise exposure across life is difficult to quantify in humans (Le Prell, 2019). Guest et al. (2017b) proposed the Noise Exposure Structured Interview (NESI) to quantify accumulated noise exposure. The NESI was included in the current assessment battery for reference. The interview identifies noisy events across the lifespan of each participant, in

either recreational and occupational settings. The accumulated noise-exposure scores were summed across the two types, yielding one measure of accumulated noise-exposure for each participant.

Have you ever experienced: Temporary change in hearing (dullness or muffled sound) after noise exposure?	
1.	Never
2.	Once in my lifetime
3.	A few times in my lifetime
4.	Several times a year
5.	Several times a month
6.	Several times a week
7.	Several times a day

Table 3.1: Temporary threshold shift (TTS) frequency questionnaire.

Additionally, a questionnaire addressing experienced temporary threshold shifts (TTS) and the frequency of such events across life was answered by the participants. The questionnaire was adapted by Brungart et al. (2019) and can be seen in table 3.1.

Self-reported hearing status questionnaire (SSQ12)

As a measure of self-reported hearing status, we measured the 12-question version of the Speech, Spatial and Qualities of hearing questionnaire (SSQ12; Gatehouse and Noble (2004) and Noble et al. (2013)). The questions address listeners' listening difficulties in everyday acoustic environments, and are designed to identify self-reported listening difficulties in specific realistic conditions concerning speech understanding, spatial separation abilities, and the perceived quality of acoustic stimuli. The 12 questions are divided into pragmatic sub-scales including speech in noise, speech in speech, multiple speech streams, localization, distance and movement segregation, identification of a sound, quality and naturalness, and listening effort. Participants are asked to rate a given situation on a scale from 1-10, 10 indicating that the participant is perfectly able to do or experience what is described in the question, and 0 indicating that the participant is unable to do or experience the described situation.

Digit span

The participants performed a reversed digit span test as a measure of working memory capacity. The listeners were asked to recall sequences of single digit numbers between 1 and 9 and report the sequence in reverse order. On subsequent trials, the listeners were presented with sequences of an increasing number of digits (2, 3, 4, ..., 8). The digit span score was then calculated by summing the number of digits which could be remembered in the correct order for a given trial (Blackburn and Benton, 1957). Digit stimuli were presented via Sennheiser HD650 headphones at a self-adjusted comfortable level.

Adaptive Categorical Loudness Scaling (ACALOS)

We measured loudness perception using adaptive categorical loudness scaling (ACALOS, Brand and Hohmann (2002)). Here, the participants were asked to rate the perceived loudness of a series of noise bursts on an 11 category perceptual scale ranging from *not heard* to *extremely loud*. The stimuli consisted of 500-ms, 1/3-octave band noises with center frequencies of 0.5, 1, 2 , and 4 kHz, presented at levels ranging from -5 to 105 dB SPL. The presentation level was determined adaptively based on previous responses. Noise stimuli were presented to the test ear only using Sennheiser HD650 headphones. Loudness perception curves were fit between categorical units (CU) and the presentation level (dB SPL), as described in Oetting et al. (2014). The fitted loudness model was then decomposed into two outcome metrics including the most comfortable level (MCL) and the slope of the loudness function.

3.2.3 Electrophysiology

Data acquisition

Electroencephalography (EEG) data were continuously recorded using the BioSemi ActiveTwo system. We recorded scalp EEG from 18 channels positioned in frontal and temporal regions of the scalp (CMS, DRL, Fp1, F3, AFz, Fz T7, C3, FC3, C4, Cz, FCz, T8, F4, Fp2, FC4, P9 and P10) using a custom EEG-cap. Additionally, EEG was recorded from gold-foil tiptrode electrodes inside the left and right ear canals. EEG recordings were digitized at 16384 Hz. The acoustic stimuli presented during the EEG experiments were presented via electromagnetically shielded (custom made) ER-3 insert earphones (Etymotic Reseach) to

the test ear. Prior to the EEG recordings, the participants were made familiar with the consequences of muscle artefacts on the quality of the recordings, and their continuous EEG time-series was shown to them in real time. Demo stimuli were presented to the participants to ensure that all stimuli and levels were comfortable. To ensure optimal positioning of the tiptrodes and the sound delivery system, otoscopy was preformed before the insertion. No further preparation of the ear canals was performed. The participants were asked to lie down on a bed in a double-walled acoustically and electromagnetically shielded booth. The participants were asked to relax and keep their eyes closed during the acoustic stimulation and EEG recording.

Auditory brainstem responses, ABR

Transient-evoked ABRs were measured using 100-μs clicks, presented at 80 dB normal hearing level (nHL) (115.5 dB ppeSPL) at presentation rate of 9 Hz. To discriminate the AP component from the earlier pre-synaptic summating potential (SP), we also measured click responses to a 40-Hz presentation rate. Compared to responses obtained with 9 Hz presentation rate, click responses at 40 Hz should reduce the AP more than the SP due to adaptation in the neural components (Grant et al., 2020; Kiang, 1965; Liberman et al., 2016). The clicks were calibrated by first adjusting a 1-kHz tone to 115.5 dB SPL. The peak-to-peak voltage (ppV) was noted on a digital oscilloscope (RET SPL, ISO389-6. 2007). The click stimuli were then adjusted in level, ensuring that the noted ppV of the click stimuli was equivalent to that of the 1-kHz tone. The calibration was preformed for both polarities. The clicks were presented with alternating polarity, including a jitter of ± 3 ms for both presentation rates. In total, the participants were presented with 3000 clicks in each polarity and for each rate (12000 in total). Continuous EEG recordings were segmented into 30-ms trials (from 10 ms preceding the onset of each click presentation to 20 ms after). Line noise (50 Hz) was removed using a comb notch filter centered around 50 Hz and the two first harmonics (100 Hz and 150 Hz). The data were bandpass filtered between 0.1 to 3 kHz, demeaned, and re-referenced to three central-frontal midline electrodes (Cz, FCz, Fz). ABR waveforms were evaluated as the electrical potential from the ipsi-lateral tiptrode to the average of the three scalp reference electrodes.

The analysis of the ABR waveforms was performed as follows. First, all click presentations were examined for artefacts, rejecting any epochs containing

EEG activity exceeding ± 20 mV. On average, 0.32% ± 0.52 % of the trials were rejected in the 9-Hz condition, and 0.56 % ± 1.31 % in the 40-Hz condition. For five of the participants, it was not possible to collect click-evoked responses due to technical difficulties during the recordings. For additional nine subjects, the 40-Hz condition was not recorded. Clean trials from the remaining participants were then weighted by the inverse of their variance and averaged (see John et al., 2001) for each individual subject.

Time-domain responses were corrected for sound-delivery and tube delay (-1.1 ms). Individually-averaged waveforms were baseline corrected by the mean response at the delay-corrected $t = 0$ point for both presentation-rate conditions (9- and 40-Hz). All averaged waveform were then visually inspected. Responses that were clearly contaminated by stimulus artefacts or abnormalities after visual inspection were excluded from further analysis. This was the case for 14 participants, leaving 92 participants with valid ABR data for further analysis.

In the ABR waveform, peak amplitudes and latencies corresponding to wave-I, SP and AP, as well as wave-V were identified by manual peak picking according to established guidelines (Stevens et al., 2013; Sutton, 2008).

Frequency-following responses, FFRs

Pure-tone FFRs, originating in the rostal-brainstem, have been shown to reduce with age, and may be sensitive to peripheral neural degeneration (Märcher-Rørsted et al., 2022). To obtain FFRs, participants listened to sequences of 250-ms long 326-Hz pure tones. The tones were presented at a rate of 2/s (250-ms stimulation, 250-ms silence) for six consecutive presentations, followed by 500 ms of silence. The tone bursts were ramped using 10-ms long sinusoidal onset/offset ramps, and presented at 85 dB SPL to the test ear only. In total, the participants listened to 486 tone presentations for each onset polarity of the stimulus. The polarity was kept constant in each condition (e.g. not true alternating).

The data were bandpass filtered from 80 Hz to 3 kHz, and re-referenced to the ipsi-lateral tiptrode. Continuous recordings were segmented into trials of 600 ms (from 100 ms preceding the onset of each tone-burst to 500 ms after), and re-sampled to 4096 Hz. Negative and positive polarity trials were subtracted from each other to eliminate phase-independent components in the response ((C-R)/2) (Kraus and Skoe, 2010; Krishnan, 2006)). Polarity-subtracted trials exceeding 25 mV were rejected. Clean trials were then weighted by the inverse

of their variance and averaged. The FFR magnitudes were evaluated in the frequency domain. The spectral magnitude of the carrier frequency (326 Hz) was first identified and then compared to the surrounding noise floor (± 20 Hz). The SNR was calculated by taking the power of the target magnitude bin, and dividing it by the average of the surrounding frequency bins. Modulation sidebands evoked from the 2-Hz presentation rate, and corresponding harmonics (± 2 Hz to 10 Hz, in steps of 2 Hz), were excluded from the noise-floor calculation. We then calculated the probability of the FFR power being different from the surrounding noise floor using an F-statistic test (Dobie and Wilson, 1996). FFR measurements were considered significantly different from noise if $p \leq 0.01$ (1 %). Non-significant responses were excluded from the statistical analysis.

Envelope-following responses, EFRs

EEG responses were also obtained for 300-ms long amplitude modulated (120 Hz) band limited noise (0.5 -2 kHz) presented at different inter-stimulus-intervals (ISI). This stimulation allowed for the examination of the envelope-following response (EFR) to the 120-Hz modulation, as well as the analysis of the cortical evoked potentials to the onset of the noise burst as a function of ISI (not analyzed in the current study). The noise bursts were presented at four discrete ISIs: 0.5, 1, 1.5 and 2 s. ISIs were varied by first presenting six consecutive 2-s ISIs, before proceeding to the next ISI (1.5 s). This was repeated until the ISI reached the lowest value (0.5 s). The ISI was then increased in a stepwise fashion, creating sweep-like ISI stimulus blocks of 48 trials. In total, the listeners were presented with 144 trials for each ISI. The noise stimuli were presented at 75 dB SPL. EFRs to the modulation frequency were extracted for each ISI condition for all participants, resulting in 576 trials per subject.

The continuous data were first bandpass filtered from 80 Hz to 2 kHz, resampled to 8192 Hz and re-referenced to the average of the two mastoid channels (P9 and P10). The recordings were then segmented into trials of 700 ms, from 100 ms preceding the onset of each noise-burst to 600 ms after the noise burst. Pre-processed trials were then subjected to artefact rejection, rejecting any trials exceeding 25 mV between 0 to 500 ms. The clean trials were weighted by their inverse variance and averaged. Spectral EFR magnitudes to the modulation rate of the stimulus (120 Hz) were then identified and compared to the surrounding noise floor, similar to the analysis for pure-tone FFRs. Modulation sidebands corresponding to the fastest ISI (0.5 ms, 2 Hz) and respective

harmonics (± 2 Hz to 10 Hz, in steps of 2 Hz) were not considered to be part of the noise floor. We then computed a SNR metric for each participant, which served as an outcome measure for further statistical analysis. The responses that were not significantly different from the surrounding noise floor (F-test) were excluded from further analysis.

3.2.4 Statistical analysis

The statistical analyses were performed in R (RStudio Team, 2020). Previous studies suggest that electrophysiological measures can be influenced by sex, documenting larger response amplitudes and shorter latencies for female participants (Don et al., 1993, 1994). To examine isolated effects of age, we fitted a linear model to each outcome measure separately, including both age and sex as predictors. Resulting p-values were corrected for multiple comparisons using the False Discovery Rate (FDR) procedure (Benjamini and Hochberg, 1995). Relationships between subjective noise-exposure questionnaire scores as well as self-reported hearing status were also compared to AP amplitudes using linear regression.

To further explore the relationship between the FFR and peripheral neural loss, we used a step-wise linear regression and model selection approach. In short, a linear model was fit using low-frequency and high-frequency pure-tone average audiometric values, AP amplitudes, age and sex. The step-wise model search then sought to optimize the Akaike information criteria (AIC) to find the model which best explained the variance seen in the FFR data.

3.3 Results

3.3.1 Hearing thresholds and OAEs

We recruited listeners across a large age range (18-77 years of age) to have normal hearing as defined by their audiometric thresholds below 4 kHz. One hundred and four participants passed the criteria set for audiometric thresholds. Their hearing threshold functions are shown in figure 3.1 A). Figure 3.1 B) shows the age distribution per decade for male (gray) and female (red) participants.

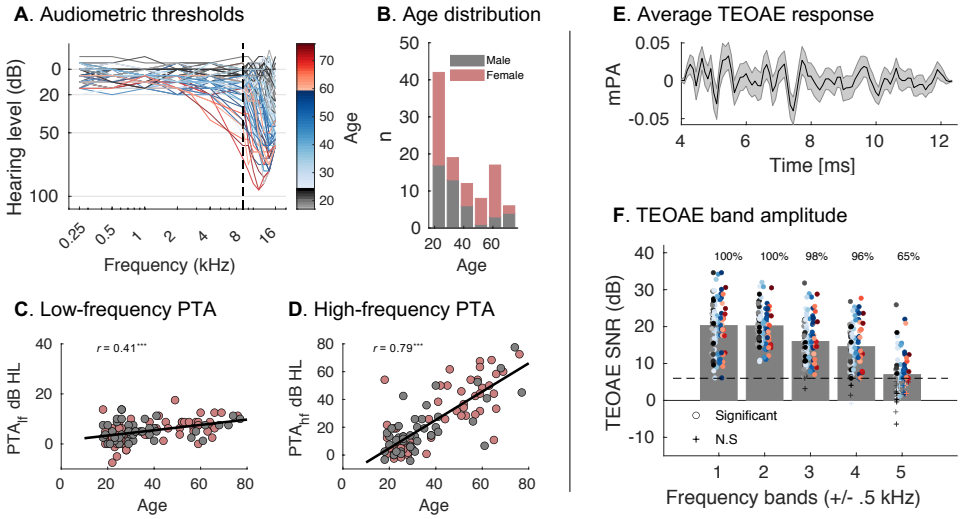

Figure 3.1: **A**) Audiometric thresholds of the test ear for all participants from 0.25 to 16 kHz. **B**) Age distribution of participants grouped by sex. Histogram blocks represent age decades. **C**) Low frequency pure-tone threshold averages (0.25 to 2 kHz) as a function of age for female (red) and male (gray) participants. **D**) High frequency pure-tone thresholds averages (9 to 16 kHz) as a function of age. **E**) Average TEOAE response across all participants. **F**) Frequency band TEOAE SNR in bands from 1 to 5 (± 500 Hz). Significant OAEs are represented as dots and non-significant responses are marked with a cross. The age of the participant is labeled according to the color bar in **A**. The dashed line indicates the significance threshold (≥ 6 dB SNR). Color indicates age according to the color bar in panel **A**. The percentage of significant responses is indicated for each band. Error bars show SEM. $\star = p < 0.05, \star\star = p < 0.01, \star\star\star = p < 0.001$.

Despite older subjects having relatively normal audiometric thresholds at lower frequencies (figure 3.1 A), thresholds at extended higher frequencies are distinctly elevated. Average high-frequency thresholds (mean threshold from 9 to 16 kHz, $\mathrm{PTA_{HF}}$) were strongly correlated with age ($t(2,101) = 12.6, p < 0.001$, figure 3.1 D)). While the participants were recruited to have normal low-frequency thresholds (≤ 20 dB HL up to 4 kHz), we also found low-frequency thresholds to be correlated with age ($\mathrm{PTA_{LF}}$, $t(2,101) = 4.708$, $p < 0.001$, figure 3.1C).

	df	Est.	SE	t	p		p corr.	
PTA_{LF}								
Age	(2,101)	0.109	0.023	4.708	**8.00e-06**	***	**6.40e-05**	***
Sex		0.777	0.788	0.986	0.326		0.560	
PTA_{HF}								
Age	(2,101)	1.017	0.081	12.60	**1.91e-22**	***	**4.59e-21**	***
Sex		-0.296	2.734	-0.108	0.914		0.924	

Table 3.2: Statistical results from multiple linear model regressions on low- and high-frequency audiogram metrics (PTA_{LF} and PTA_{HF}) as predicted by age and sex. The p corr. coloum represents the p-value after Benjamini-Hochberg correction for multiple comparisons. $\star = p<0.05$, $\star\star = p<0.01$, $\star\star\star = p<0.001$

	$TEOAE_{SNR}$				
	df	Est.	SE	t	p	p corr.
1 kHz						
Age	(2,101)	0.006	0.040	0.158	0.875	0.972
Sex		2.470	1.355	1.822	0.071	0.285
2 kHz						
Age	(2,101)	0.046	0.027	1.691	0.094	0.225
Sex		0.503	0.921	0.547	0.586	0.827
3 kHz						
Age	(2,99)	-0.019	0.033	-0.564	0.574	0.725
Sex		-0.159	1.132	-0.140	0.889	0.924
4 kHz						
Age	(2,97)	-0.021	0.032	-0.637	0.526	0.701
Sex		-0.630	1.083	-0.581	0.562	0.827
5 kHz						
Age	(2,65)	-0.004	0.035	-0.104	0.918	0.972
Sex		-1.950	1.212	-1.609	0.112	0.385

Table 3.3: Statistical results from multiple linear model regressions on $TEOAE_{SNR}$ at 5 frequencies as predicted by age and sex. The p corr. coloum represents the p-value after Benjamini-Hochberg correction for multiple comparisons. $\star = p<0.05$, $\star\star = p<0.01$, $\star\star\star = p<0.001$

Click-evoked TEOAEs were also measured as an objective correlate of OHC function, the main determinant of threshold sensitivity. Figure 3.1 E) shows the average TEOAE response from 4 to 12.5 ms after the click stimulus. The Fourier transform of the time-domain responses was calculated for each participant, and the frequency-domain power was averaged in 1-kHz wide frequency bands from 1 to 5 kHz. Figure 3.1 F) shows the average SNR for the five frequency bands. When excluding non-significant responses, we found no correlation between age and each frequency band (1 kHz: $t(2,101) = 0.158, p = 0.972$; 2 kHz: $t(2,101) = 1.691, p = 0.225$; 3 kHz: $t(2,99) = -0.564, p = 0.725$; 4 kHz: $t(2,97) =$

0.526, $p = 0.701$; 5 kHz: $t(2,65) = -0.104$, $p = 0.972$, corrected). When including non-significant responses, we observed a negative correlation between the $\text{TEOAE}_{\text{SNR}}$ for the highest frequency band and age (5 kHz, $t(2,101) = -2.551$, $p = 0.0279$, corrected), consistent with elevated audiometric thresholds at high frequencies for older listeners.

3.3.2 Clinical profiles

Figure 3.2 A) shows the results from the backwards digit-span test for all participants. Digit-span scores were significantly correlated with age ($t(2,98) = -2.73$, $p = 0.029$), suggesting a lower cognitive performance for the older participants. Figure 3.2 B) shows results from the two noise exposure questionnaires. We found no effect of age on either of the questionnaires (NESI: $t(2,98) = 0.087$, $p = 0.972$, TTS: $t(2,98) = 1.112$, $p = 0.461$). Figure 3.2 C) shows SSQ-12 scores, averaged over the 12 questions for each participant, as a function of age. We found no effect of age on SSQ-12 scores either ($t(2,100) = 1.608$, $p = 0.242$).

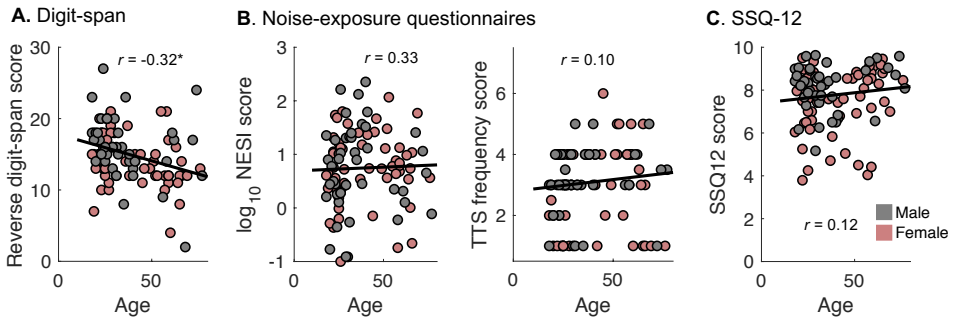

Figure 3.2: **A**) Backwards digitspan score as a function of age. **B**) Noise exposure scores from the NESI- and TTS frequency questionnaire as a function of age. **C**) Averaged SSQ-12 score as a function of age. $\star = p < 0.05, \star\star = p < 0.01, \star\star\star = p < 0.001$.

3.3.3 ACALOS

We measured the perceived loudness of four different band-limited noise stimuli using the ACALOS test. Figure 3.3 shows grand-average response functions for the band-limited noise stimuli with center frequencies of 500 Hz, 1 kHz, 2 kHz and 4 kHz (left panel), as well as the slope for each of the conditions as a function of age (right panels). We found no correlation between the age of the participants and the slope of the loudness perception curves for any of the

stimuli (500 Hz: $t(2,99) = 0.828, p = 0.655$; 1 kHz, $t(2,99) = 0.649, p = 0.701$; 2 kHz: $t(2,99) = 0.665, p = 0.701$; 4 kHz: $t(2,99) = 1.872, p = 0.193$).

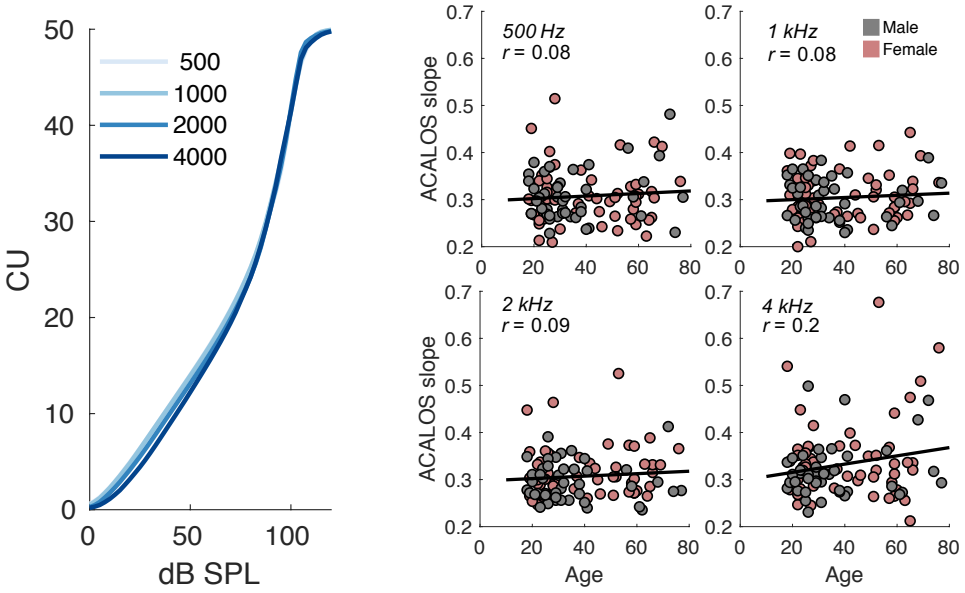

Figure 3.3: Grand average loudness perception curves from the ACALOS test. The y-axis represents catagorical units (CU) in relation to the physical sound pressure level (left panel). The legend indicates the center frequency in Hz of the band-limited noise stimulus. The right panel shows correlation scatter plots between the slope of the ACALOS function and the age of the participant. $\star = p < 0.05, \star\star = p < 0.01, \star\star\star = p < 0.001$.

3.3.4 MEMRs

Age-related reductions of the MEMR have been argued to reflect a degeneration of low spontaneous-rate fibers in the AN, and the strength of the MEMR may therefore potentially represent a proxy for the amount of functioning nerve fibers (Bharadwaj et al., 2019, 2021; Valero et al., 2016). Here, we measured MEMRs as the change in ear-canal sound pressure after presentation of a wide-band noise elicitor at levels ranging from 75 to 105 dB SPL. Larger responses indicate a larger change in the absorbed sound power induced by the stiffening of the tympanic membrane, and thereby a larger MEMR activation. Figure 3.4 A) shows the grand average MEMR as a function of frequency (left), and the resulting summed absolute change in absorbance as a function of level, averaged across frequency (right). Figure 3.4 B) shows the slope of the MEMR growth curve for each participant as a function of age. Male and female participants are

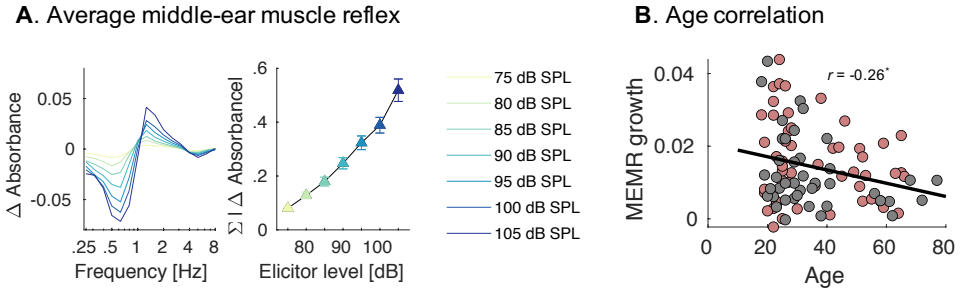

Figure 3.4: **A**) Left panel shows average middle-ear muscle reflex responses (MEMRs) across all participants. Responses are plotted according to elicitor level. Right panel shows the average sum of change in absorbance as a function of elicitor level. **B**) MEMR growth (fitted linear coefficients) as a function of age for female (red) and male (gray) participants. Error bars show SEM. $\star = p < 0.05, \star\star = p < 0.01, \star\star\star = p < 0.001$.

indicated as gray and red symbols, respectively. We observed a main effect of age on the MEMR growth ($t(2,91) = -2.692, p = 0.029$), suggesting a more shallow MEMR growth-function with increasing age and consistent with previous results (Märcher-Rørsted et al., 2022). Although age was significantly correlated with MEMR growth, a large spread among the younger participants was observed. Since the MEMR is thought to be sensitive to a noise-induced loss of low spontaneous-rate fibers (Bharadwaj et al., 2019), lower MEMRs may reflect accumulated noise exposure among younger participants. However, for the young participants (18-30 years of age), no significant correlation could be observed between the MEMR growth and the noise exposure questionnaire scores (Pearson's correlation, NESI, $r = -0.02, p = 0.9116$; TTS, $r = 0.012, p = 0.9363$).

	df	Est.	SE	t	p		p corr.	
MEMR								
Age	(2,91)	0.000	0.000	-2.692	**0.008**	**	**0.029**	*
Sex		-0.003	0.002	-1.484	0.141		0.343	

Table 3.4: Statistical results from multiple linear model regressions MEMR growth as predicted by age and sex. The p corr. coloum represents the p-value after Benjamini-Hochberg correction for multiple comparisons. $\star = p<0.05$, $\star\star = p<0.01$, $\star\star\star = p<0.001$

3.3.5 ABRs

Figure 3.5 A) shows the measured grand-average ABRs to clicks presented at 9 Hz (grey) and 40 Hz (blue). Traditional response peaks (SP, AP and wave V) were identified in terms of their amplitude and latency in the 9-Hz condition. The

SP was characterized as the first positive peak after the onset of the stimulus. On average, the SP component was identified at a latency of 0.81 ms ± 0.23 ms. Following the SP, the AP component occurs, typically producing much

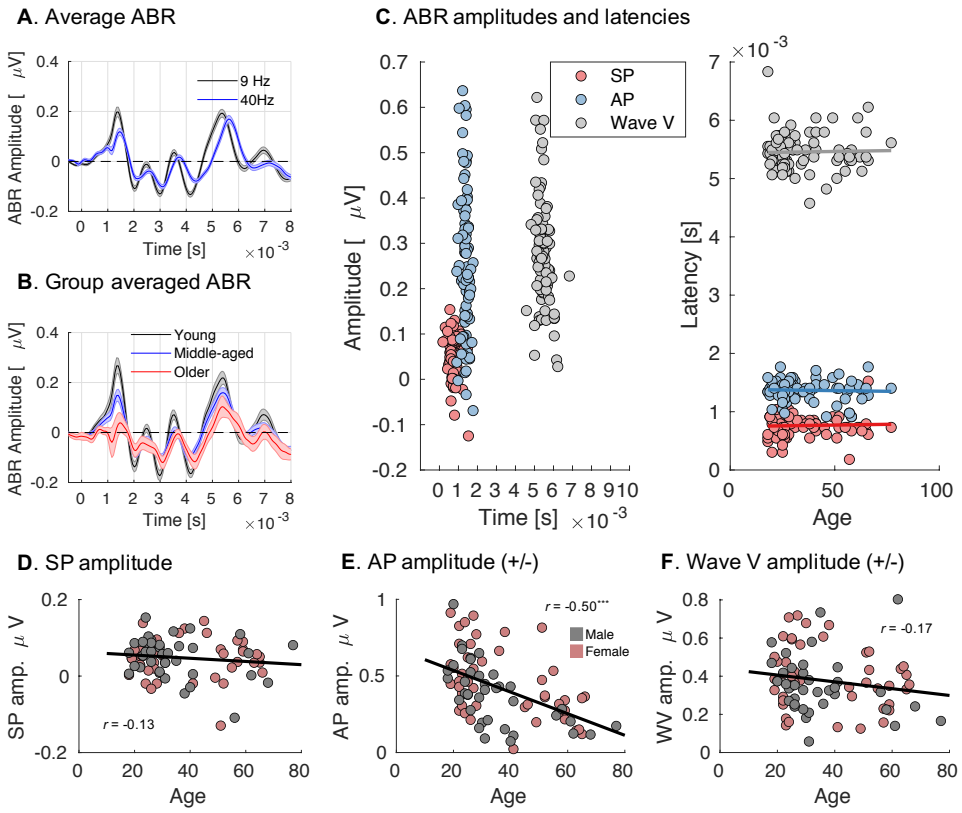

Figure 3.5: **A**) Average click-evoked ABR for 9-Hz (black) and 40-Hz (blue) presentation rates. **B**) Group averaged ABR for young (black, age ≤ 25, $n = 31$), middle-aged (blue, 25 < age > 60, $n = 52$), and older listeners (red, age ≥ 60, $n = 15$). **C**) The left panel shows quantified SP (red), AP (blue) and wave-V (gray) amplitudes as a function of latency. The right panel shows latencies of the three peaks as a function of age. **D**) SP amplitude as a function of age for female and male participants. **E**) AP amplitude (peak-to-trough) as a function of age. **F**) Wave-V amplitude (peak-to-trough) as a function of age. Error bars show SEM. $\star = p < 0.05, \star\star = p < 0.01, \star\star\star = p < 0.001$.

higher amplitudes. It has been shown that the first two components of the ABR (i.e., SP and AP) are differently affected by stimulation rate (Liberman et al., 2016). As the SP is considered to be mainly pre-synaptic (i.e., generated by the hair-cells), neural adaptation should not contribute to this component, and the increase in presentation rate should mainly reduce the AP. Accordingly, the AP component was identified by comparing the 9-Hz and 40-Hz traces, and defining the first positive peak after the SP component. The AP component

was, on average, identified at a latency of 1.4 ms ± 0.18 ms. For peak-to-trough identification, the first negative deflection following the AP component was also identified. Lastly, ABR wave-V was identified as the fifth peak following the AP component, occurring, on average, at a latency of 5.45 ms ± 0.23 ms. As for the AP component, the first negative deflection was also identified.

	df	Est.	SE	t	p		p corr.	
SP								
Amplitude								
Age	(2,82)	0.000	0.000	-1.178	0.242		0.450	
Sex		0.001	0.011	0.096	0.924		0.924	
Latency								
Age	(2,82)	0.000	0.000	-0.135	0.893		0.972	
Sex		0.000	0.000	-0.294	0.769		0.924	
AP								
Amplitude								
Age	(2,82)	-0.007	0.001	-5.672	**2.11e-07**	***	**2.53e-06**	***
Sex		-0.096	0.040	-2.379	**0.020**	*	0.127	
Latency								
Age	(2,82)	0.000	0.000	-1.174	0.244		0.450	
Sex		0.000	0.000	0.108	0.914		0.924	
Wave-V								
Amplitude								
Age	(2,82)	-0.002	0.001	-1.786	0.078		0.207	
Sex		-0.049	0.034	-1.454	0.150		0.400	
Latency								
Age	(2,82)	0.000	0.000	-0.011	0.991		0.991	
Sex		0.000	0.000	2.351	**0.021**	*	0.127	

Table 3.5: Statistical results from multiple linear model regressions on ABR outcome measures as predicted by age and sex. The p corr. coloum represents the p-value after Benjamini-Hochberg correction for multiple comparisons. $\star = p<0.05$, $\star\star = p<0.01$, $\star\star\star = p<0.001$

Figure 3.5 B) shows the group-averaged ABRs for young (≤ 25 years), middle-aged (between 26 and 59 years) and older (≥ 60) participants. The quantified peak amplitudes and latencies are shown in figure 3.5 C). The correlation of the SP amplitude, AP peak-to-trough amplitude, and wave-V peak-to-trough amplitude with age are illustrated in the scatter plots in figure 3.5 D), E) and F), respectively. A significant negative correlation between age and AP amplitudes was observed ($t(2,81) = -5.672, p < 0.001$), indicating lower AP amplitudes with increasing age. Interestingly, we found no correlation between age and either the SP component ($t(2,82) = -1.178, p = 0.450$) nor wave-V amplitude ($t(2,81) = -1.786, p = 0.207$). We also found no correlation between age and

latency for any of the three components (SP, $t(2,82) = -0.135, p = 0.972$; AP, $t(2,82) = -1.173, p = 0.450$; Wave-V, $t(2,82) = -0.010, p = 0.991$). The results are summarized in table 3.5.

3.3.6 Sustained responses

Pure-tone FFRs

Figure 3.6 A) shows topographic maps of the SNR of the FFR (FFR_{SNR}) component to the low-frequency (326 Hz) pure tones, interpolated across the 16 scalp EEG channels. The broad excitation pattern seen in the topographic maps suggests sub-cortical or peripheral sources (i.e., non-cortical). The response SNR decreases with increasing age group. Since all channels seemed to be correlated, we conducted a further analysis on the vertex electrode (Cz), typically used in FFR studies. Figure 3.6 B) shows group-averaged time-domain responses to the stimulus (250 ms) for young, middle-aged and older participants at Cz. A clear response phase-locked to the stimulus frequency (first 250 ms) can be seen for all age groups, followed by EEG noise during the silent period (last 250 ms).

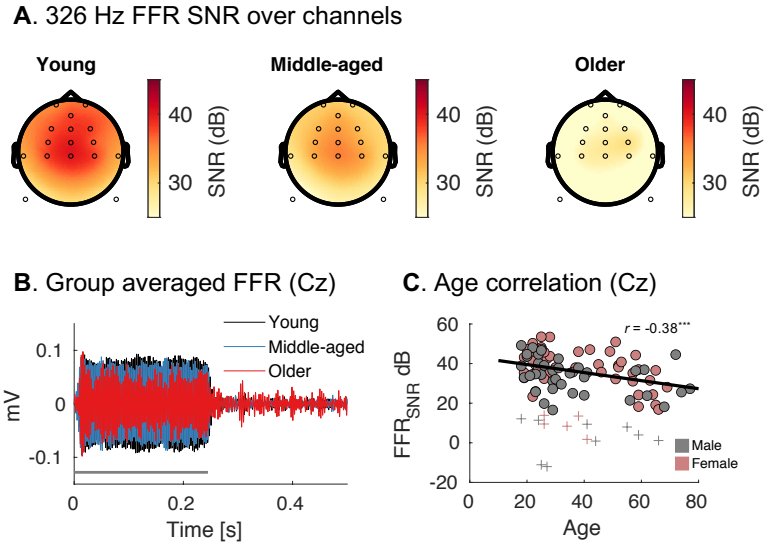

Figure 3.6: **A**) SNR of the 326 Hz component over 16 scalp electrodes for young (black, age ≤ 25, $n = 31$), middle-aged (blue, $25 <$ age > 60, $n = 52$) and older participants (red, age ≥ 60, $n = 15$). **B**) shows time-domain FFR averages over young, middle-aged and older listeners at Cz. The solid line indicates the stimulation period (250 ms) **C**) FFR_{SNR} at Cz as a function age for male (gray) and female (red). Responses which were not significantly different from the surrounding noise floor are marked by +. Error bars show SEM. $\star = p < 0.05, \star\star = p < 0.01, \star\star\star = p < 0.001$.

Figure 3.6 C) shows the 326 Hz FFR_{SNR} as a function of age for the male (black) and the female (red) participants. Non-significant responses are indicated as crosses. We found a significant negative correlation with age ($t(2,82) = -4.123, p < 0.001$), suggesting a lower SNR with increasing age, consistent with previous studies (Clinard and Cotter, 2015; Märcher-Rørsted et al., 2022; Marmel et al., 2013). It is possible that age affects the overall noise level of the recordings. To investigate this, we correlated the extracted noise level used for SNR analysis with the age of the participants. No significant correlation between age and the noise level of the recordings was found ($r = 0.17, p = 0.1008$).

Envelope-following responses

EFR magnitudes have been associated to AN degeneration both in animal studies (Lai et al., 2017; Parthasarathy et al., 2010; Parthasarathy and Kujawa, 2018; Parthasarathy et al., 2016; Shaheen et al., 2015) and human studies (Bharadwaj et al., 2015; Bramhall et al., 2021; Encina-Llamas et al., 2019). Figure 3.7 A) shows the grand-average EEG time-series in response to the 120 Hz amplitude modulated noise at scalp electrode Cz. The stimulation period of the noise burst is indicated by the horizontal black line. Figure 3.7 B) shows the SNR of the

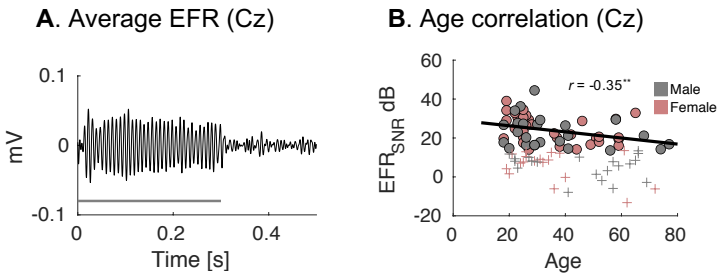

Figure 3.7: **A**) Average 120 Hz EFR over all significant responses at Cz. Solid line indicates stimulation period (300 ms). **B**) EFR SNR (dB) for male (gray) and female (red) participants. Non-significant responses are indicated by crosses. $\star = p < 0.05, \star\star = p < 0.01, \star\star\star = p < 0.001$.

EFR (EFR_{SNR}) for male (gray) and the female (red) participants. Non-significant responses are indicated by crosses. We found a significant correlation between the age of the participant and the EFR_{SNR} using only significant responses ($t(2,57) = -2.767, p = 0.023$), suggesting a lower SNR with increasing age. We observed that the amount of non-significant responses was higher in the EFR results than for the FFR measurement. This is most likely due to the difference in level (FFR: 85 dB SPL, EFR: 75 dB SPL), and the fact that we only considered

single-polarity recordings and fewer trials in the EFR measurements (FFR: 486 in both polarities, EFR: 576 in total). Despite these discrepancies, we sought to investigate whether the two measurements were similar across stimuli. We correlated EFR_{SNR} with FFR_{SNR} for all participants. We found no significant correlation between the two measures ($r = 0.23, p = 0.09$), also when including the non-significant responses ($r = 0.13, p = 0.20$).

	df	Est.	SE	t	p		p corr.	
FFR								
Age	(2,82)	-0.217	0.053	-4.123	**8.90e-05**	***	**5.34e-04**	***
Sex		-4.516	1.775	-2.544	**0.013**	*	0.127	
EFR								
Age	(2,57)	-0.155	0.056	-2.767	**0.008**	**	**0.029**	*
Sex		-1.594	1.767	-0.902	0.371		0.593	

Table 3.6: Statistical results from multiple linear model regressions on FFR and EFR outcome measures as predicted by age and sex. The p corr. coloum represents the p-value after Benjamini-Hochberg correction for multiple comparisons. $\star = p<0.05$, $\star\star = p<0.01$, $\star\star\star = p<0.001$

3.3.7 Predictors of the AP amplitude

We sought to investigate whether subjective noise-exposure questionnaires as well as subjective evaluation of hearing status of the participants could explain the observed variance in the AP amplitude. Additionally, physiological measures attributed to be influenced by peripheral loss (e.g., MEMR growth, FFR_{SNR} and EFR_{SNR}) were used to predict AP amplitudes. Figure 3.8 A) shows correlation scatter plots between the noise-exposure questionnaire scores (NESI and TTS) as a function of the AP amplitude. We observed that the TTS scores were significantly correlated with the AP amplitudes ($t(1,79) = -2.413, p = 0.036$), suggesting that higher TTS scores were related to lower AP amplitudes. In contrast, NESI scores were not correlated with AP amplitudes($t(1,79) = 0.372, p = 0.710$).

Figure 3.8 B) shows a correlation scatter plot between the subjective hearing status scores from the SSQ12 questionnaire and the AP amplitudes. Here, we did not find any relationship between mean SSQ12 scores and the amplitude of AP ($t(1,81) = -0.945, p = 0.428$).

Figure 3.8 C) shows correlation scatter plots for MEMR growth, FFR_{SNR} and EFR_{SNR} as a function of AP amplitude. We found that a lower MEMR growth was related to lower AP amplitudes ($t(1,78) = 2.512, p = 0.036$). Furthermore, lower SNRs of the FFR were also related to lower AP amplitudes ($t(1,72) = 3.883, p =$

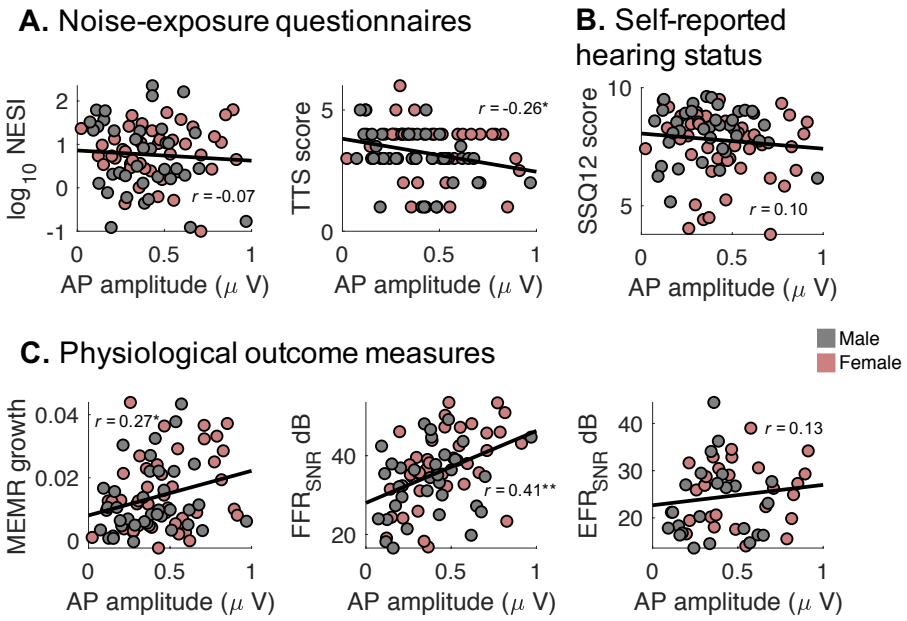

Figure 3.8: **A**)Scatter plot of NESI and TTS scores as a function of AP amplitude. **B**) Scatter plot of self-reported hearing status (SSQ12 scores) as a function of AP amplitude. **C**) Scatter plot of MEMR growth (left), FFR_{SNR} (middle) and EFR_{SNR} (right) as a function of AP amplitude. $\star = p < 0.05, \star\star = p < 0.01, \star\star\star = p < 0.001$.

0.0013). In contrast, the SNR of the EFR was not significantly related to the amplitude of the AP ($t(1,49) = 0.930, p = 0.428$).

	df	Est	SE	t	p		p corr.	
TTS	(1,79)	-1.360	0.564	-2.413	**0.018**	*	**0.036**	*
NESI	(1,79)	6.790	18.194	0.373	0.710		0.710	
SSQ12	(1,81)	-0.642	0.679	-0.945	0.347		0.428	
MEMR	(1,78)	0.014	0.006	2.512	**0.014**	*	**0.036**	*
FFR_{SNR}	(1,72)	18.291	4.711	3.883	**2.27e-4**	***	**1.36e-3**	**
EFR_{SNR}	(1,49)	4.316	4.641	0.930	0.357		0.428	

Table 3.7: Statistical results from multiple linear model regressions on NESI, TTS, SSQ, MEMR, FFR and EFR outcome measures as predicted by AP amplitude. The p corr. coloum represents the p-value after Benjamini-Hochberg correction for multiple comparisons. $\star = p<0.05$, $\star\star = p<0.01$, $\star\star\star = p<0.001$

3.3.8 FFR as a measure of peripheral neural integrity

We examined the relationship between ANF integrity and the low-frequency, high-level FFR. The AP component of the ABR reflects synchronized neural

activity at the level of the AN, and is still considered as the most direct non-invasive measure of the ANF status in humans. We found a strong correlation

A: Step-wise model selection

		Sum of Sq	RSS	AIC
Start: AIC=314.51				
	- PTA_{HF}	23.711	4435.6	**312.91**
	- PTA_{LF}	44.377	4456.2	313.25
	- AP	118.129	4530	314.47
	- Sex	236.07	4647.9	316.37
	- Age	257.459	4669.3	316.71
Step 1: -PTA_{HF}				
	- PTA_{LF}	27.94	4463.5	**311.37**
	- AP	129.53	4565.1	313.04
	- Sex	224.82	4660.4	314.57
	- Age	619.86	5055.4	320.59
Step 2: -PTA_{LF}				
	- AP	149.68	4613.2	311.81
	- Sex	205.9	4669.4	312.71
	- Age	613.49	5077	318.9
	none		4463.5	**311.37**

B: Final model
FFR ∼ AP+ Age + Sex

	Estimate	Std Error	t	p	
AP	8.253	5.39	1.532	0.13	
Age	-0.219	0.07	-3.102	**2.77e-03**	**
Sex	-3.476	1.93	-1.797	0.077	

Table 3.8: **A)** Stepwise model selection outcome for FFR ∼ AP+ Age + Sex + PTA_{LF} + PTA_{HF}. **B)** model parameters for the most optimal model predicting FFR_{SNR}. $\star = p < 0.05$, $\star\star = p < 0.01$, $\star\star\star = p < 0.001$

between the two measures ($t(1,72) = 3.883$, $p = 0.0013$), suggesting that a higher FFR_{SNR} is associated with a higher AP amplitude. Although encouraging, it is possible that the correlation between the two measures is driven by common confounding variables, such as age, sex, and the hearing status of the participants. To this end, we sought to find the linear model that might best explain the variance of the FFR by using a step-wise model-selection approach. The first model included only age, and was the least accurate model. AP was significantly better at explaining the variance in the FFR. When adding age, sex, PTA_{LF} and PTA_{HF}, the AIC was further reduced. By using a step-wise model selection from

this point, the model was further improved by removing both PTA_{LF} and PTA_{HF}, resulting in a final model including only AP, age and sex. The results from the step-wise model selection can be seen in table 3.8 A).

Table 3.8 B) shows the final model parameters from the step-wise model selection analysis. Here, we found a significant effect of age ($t(3,70) = -3.102$, $p < 0.01$), but no main effects on either the AP ($t(3,70) = 1.53, p = 0.13$) or sex ($t(3,70) = -1.797, p = 0.077$).

3.4 Discussion

The current study investigated the potential correlation between the AP component of the click-evoked ABR and the FFR evoked by low frequency pure tones across a group of aging listeners. It has been speculated that the FFR recorded at the scalp may reflect age-related peripheral neural loss, yet experimental evidence is missing. Here, we recruited listeners across a wide age span with normal or near-to-normal audiometric thresholds at lower frequencies. We first confirmed that measures of OHC function at lower frequencies were similar between younger and older listeners. Younger and older listeners were found to have similar SP amplitudes, similar TEOAE amplitudes, and audiometric thresholds within the normal range up to 2 kHz, suggesting similar status of apical hair cells. Consistent with previous studies, we found a strong effect of age on the AP component of the ABR (Carcagno and Plack, 2020). We interpret this result as an indication of age-related neural degeneration at the level of the AN. Consistent with this, we also found shallower MEMR level growth functions for older participants, also consistent with age-related loss of low spontaneous-rate ANFs (Bharadwaj et al., 2021; Märcher-Rørsted et al., 2022; Thompson et al., 1980). We further confirmed strong age-related decreases in the SNR of the vertex FFR in response to pure-tone stimulation (326 Hz). Additionally, the SNRs of EFRs to amplitude modulated noise (120 Hz) were also similarly reduced in older listeners, although this effect was less pronounced. The age-related reductions in AP amplitude of the ABR and in the FFR were strongly correlated. When further exploring the relationship between peripheral loss (AP amplitudes) and the brainstem generated FFR, we found that adding age to the linear model best explained the variance in the participants. This might suggest that age-related reductions in brainstem phase-locking to longer sustained stimuli may be, at least in part, driven by the status of periphery, but we cannot rule out other

age-related deficits in the central auditory system.

Although participants were recruited to have relatively normal low-frequency thresholds (up to 2 kHz), significant loss of sensitivity at extended high frequencies (>8 kHz) were observed in older listeners. In consequence, high-frequency thresholds were highly correlated with age and with the decrease in AP amplitudes. This could imply that the age-related changes seen in physiological outcome measures (e.g., AP and FFR) are driven by OHC loss in basal parts of the cochlea. However, recent modeling work has suggested that OHC loss does not influence ABR wave I amplitudes (Buran et al., 2022; Verhulst et al., 2018) or AN FFR amplitudes significantly (Märcher-Rørsted et al., 2022). Carcagno and Plack (2020) argued that age-related reductions in the ABR and the FFR are primarily driven by basal ANF loss and/or IHC loss, since high-frequency masking removed the age-related effects on both measures. Although the effects may be driven by basal loss of IHC or ANF loss, this does not rule out that more apical ANF loss is also driving age-related differences in the FFR. If nerve loss supersedes the loss or dysfunction of sensory cells (i.e., OHCs and IHCs), as suggested by animal studies (Sergeyenko et al., 2013) and results from human temporal bones (Wu et al., 2019), the high frequency audiogram may in itself be a proxy for neural degeneration also in more apical parts of the cochlea, as suggested by others (Liberman et al., 2016). More selective analysis of the current dataset is required to shed light on such questions.

Later waves of the click ABR were not affected by age, as we observed similar wave-V amplitudes in both young and older listeners. The fact that the transient evoked response levels are restored is consistent with a central gain mechanism that help to restore mean activity levels in the central auditory system with reduced peripheral input, which may hide potential age-related central deficits (Chambers et al., 2016). Previous studies have shown that cortical activity entrained to slow envelope fluctuations are enhanced in older normal-hearing (Goossens et al., 2016; Prendergast et al., 2019; Presacco et al., 2016a; Walton, 2010) and hearing-impaired listeners (Aiken and Picton, 2008; Fuglsang et al., 2020; Goossens et al., 2018). If these changes already restore, at least in part, the transient responses (i.e., onset responses) from brainstem level, this may hide potential age-related central deficits, especially to transient stimuli. Interestingly, sustained responses thought to arise from the same generator as the wave-V (FFRs and EFRs) were both affected by age, consistent with previous investigations (Anderson et al., 2012; Prendergast et al., 2019; Presacco et al.,

2016a; Walton, 2010). This may add to arguments by Rumschlag et al. (2022), who suggested that overall amplitude is compensated for while the precision of rapid phase-locked activity can be compromised in the aging system. Given these results, a proposed diagnostic measure should consider a combination of both transient and sustained stimuli to be sensitive to effects related to both the overall response amplitude and the response synchrony in the auditory system. Although this may point in the direction of age-related central deficits, it still remains unclear whether peripheral loss in itself could be responsible for deficits seen more centrally.

Many studies have attempted to quantify the relationship between noise-exposure and peripheral measures of ANF loss in humans (see Le Prell (2019) for review). While the acute effects of noise exposure on ANF loss are now well established in various animal models (Kujawa and Liberman, 2009; Parthasarathy et al., 2018; Shaheen et al., 2015; Valero et al., 2017; Valero et al., 2016), evidence in humans was lacking. Here, we confirmed previous reports that life-time exposure evaluated by the NESI questionnaire was not correlated with AP amplitude (Grinn et al., 2017; Guest et al., 2017b; Prendergast et al., 2019; Presacco et al., 2016b). We also did not find any correlation between AP amplitudes and self-reported hearing status measured by the SSQ12. Given that memory recall of past noise-exposure events is subjective and difficult to quantify, unintended variability in the estimation of the accumulated noise-exposure through life is inevitable. The use of questionnaires to estimate the amount of noise exposure received by an individual during his/her whole live may not be well associated to the real received physical magnitude, and hence not well associated to the inflicted physiological damage. It is likely that high variability in subjective questionnaires implies that correlations with physiological measures of AN health can only be meaningfully assessed in very high-powered studies (many thousands of participants). Interestingly, however, we found a correlation between the estimated recurrence of TTS-inducing events and the AP amplitude. This connection could suggest that noise-induced synaptopathy only occurs with traumatic doses of noise. Although extreme exposure is known to produce OHC damage associated with threshold elevation, mild-to-severe events leading to temporary perceptual changes in hearing may lead to significant denervation without the presence of a threshold shift. Although speculative, this result may argue along these lines.

Limitations and future directions

The present results suggest that the FFR could, at least in part, be driven by peripheral neural loss. However, it is unclear whether other age-related effects could influence the observed FFR reductions. We found a strong correlation between age and EHF thresholds, which made hard to disentangle the effects of peripheral loss from age and high-frequency hearing-loss. To examine some of these controversies, more restricted analysis should be performed on a subset of listeners (e.g., super-normal hearing-aged listeners). Furthermore, histopathological evidence suggests a peripheral neural degeneration linearly associated with age, leading to the assumption that even normal-hearing older listeners will tend to have higher degrees of ANF degeneration than younger listeners (Wu et al., 2020). However, this assumption may not hold when examining individual subjects. The status of the AN is not assessed directly in individual subjects, but we assume that the AP of the ABR wave-I is a direct measure of AN health. To finally conclude on correlates of AN health, a more direct measure of AN health is needed. If micro-structural magnetic resonance imaging (MRI), computed tomography (CT) or optical tomography (OCT) imaging succeeds in advancing towards reliable in-vivo structural estimates of AN status, this could in turn help to reveal the relation to electrophysiological correlates. Lastly, the current analysis focused on electrical potentials arising from sub-cortical sources. The consequences of sub-cortical processing deficits have been speculated to be associated with enhanced cortical responses (i.e., central gain, lack of inhibition) often associated with perceptual deficits (Chambers et al., 2016). The connection between peripheral loss and perception is still unclear, and effects on cortical processing should be further examined. If peripheral loss leads to strong cortical effects, it may be more readily compared to future behavioral studies in the same cohort of listeners. To explore this further, the disentanglement of peripheral and central responses is needed. If the periphery is driving the decrease seen at the level of the brainstem, it should be possible to see similar reductions in the isolated peripheral response.

3.5 Conclusion

In the present study, we provided evidence that the FFR to low-frequency tones is correlated both with age, and the AP component of the ABR. It is known

that age is correlated with progressive cochlear neural degeneration, and our interpretation of these results further demonstrate potential diagnostic value of the FFR. Although we found correlations between AP amplitudes and the FFR, it is still assumed that AP is correlated with cochlear neural loss. More direct measures of AN health, as well as more direct electrophysiological measures generated at the level of the cochlea are needed to further conclude on these finding.

Acknowledgments

This work was supported by the Novo Nordisk Foundation synergy grant NNF-17OC0027872 (UHeal).

4

Measures of temporal coding in aging humans using electrocochleography [d]

Abstract

Auditory nerve-fibers that innervate inner hair cells in the cochlea degenerate with advancing age. It has been proposed that age-related reductions in the brainstem frequency-following response (FFR) elicited by low-frequency pure tones may be sensitive to such neural loss in the cochlea. If auditory nerve-fiber loss is the main contributor to age-related changes in the brainstem FFR, then the FFR may be a proxy for cochlear neural degeneration. To further explore this possibility, synchronized neurophonic potentials generated at the level of the auditory nerve need to be compared to brainstem FFR responses obtained with the same stimulation. However, stimulation with sustained tones complicates the dissociation of temporally overlapping responses from peripheral and central sources. In the present study, we recorded responses to pure tones and clicks using both electrocochleographic (ECochG) recordings at the tympanic membrane (TM) as well as 'classical' scalp recordings of the FFR in younger and older normal-hearing human listeners. In the ECochG montage, both the auditory nerve neurophonic response (ANN) to the tonal stimulation and the click-evoked compound action potential were strongly reduced in the older normal-hearing listeners. Scalp FFRs to low-frequency (516 Hz) tones (250 ms, 80 dB sound pressure level) were also found to be reduced for the older listeners. The amplitudes of the ANNs and FFRs were similarly reduced with increasing age. The results support the hypothesis

[d] This chapter is based on Märcher-Rørsted, J. & Temboury-Gutierrez, M., Bille, M., Yde, J.B., Encina-Llamas, G., Hjortkjær, J. & Dau, T. , (In preparation). "Electrocochleographic frequency-following responses as a potential marker of age-related peripheral degeneration."

that the reduction of the scalp-recorded FFR with age reflects, at least in part, neural loss at the level of the auditory nerve.

4.1 Introduction

Declines in speech-in-noise perception in older people without loss of threshold sensitivity have been widely reported, but the cause is uncertain (Hind et al., 2011). Recent evidence suggests that such 'hidden hearing loss' (HHL) could be linked to deafferentation of inner hair cells (IHC) or cochlear synaptopathy, the disconnection of auditory-nerve fibers (ANF) from IHCs in the cochlea. Neural degeneration may precede damage to outer hair cells (OHC) (Kujawa and Liberman, 2009; Sergeyenko et al., 2013) and can therefore occur in subjects with clinically-normal or near-normal hearing thresholds (Schaette and McAlpine, 2011). However, a direct link between these suprathreshold behavioral effects and peripheral neuropathy remains unclear. If this link is to be investigated, further understanding of the consequences of a peripheral neural loss on more central (e.g., brainstem) auditory processing is needed. Disentangling responses from the auditory nerve (AN) and the brainstem may be useful if a relationship between ANF loss and reduced brainstem neural activity is to be established.

Age-related changes have been reported for frequency-following responses (FFR) phase-locked to the period of low-to-mid frequency (i.e., 100-1000 Hz) acoustic stimuli, where the main generators are considered to be of central (i.e., brainstem) origin (Clinard and Tremblay, 2013; Johnson and Brown, 2005; Werff and Burns, 2011). Age-related reductions in FFRs evoked by low-frequency pure tones have also been reported for older listeners with normal or near-normal audiometric thresholds (Anderson et al., 2012; Mamo et al., 2016; Märcher-Rørsted et al., 2022; Presacco et al., 2016a; Roque et al., 2019). Most of these studies have interpreted such FFR reductions to indicate age-related deficits in central processing (e.g., central desynchronization, Frisina and Frisina, 1997; Pichora-Fuller et al., 2007; Schneider et al., 1998). However, peripheral deafferentation may, at least in part, contribute to the FFR reduction. Recent modeling work suggested that ANF loss can cause a decrease in phase locking across ANFs which could drive the reduction in FFR amplitudes observed experimentally in older listeners (Märcher-Rørsted et al., 2022). However, more experimental evidence is needed to confirm this hypothesis. This requires a comparison of the centrally generated FFR with the synchronized response generated by the

same stimulation at the level of the AN (i.e., the auditory nerve neurophonic, ANN).

Reduced wave-I amplitudes of click-evoked auditory brainstem responses (ABR) have also been reported in older near-normal hearing listeners (e.g., Carcagno and Plack, 2020; Grant et al., 2020). The ABR evoked by transient stimuli (e.g., clicks, short tones or chirps) is composed of several wave peaks, each associated with a unique latency. The consecutive peaks are thought to reflect neuronal activity at distinct generator sites (i.e., auditory nuclei) along the auditory pathway from the cochlear sensory cells to the auditory cortex. Presynaptic hair-cell activity is reflected in the first deflection in the ABR (i.e., the summating potential, SP, Zheng et al., 1997), which is followed by the compound action potential (CAP) arising from the population response of the AN (Ferraro, 1998). Waves III through V are considered to be generated by more central ascending auditory nuclei, from the cochlear nucleus (CN) to the inferior colliculus (IC), respectively (Møller et al., 1988). In relation to diagnostics of peripheral neural deficits, the loss of ANFs in animal models of cochlea synaptopathy has been associated with reduced suprathreshold amplitudes of ABR wave-I (Kujawa and Liberman, 2009; Parthasarathy et al., 2018; Shaheen et al., 2015; Valero et al., 2017; Valero et al., 2016). Wave-I of the ABR has also been considered as a potential diagnostic measure of age-related or noise-induced ANF loss in humans (Carcagno and Plack, 2020; Garrett and Verhulst, 2019; Grant et al., 2020; Guest et al., 2017a; Liberman et al., 2016; Prendergast et al., 2019).

In scalp electroencephalography (EEG) measurements in humans obtained with a traditional mastoid-to-vertex recording montage, later waves of the click ABR can be identified even at stimulation levels close to hearing threshold (Hecox and Galambos, 1974). However, earlier components are only observed with high-intensity stimuli where a sufficient amount of neurons are synchronously activated (Dau et al., 2000). These responses are often difficult to identify in clinical settings, especially in older and hearing-impaired listeners (e.g., Steinhoff et al. (1988). The use of electrodes positioned closer to the cochlea (i.e., on the tympanic membrane, TM) improves the signal-to-noise ratio (SNR) of potentials arising from the sensory organ (e.g., Harris et al., 2021; Simpson et al., 2020; Stamper and Johnson, 2015). This may improve the fidelity of the early ABR components. Here, we utilized this recording technique, along with classical EEG recordings, in an attempt to isolate potentials arising from

the AN from potentials generated in the auditory brainstem.

Sustained acoustic stimulation (e.g., with a sustained tone) elicits synchronized responses at several stages along the auditory pathway. These evoked responses can be captured with scalp electrodes, and are generally referred as FFRs. Sustained 'microphonic' responses are elicited by presynaptic sources in the cochlea (i.e., the cochlear microphonic, CM, arising from the cochlear hair cells). 'Neurophonic' responses are elicted by the auditory nerve (i.e., the ANN), the auditory brainstem (i.e., responses generated at the cochlear nuclei, the medial superior olive, MSO, and the IC), as well as the auditory cortex (Worden and Marsh, 1968). The temporal overlap between responses makes it difficult to separate the different generators of the scalp FFR (Gardi et al., 1979). It is known that the ascending auditory system exhibits a low-pass characteristic, as the limits of phase locking declines towards the cortex. While the AN population response can phase lock to several 1000s of Hz (Dynes and Delgutte, 1992; Johnson, 1980), neurons in the rostral brainstem have been estimated to show phase locking up to about 1 kHz (Bidelman, 2015; Liu et al., 2006) and are most prominent in the range of 100s of Hz. By utilizing the fact that different neural generators have different phase-locking characteristics, it may be possible to isolate phase-locked responses from pre-synaptic, AN and brainstem sources.

In this study, we measured sustained responses to different stimulation frequencies likely to yield responses dominated by different sources. In particular, we used tones of 516 Hz to generate responses dominated by brainstem activity, 1032 Hz to yield AN activity, and 3096 Hz to yield pre-synaptic activity. We anticipated that responses to higher frequencies may be more difficult to record, comparable to the recording of ABR wave-I. To ensure that a sufficient population of ANFs would be responding to these frequencies, we used high-intensity (100 dB sound pressure level, SPL) tone bursts. Given that these levels may be harmful to the cochlea for longer exposure times, we limited the duration of the tones to 10 ms.

We measured both transient evoked and sustained evoked potentials in both young and older listeners. Clinical near-normal hearing thresholds were verified by means of standard audiometry. Extended high-frequency (EHF) audiometry as well as distortion-product otoacoustic emissions (DPOAE) were also collected. We measured EEG and ECochG to broadband high-level clicks and 10-ms tone pulses at low (516 Hz), mid (1032 Hz) and high (3096 Hz) frequencies . Furthermore, we measured the FFR to longer-duration (250-ms)

lower-level (80 dB SPL) tones at low (516 Hz) and mid (1032 Hz) frequencies. We hypothesized that different montages would allow disentangling peripheral sources from central sources, which could be validated using the responses to transient stimuli. We expected to observe reduced peripheral responses to both transient and sustained stimuli in the older listeners. If the peripheral component of the FFR would be confirmed to be reduced, this would further support the hypothesis that ANF loss contributes to the brainstem generated FFR.

4.2 Materials and Methods

4.2.1 Participants

Twenty-nine subjects participated in the study. The participants were recruited from our patient database based on age and audiometric sensitivity (<25 dB hearing level (HL) from 125 Hz to 6 kHz), and divided into a young group (n=15, ages 20–31 yr, mean age 23.5 yr, standard deviation 3 yr, 5 men) and an older group (n=14, ages 58–79 yr, mean age 64.7 yr, standard deviation 7.1 yr, 5 men). Ear-canal status was checked via otoscopy prior to measuring the pure-tone audiogram. To verify audiometric thresholds used to recruit the participants, we measured air conduction thresholds from 125 Hz to 8 kHz using IP30 insert earphones (RadioEar) as well as extended high frequency (EHF) thresholds from 10 to 16 kHz using DD450 circumaural headphones (RadioEar). The ear used in the measurements (referred to throughout the manuscript as the "test ear") was the ear with the lowest audiometric thresholds. After audiometric assessment, the participants filled out a short questionnaire reporting the number of years of formal musical training, the presence and degree of tinnitus, the recall of potential long-term exposure to ototoxic chemicals, any medical history of middle ear, head trauma and neurological disease, as well as the frequency of perceived temporary threshold shifts (TTS). All subjects gave their written consent to participate in the study, and the project was approved by the Science Ethics Committee of Capital Region of Denmark (protocol H-21049895). The study was conducted in accordance with the Declaration of Helsinki. All measurements took place at the Copenhagen Hearing and Balance Center at Rigshospitalet in Copenhagen, Denmark.

4.2.2 Distortion product otoacoustic emissions (DPOAEs)

As an objective measure of OHC function, DPOAEs were measured in the participants' test ear using the Interacoustics Titan system. We measured DPOAEs using two pure tones, or primaries (F1 and F2), fixed at a 1.22 ratio (F2/F1). The difference in level between the primaries was fixed to 10 dB, such that F2 = F1 – 10 dB. DPOAE amplitudes were evaluated at the distortion product defined by 2F1-F2. DPOAEs were measured both as a function of frequency (500 Hz to 10 kHz at F1=65 dB SPL), and level (F1=40 to 65 dB SPL at 1, 3, 8 and 10 kHz in 5 dB steps). For the frequency dependent DPOAEs, the level of the two primaries remained constant (F1 at 65 dB SPL and F2 at 55 dB SPL), while the frequency of F2 varied (0.5, 1, 1.5, 2, 3, 4, 5, 6, 7, 8, 9, 10 kHz). The level-dependent DPOAEs were measured at two frequencies also used for the electrophysiological measurements (F2 = 1032 and 3096 Hz) to control for local ('on-frequency') OHC dysfunction. Additionally, two higher frequencies (F2 = 8 and 10 kHz) were measured to assess the status of basal OHCs.

4.2.3 Electrophysiology

Stimuli

Transient-evoked potentials were recorded in response to 100-μs clicks, which were presented at 115.5 dB peak-to-peak equivalent (ppe)SPL at presentation rates of 12 and 40 Hz. The clicks were presented 6000 times in alternating polarity for each presentation rate. To elicit the FFR, we used 10-ms pure tones (1-ms rise/fall sinusoidal ramp) at 516, 1032 and 3096 Hz, presented at 100 dB ppeSPL. We presented 3000 repetitions at each frequency separately for both onset polarities[e]. To have a condition with sufficient frequency resolution and to compare with previous results (e.g., Märcher-Rørsted et al., 2022), we also presented 150 repetitions of 250-ms long pure tones (1-ms rise/fall sinusoidal ramp) at 516 and 1086 Hz at 85 dB SPL in each polarity. All stimuli were presented monaurally using ER-3 insert earphones. The ER-3 transducers were placed in small, custom-made metal boxes to shield them from electrical noise. The cables connecting the earphones to the soundcard were also electrically shielded. Additionally, the inside of the box was soldered to an extra cable, which

[e] The polarities for the pure tones were presented separately, i.e., not in a true alternating manner.

was connected to ground outside of the booth. This grounding was added to avoid further electric artifacts, since it drains the extra charge that can accumulate in the transducers (Simpson et al., 2020). In total, the stimulation paradigm lasted one hour, and the participants were offered 5-minute breaks between the recordings obtained with clicks, the short and the longer tone bursts recordings, respectively.

Data acquisition

Electrophysiological data were recorded with the BioSemi ActiveTwo system using speed-mode 3 and a sampling frequency of 16384 Hz. The ground electrode with the BioSemi ActiveTwo system is divided into the common mode sense (CMS) and the driven right leg (DRL) electrodes, which were placed on C1 and C2, respectively. EEG and ECochG data were continuously recorded using the commercially available ABR module of the ActiveTwo AD box, which provides improved SNRs compared to the traditional BioSemi inputs. The participants were positioned on a bed in a double walled, sound treated, electromagnetically shielded booth and were instructed to keep their eyes closed. Participants were encouraged to sleep or relax. We measured EEG using two inputs to the ABR module from BioSemi's ActiveTwo AD box. Ambu Neuroline 720 neurology surface electrodes were placed on the ipsilateral mastoid (inverting, P3 or P10) and on the lower forehead (reference, PFz). The skin was disinfected with alcohol (85% ethanol) prior to the application of the electrodes.

Electrocochleography (ECochG)

A TM electrode (Sanibel), connected to the remaining input of the ABR module, was placed in the test ear of each participant. First, a trained medical doctor (ENT) inspected the ear canal using an otomicroscope, followed by the application of liquid local anesthesia (Xylocaine, lidocaine). The tip of the TM electrode was immersed in conductive gel (Signagel, Parker Laboratories) for 10 minutes prior to insertion. After 10 minutes, the anesthetic was removed from the ear canal via microsuction (typically used in clinics for earwax removal). The TM electrode was placed on the tympanic membrane by the medical doctor. The electrode was fixed in place by a foam ER-3 insert tip, which was later connected to the sound delivery system. Correct positioning of the electrode was verified by visual inspection of the continuous electrical activity after insertion.

Data pre-processing

The continuous electrophysiological data were high-pass filtered at 100 Hz by the BioSemi built-in ABR module. The data were pre-processed in MATLAB using the FieldTrip Toolbox (Oostenveld et al., 2011). At this stage, the trial labels and channels were extracted and a comb-notch filter was applied at 50 Hz and its harmonics up to 1500 Hz to remove the line noise. The data were subsequently divided into epochs: from 10 ms before stimulation to 50 ms after stimulation for the clicks and the 10-ms tone bursts, and from -100 ms to 500 ms for the 250-ms tone bursts. Epochs with values over 90 mV were rejected from further analysis. The epochs were averaged using the inverse of the epoch variance as weights (John et al., 2001). The condensation (C) and rarefaction (R) polarities, as well as polarity dependent ((C-R)/2) and independent ((C+R)/2) responses, were computed for each stimulus. The average responses were band-pass filtered between 100 and 4000 Hz. The acoustic delay in the sound delivery system (1 ms) was compensated for in all analyses.

Compound action potential (CAP) and auditory brainstem response analysis (ABR)

We sought to isolate both peripheral activity (i.e., from the AN) from more central activity (i.e., from the brainstem) in response to transient and periodic stimuli. As a measure of peripheral synchronized neural activity to transient stimuli, we extracted the CAP N1 peak to the 12/s and 40/s rate clicks, recorded with the ECochG configuration (ipsilateral mastoid-to-TM electrode). The following parameters were extracted from the CAP: onset latency, peak latency, peak amplitude, trough amplitude and half-width latency as in Harris et al. (2021). The peak latency, peak amplitude, trough amplitude, and onset latency were obtained using a modified version of the *localpeak()* function in the ERPlab toolbox (Lopez-Calderon and Luck, 2014). In short, the function searches for the local maxima between 0 and 3 ms of the responses. Additionally, the latency and peak of the SP was obtained from the participants where it was detectable using the same modified function. The amplitudes were measured from the peak to the trough and responses were corrected to a baseline, computed as the average of the 2 ms prior to the onset of the stimulation. The amplitudes and latencies obtained from the function were inspected visually and corrected when needed using the ABR wave-I waveform as a reference. The half-width

latency was calculated as the latency from the onset of the peak to the peak of the CAP.

As a measure of synchronized central (i.e., brainstem) activity, we recorded ABRs to the same clicks using the classic ABR ipsilateral mastoid-to-forehead EEG configuration. As for the CAP, we estimated onset latency, peak latency and peak amplitude of wave-V, using limits of 4.5-6.5 ms (Jerger and Johnson, 1988; Lightfoot, 1993). Again, the output of the function was checked and corrected by visual inspection. Additionally, we computed the phase-locking value (PLV) of the response, which indicates the level of neural synchrony across n epochs. The PLV was derived by using the following expression (Delorme and Makeig, 2004):

$$PLV(f,t) = \frac{1}{n}\sum_{k=1}^{n}\frac{F_k(f,t)}{|F_k(f,t)|} \tag{4.1}$$

where $Fk(f,t)$ indicates the complex spectral estimate at time t and frequency f of epoch k. PLVs range from 0 (i.e., completely unsynchronized) to 1 (i.e., completely synchronous). The function *newtimef()* from the EEGlab toolbox was used to perform the time-frequency analysis, with Hanning tapers, a window size of 32 samples, pad ratio of 2, and using 20 linearly-spaced frequencies from 250 to 5120 Hz. The PLV was then obtained as the maximum value in the 2-ms windows around the two peaks (CAP and w-V).

ANN and FFR analysis

We recorded ANNs to both short (10 ms) high-intensity (100 dB ppeSPL) tones, and ANNs and FFRs to longer (250 ms) lower-intensity tones (80 dB SPL). The magnitudes of the responses were estimated in the frequency domain at the bin of the stimulus frequency, after computing the spectrum of the response between 0 and 12 ms and 0 and 250 ms, for the 10-ms and 250-ms tone bursts, respectively. For the ANNs and FFRs evoked by the longer tones, the SNR was calculated. The spectral magnitude of the carrier frequency was first identified and then compared to the surrounding noise floor (± 20 Hz). The SNR was calculated by taking the power of the target magnitude bin, and dividing it by the average of the surrounding frequency bins. Modulation sidebands evoked from the 2-Hz presentation rate, and corresponding harmonics (± 2 Hz to 10 Hz, in steps of 2 Hz), were excluded from the noise-floor calculation. We then calculated the probability of the response power being different from the surrounding noise floor using an F-statistic test (Dobie and Wilson, 1996). The

FFR measurements were considered significantly different from noise if $p \leq 0.01$ (1 %). Non-significant responses were excluded from the statistical analysis.

As an additional measure of synchronized activity in the response, we calculated the PLV of the responses. The PLV was obtained by averaging the PLVs of the 0-to-12 ms and 0-to-250 ms responses, for the 10-ms and 250-ms tone bursts, respectively, around each of the frequencies of stimulation (f/2 – 2f).

4.2.4 Statistical analysis

We examined group differences and differences between montages using t-test and ANOVA functions. Differences in the pure-tone average (PTA) of audiometric thresholds and DPOAE amplitudes were examined using a t-test. Results were corrected for multiple comparisons using the Bonferroni correction method. The normality of the data was verified by examining the normal Q-Q plots (qqnorm and qqline) of the residuals of the models. All statistical analyses were performed with RStudio (RStudio Team, 2020).

4.3 Results

4.3.1 Hearing thresholds and OAEs

Figure 4.1A) shows the pure-tone thresholds for the test ear for all participants. The group-averaged thresholds are illustrated by thick lines for the younger group (orange) and the older group (purple). Individual participants' audiograms are shown as thin lines.

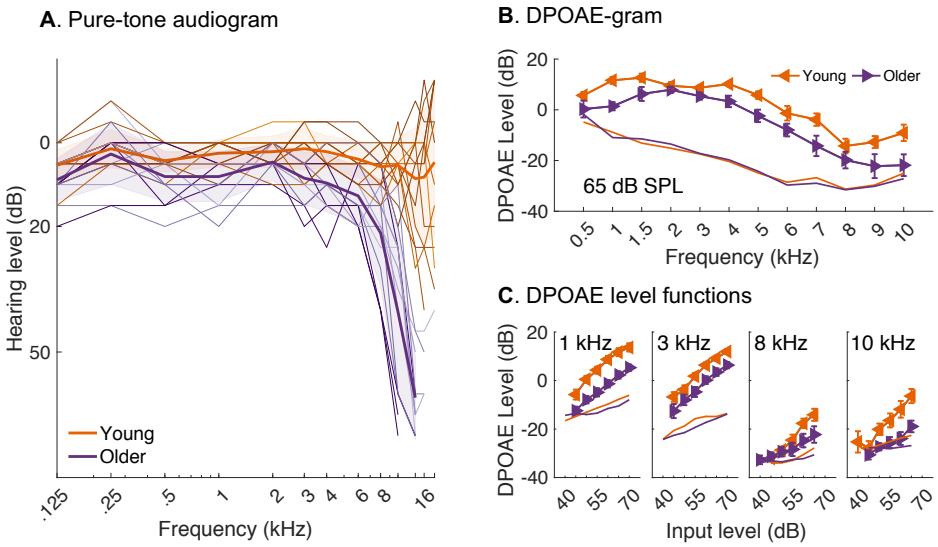

Figure 4.1: **A**) Pure-tone thresholds from 125 Hz to 16 kHz of the younger (orange) and older (purple) participants. Thick lines show the group average thresholds. The shaded region illustrates the standard deviation and the thin lines represent the thresholds of the individual listeners. **B**) Average DPOAEs at 65 dB SPL from 500 Hz to 10 kHz for the younger (orange triangles pointing left) and older (purple triangles pointing right) participants. **C**) Average DPOAE level functions from 40 to 70 dB SPL at 1, 3, 8 and 10 kHz for the younger (orange triangles pointing left) and older (purple triangles pointing right) participants. Error bars indicate standard error, solid lines without markers indicate the averaged noise floor and gray dashed lines indicate threshold for significant responses (-10 dB).

All participants were confirmed to have audiometric thresholds below 25 dB HL up to 6 kHz. Despite this, we found statistical differences between the two groups on the PTA of these frequencies (PTA from 0.125 to 6 kHz, t-test, $t(19.3) = -3.22, p = 0.0221$) suggesting higher low-frequency thresholds in the older group. For EHF thresholds (> 8 kHz), we found significant differences between the young and the older group (PTA from 8 to 16, t-test, $t(25.9) = -10.1, p = 4.7e-10$) suggesting higher EHF thresholds with increasing age. At the lowest two frequencies used for electrophysiological stimulation (516

Hz and 1032 Hz), there were no significant differences between the groups (t-test; 500 Hz: $t(17.2) = -1.79, p = 0.4543$; 1 kHz: $t(19.3) = -2.82, p = 0.0543$). However, hearing thresholds at 3 kHz were significantly affected by age ($t(25.8) = -2.93, p = 0.0349$).

Figure 4.1B) shows group-averaged DPOAE amplitudes for young (orange) and older (purple) listeners for the fixed-level condition (65 dB), measured as a function of F2 frequency (500 Hz to 10 kHz). We observed consistently lower DPOAE amplitudes across frequency in the older group compared to the young group. Averaged DPOAE amplitudes from frequencies where all participants were considered to be "normal hearing" (0.5 to 6 kHz) were still found to be significantly different (t-test, $t(22.2) = 2.74, p = 0.0383$), also suggesting lower DPOAE amplitudes in the older group. At higher frequencies (8 to 10 kHz), we detected a much lower number of significant DPOAE responses across groups (50% and 85.71% of significant responses in the older and young groups, respectively). This led us to conclude that the instrumentation was not adequate for assessing DPOAE thresholds at high frequencies (>8kHz).

Figure 4.1C) shows group-averaged DPOAE amplitudes measured in the fixed-frequency condition (1, 3, 8 and 10 kHz) as a function of F2 level (40 to 70 dB in steps of 5 dB) for the young and the older group. The level-growth functions confirmed differences in DPOAE amplitudes between the young and the older participants, suggesting that the older listeners elicit lower DPOAE amplitudes, consistent with (small) differences in the pure-tone thresholds.

4.3.2 Disentangling peripheral potentials

Evoked potentials were recorded with three electrodes located on the ipsilateral mastoid, the lower forehead (i.e., vertex), and the ipsilateral tympanic membrane. Figure 4.2 shows the across-group average potentials recorded simultaneously with the two different electrode configurations: Mastoid-to-vertex (4.2A), and TM-to-mastoid (4.2B). Figure 4.2.1 shows the average response to a 115.5 dB-ppSPL click. Figure 4.2.2 and 4.2.3 show the average response to a 100-dB-ppSPL 10-ms tone bursts at 516- and 1032-Hz, respectively.

Mastoid-to-vertex

Figure 4.2.1A) shows click-evoked responses recorded between the ipsilateral mastoid and vertex electrodes, referred to as the mastoid-to-vertex montage.

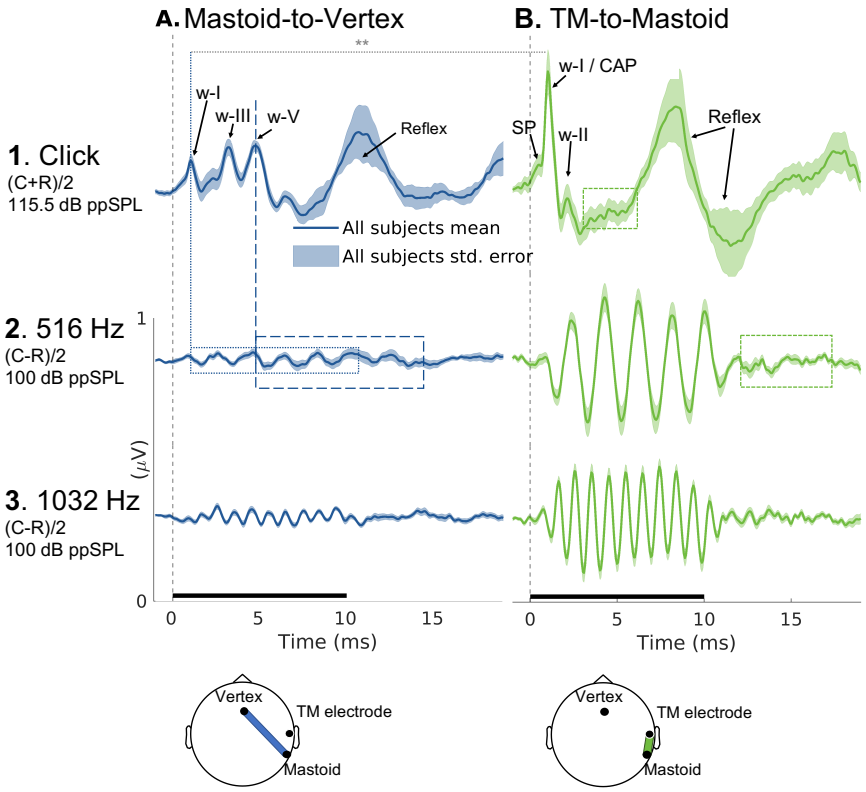

Figure 4.2: Average delay-corrected ABR and FFR measured simultaneously with different electrode configurations. The top row (**1**) shows polarity-independent ABR / CAP responses, (C+R)/2, the middle (**2**) and bottom (**3**) rows show 516-Hz and 1032 Hz polarity-dependent FFR / ANN responses, respectively, (C-R)/2. **A**) shows responses collected using the mastoid-to-vertex montage (P10-FPz). This configuration is shown to capture both peripheral (wave I) and brainstem (wave III and V) potentials. **B**) shows responses collected using the TM electrode-to-mastoid montage. Here, only peripheral potentials are present (i.e., SP, w-I/CAP, w-II). Responses to sustained stimuli show the isolated ANN. Solid lines indicate average responses of all participants, shaded areas indicate standard error. Black horizontal lines in the bottom panels indicate the duration of the pure-tone stimuli.

Waves-I, -III and -V were observed in the first milliseconds of the response to the click. Figure 4.2.2A) shows the average response to a 516 Hz tone. Here, the response can be seen to phase lock to the frequency of the tone. The onset of the response corresponds to the onset of the click ABR wave-I. The phase-locked response continues to latencies beyond the stimulation period (approximately 15 ms), consistent with a brainstem source. Figure 4.2.3A) shows the average response to a 1032 Hz tone. The onset of the response also corresponds to the wave-I latency, but the phase-locked response ends at around 10 ms, similar to the stimulus duration (indicated as a black horizontal line). The amplitude of the

response is relatively small. This may indicate that brainstem contributions are almost negligible and that the response is dominated by peripheral generators (i.e., AN and hair-cell potentials).This is consistent with the limits of phase locking of brainstem neurons (Liu et al., 2006).

TM-to-mastoid

Figure 4.2.1B) shows click-evoked potentials recorded from the TM electrode to the ipsilateral, referred to as the TM-to-mastoid montage. CAP amplitudes from this configuration were significantly larger than for the mastoid-to-vertex montage (t-test, $t(31.4) = -3.22, p = 0.0029$), suggesting that peripheral sources are dominant when recording from the TM. Later potentials (i.e., wave III-V) are diminished. Therefore, this montage is primarily sensitive to peripheral activity arising from the hair cells and the AN. Figure 4.2.2B) and 4.2.3B) show the average recorded responses to the 516 Hz and 1032 Hz tone bursts, respectively, for the TM-to-mastoid montage. The phase-locked responses arising at the latency of wave I and lasting 10 ms in duration suggest isolated peripheral phase-locked responses (i.e., ANNs).The responses observed here are larger in amplitude than for the mastoid-to-vertex configuration, consistent with the enhanced CAP amplitude. For this condition, it is assumed that the response is dominated by phase-locked AN activity due to the stimulation frequency.

4.3.3 Effects of age on CAP and ABR

Figure 4.3A) shows the across-group average click evoked response to 12/s and 40/s presentation rate conditions, recorded from the TM-to-mastoid montage. The response shows distinct SP and action potential (AP) amplitudes (i.e., CAP). For the 40/s condition, the AP amplitude is significantly reduced compared to the 12/s condition (t test, $t(37.8) = 3.03, p = 0.0087$), suggesting neural adaptation effects (Kiang, 1965; Pérez-González and Malmierca, 2014; Sumner and Palmer, 2012).

Figure 4.3B) shows group averaged click responses to the 12/s condition for young (orange) and older (purple) listeners. The CAP, which reflects compound activity from the AN, was reduced by 60.7% for the older participants ($t(27) = 8.97, p = 0.0058$). Figure 4.3C) shows a spider diagram reflecting the CAP amplitude, half-width latency and PLV, similar to Harris et al. (2021). On average, the CAP PLV was reduced by 50.8% in the older group compared to the

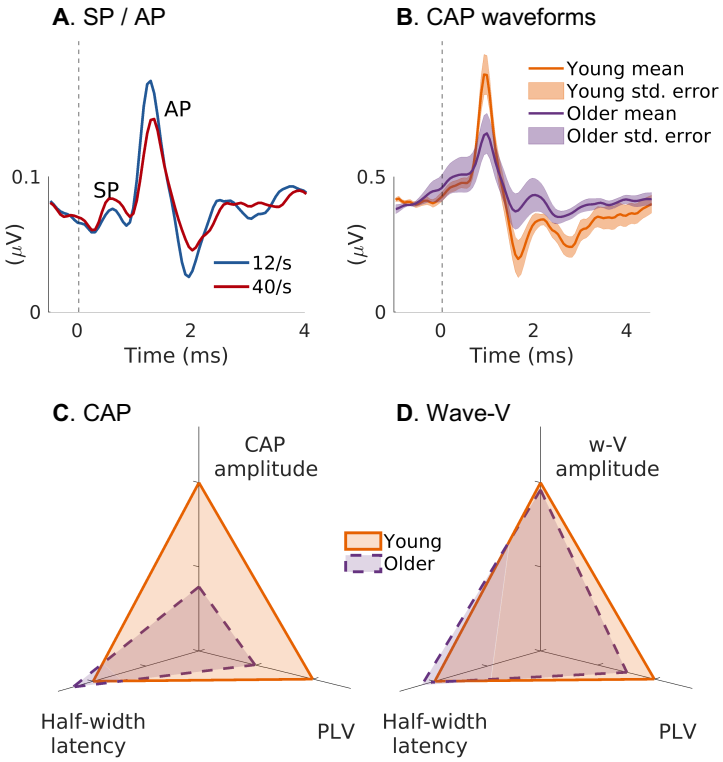

Figure 4.3: **A**) Averaged SP and AP across all participants in response to clicks presented at rates of 12 (blue) and 40 / second (red). **B**) Group-average click responses to the 12/s condition for young (orange) and older (purple) listeners. Shaded areas represent standard errors. **C**) Spider diagram showing the CAP amplitude, half-width latency and PLV for young (orange, solid) and older (purple, dashed) participants, measured with the TM-to-mastoid configuration. **D**) Spider diagram showing wave-V amplitude, half-width latency and PLV, measured with the mastoid-to-vertex configuration.

younger group ($t(27) = 6.50, p = 0.0164$), indicating a reduced neural activity at the level of the AN in the older subjects. The half-width latency of the CAP was not significantly different between the young and the older listeners.

Figure 4.3D) shows a spider diagram reflecting the wave V amplitude, half-width latency and PLV recorded from the mastoid-to-vertex montage. Here, we found no differences in the amplitude and PLV or the half-width latency between the two age groups.

4.3.4 Effects of age on long-tone ANNs and FFRs

Figure 4.4 shows a box plot of the ANN- and FFR SNR elicited by longer tone bursts (250 ms) of different frequencies (516 and 1032 Hz) for young (orange)

and older participants (purple), recorded from the TM-to-mastoid montage (e.g., ANN, figure 4.4A) and from the mastoid-to-vertex montage (e.g., FFR, figure 4.4B).

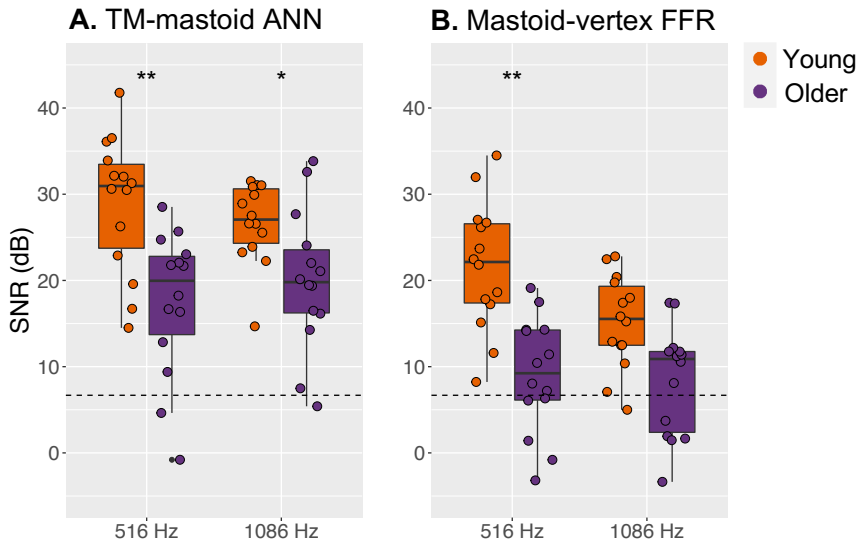

Figure 4.4: Box plots of the response SNR from young (purple) and older (orange) participants at 516 and 1086 Hz recorded with the TM-to-mastoid montage (e.g., ANN, **A**) and with the mastoid-to-vertex configuration (e.g., FFR, **B**). Individual SNRs are indicated with dots for young (orange) and older (purple) listeners.

Significant age effects were observed in the SNR of ANNs recorded with the TM-to-mastoid montage that enhances peripheral contributions at 516 Hz (figure 4.4A, $t(24) = 10.467, p = 0.0035$) and at 1032 Hz ($t(25) = 5.723, p = 0.0245$). SNRs in the older group were lower than those in the younger group. Additionally, we observed a similar age effect on the spectral amplitudes of both stimulation frequencies (not shown, 516 Hz: $t(24) = 5.98, p = 0.0221$, 1086 Hz: $t(25) = 6.63, p = 0.0162$).

For the mastoid-to-vertex montage, the SNR of the 516 Hz FFR was also reduced with for older participants (figure 4.4B, $t(21) = 10.277, p = 0.0042$). The FFR SNR for the 1086 Hz stimulation was not statistically different between the groups ($t(20) = 3.807, p = 0.0651$). These effects are similar and comparable to those reported in Märcher-Rørsted et al. (2022), although the exact frequencies, level and montage are not identical in both studies. Responses from both recording montages were similarly reduced with age, suggesting that potentials recorded with the more classic (mastoid-to-vertex) electrode montages reflect effects observed in the potentials reflecting peripheral activity (i.e., TM-to-

mastoid).

4.3.5 Effects of age on tone-pulse ANNs

We also measured ANNs to short (10-ms) high-intensity (100 dB ppeSPL) pure tones. Figure 4.5A) shows the group-averaged waveforms from the TM-to-mastoid montage for high- (3096 Hz), mid- (1032 Hz) and low- (516 Hz) pure tones for the young (orange) and the older (purple) listeners. We observed phase-locked responses to the periodicity of the tones for 516 Hz and 1032 Hz conditions for both listener groups. At the highest frequency (3092 Hz), the amplitude of the response was small compared to the two lower frequencies.

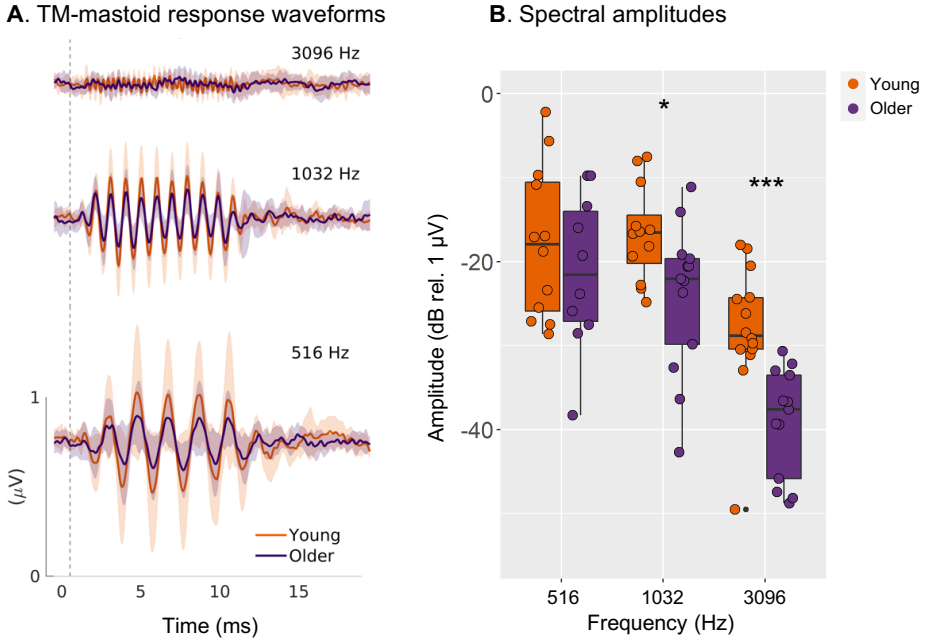

Figure 4.5: Average ANNs for young (orange) and older (purple) participants to 100-ms 100 dB ppSPL pure tones, measured with the TM-to-Mastoid configuration. **A**) Time domain waveforms for the 3096 (top), 1032 (middle) and 516 Hz (bottom) stimulation frequencies. **B**) FFR amplitudes estimated as the power of the response at the frequency of stimulation.

Figure 4.5B) shows the estimated ANN spectral amplitudes as a function of the stimulation frequency for the young (orange) and the older (purple) listeners. The amplitudes of the responses were estimated in the frequency domain, by taking the FFT of the averaged response from 0 to 12 milliseconds post onset, and evaluating the spectral energy at the frequency bin of stimulation. We observed significantly reduced spectral amplitudes at the two highest frequencies (1032

Hz: $t(23) = 6.3, p = 0.0195$; 3092 Hz: $t(25) = 16.03, p = 0.0004$) in the older group compared to the younger group. For 516 Hz, we did not find significant age effects ($t(20) = 0.78, p = 0.3873$).

4.4 Discussion

The present study investigated the effect of age on peripheral potentials recorded using ECochG. In a previous study, we introduced the possibility that age-related loss of ANFs may contribute to reductions seen in the scalp FFRs elicited by pure tones (Märcher-Rørsted et al., 2022). By dissociating peripheral responses (ANNs) from more central responses (FFRs) using different recording montages, we sought to investigate the upstream consequence of a peripheral changes. If the central response is reduced by a peripheral loss, the FFR recorded at the scalp may demonstrate diagnostic properties that could be valuable in clinical settings.

The different responses measured with high-level transient stimuli (clicks) showed distinct latencies corresponding to different generators. We first confirmed ABR waveforms for the classic mastoid-to-vertex configuration, where all characteristic waves (waves I-V) were identified. With a TM-to-mastoid montage, we found that the peripheral components (SP and CAP) were significantly enhanced compared to the ECochG mastoid-to-vertex configuration, as expected. However, the later waves of the ABR were not present, suggesting that this montage better captures isolated peripheral activity from cochlear sensory and neural cells, in line with previous work (Harris et al., 2018, 2021; Simpson et al., 2020; Stamper and Johnson, 2015). The CAP, which is considered to originate from the population response of the AN, was significantly decreased with increasing presentation rate. In contrast, the SP component arising from pre-synaptic sources was found to be unchanged in amplitude, consistent with previous results in humans (Grant et al., 2020; Liberman et al., 2016). We found strong age-related reductions of the CAP amplitude, as well as on the CAP PLV, adding evidence to the hypothesis that AN damage is present in older humans despite clinically near-normal hearing thresholds (Wu et al., 2020).

Previous studies have argued that age-related reductions in the brainstem FFR may be driven by reduced population phase locking in the auditory periphery. To investigate this, we measured neurophonic responses to 250-ms long tone-bursts, presented at 80 dB SPL. ANN responses measured with the EcochG

TM-to-mastoid electrode montage were indeed reduced in the older listeners both at low- (516 Hz) and mid- (1032 Hz) frequencies. As in previous reports, the brainstem FFR to the same stimulation measured in the mastoid-to-vertex montage was also reduced in the older normal-hearing listeners (Clinard and Cotter, 2015; Clinard and Tremblay, 2013; Clinard et al., 2010; Mamo et al., 2016; Märcher-Rørsted et al., 2022; Presacco et al., 2019; Roque et al., 2019). The neurophonic responses captured in the TM-to-mastoid and mastoid-to-vertex montages were both reduced for the low-frequency stimulation, supporting the notion that ANF loss could drive the age-related reductions in the brainstem FFR (Märcher-Rørsted et al., 2022), even though the peripheral contribution to the FFR in the mastoid-to-vertex montage measures is assumed to be minimal.

We also explored responses to short (10 ms) tone bursts that allowed higher presentation levels (100 dB SPL). We found significantly reduced spectral amplitudes of the ANN in the older group at 1032 Hz. It is possible that the reduction observed at 1032 Hz reflects a reduced CM response. Arguably, the neural response at this frequency (1032 Hz) is a superposition of the pre-synaptic CM and the neural generators at the level of the AN. We found decreased OAE amplitudes in the older listeners, indicating OHC dysfunction in the basal parts of the cochlea (Probst et al., 1991; Shera and Guinan, 1999). Furthermore, we found extended high-frequency audiometric threshold elevations in the older listeners. Although modeling work suggests that OHC loss in itself would not decrease the ANN (Märcher-Rørsted et al., 2022), basal OHC loss could reduce the CM. If the pre-synaptic response from the OHCs is significantly reduced and superimposed on the neural ANN, it may lead to false conclusions regarding the origin of the reduced ANN observed here. For short, high-intensity, high-frequency (3096 Hz) tones, it can be assumed that phase-locked responses from both the AN and the brainstem are negligible (Snyder and Schreiner, 1984; Worden and Marsh, 1968). For this condition, we observed a significant effect of age, suggesting lower response amplitudes in the older group. Assuming that this response mainly represents of hair-cell activity, we concluded that the CM is significantly reduced in the older group of listeners. The isolated CM response was though of much lower amplitude (-30 to -40 dB rel 1 mu V), than the ANN amplitude observed at the 1032 Hz condition (20 dB rel 1 muV). Assuming that the amplitude of the CM is of relatively constant amplitude across stimulation frequency (i.e., frequency independent, Snyder and Schreiner, 1984) argues against a significant contribution from a reduced CM response in the ANN

reduction observed here.

We did not find significant age-related reduction in the ANN to short low-frequency tones (516 Hz). The AN population response at this frequency may be less sensitive to AN loss than at ascending nuclei in the auditory system when recording isolated peripheral responses. Enhanced phase locking to the fine-structure of low-frequency tones has been demonstrated in ascending auditory nuclei (i.e., the CN, Joris et al., 1994a,b). When stimulating with lower-frequency, high-intensity tones, the population response of the nerve may, in itself, not be affected significantly, whereas neural generators higher up in the system may suffer, due to decreased AN coincidence across fibers in ascending auditory nuclei (Chanda and Xu-Friedman, 2010; Rothman and Young, 1996). This may explain why FFRs measured at the scalp at lower frequencies demonstrate age-related reductions, but not at the level of the AN. Although intriguing, more isolated measures of AN, CN and IC activity should be investigated.

We found no differences between the participant groups regarding the later waves of the ABR. In particular, the amplitude and PLV of wave-V were comparable between the young and the older listeners. Central processes involved in compensation processes of decreased peripheral input may explain these findings (Caspary et al., 2008). Such effects have been extensively documented for cortical signals evoked by transient or slowly fluctuating stimuli in older normal-hearing and hearing-impaired listeners (e.g., Fuglsang et al., 2020; Goossens et al., 2016; Parthasarathy et al., 2019; Presacco et al., 2016a, 2019). It has also been suggested that transient and sustained responses of subcortical origin result from different mechanisms of temporal processing (Johnson and Brown, 2005). This may suggest that responses to transient stimuli do not capture processing deficits arising at brainstem level.

4.5 Conclusion

The present study investigated neural deficits found in older listeners at the level of the AN using ECochG. The results presented here suggest that age-related ANF loss is reflected both for transient and sustained stimuli when using sensors positioned close to the cochlea. Brainstem FFR amplitudes to sustained tone stimulation were found to be reduced with age, whereas click-evoked ABR wave-V from similar brainstem sources were not. The results further report that the FFR recorded in the far field to low-frequency tones may be sensitive to neural

deficits already at the level of the cochlea, and could be valuable for robust diagnostics of ANF loss in humans.

Acknowledgments

This work was supported by the Novo Nordisk Foundation synergy grant NNF-170C0027872 (UHEAL) and the Oticon Centre of Excellence for Hearing and Speech Sciences (CHESS).

5

Measures of temporal coding in a chinchilla model of noise-induced cochlear synaptopathy [f]

Abstract

Scalp-recorded frequency following responses (FFRs) from the auditory brainstem in humans reduces in amplitude with advancing age. This reduction is also observed in listeners with clinically normal hearing thresholds and could be caused by an age-related decline in temporal processing in the central auditory system. Alternatively, age-related loss of auditory nerve fibers may reduce synchronized activity already in the auditory periphery, and this peripheral loss may also contribute to reduced FFR responses in the brainstem. If primarily driven by peripheral loss, the FFR may have potential diagnostic value as a proxy for cochlear neural degeneration. To investigate the causal effects of cochlear neural loss, we recorded simultaneous brainstem FFR responses and electrocochleography (ECochG) in noise-exposed chinchillas. The chinchillas were exposed to two hours of 100 dB SPL octave-band noise (centered at 1 kHz), producing a significant temporary threshold shift (TTS) measured one day post exposure. Such exposure creates a broad region of significant (up to 50%) cochlear synaptopathy with minimal loss of outer hair cells. The different electrophysiological responses were measured in four exposed chinchillas at least two weeks post exposure. The same recordings were also performed in four unexposed but aged (4-5 years) chinchillas to observe potential age effects.

[f] This chapter is based on Märcher-Rørsted, J.,Hjortkjær, J., Encina-Llamas, G., Dau, T. , & Heinz M., (In preparation). "Interactions between peripheral and central measures of temporal coding in a chinchilla model of noise-induced cochlear synaptopathy".

Four additional unexposed young chinchillas served as controls. FFRs to the carrier frequency of 10-ms tone pulses at low (516 Hz), mid (1032 Hz) and high (4128 Hz) frequencies, presented at sound pressure levels (SPL) ranging from 40 to 80 dB, were recorded. Additionally, responses to clicks from 0-80 dB SPL were also recorded to quantify level-dependent latencies of different sources in the auditory pathway. Both FFR and ECochG responses to the carrier of low (516 Hz) frequency tones were reduced in both exposed and aged animals compared to the controls. Reductions of the phase-independent second harmonic of the tonal carrier (two times the fundamental) were also observed in the ECochG responses, consistent with a neural origin of the reduced response. In contrast, brainstem FFR responses to low-frequency tones showed enhanced amplitude responses for exposed animals compared to aged and control animals. Although this may suggest central compensation, it may be possible that this is a result of phase interactions between peripheral and central generators.

5.1 Introduction

Neural degeneration in the peripheral auditory system may have perceptual consequences when listening in complex acoustic environments. Although many potential diagnostics have been proposed, it still remains unclear whether cochlear synaptopathy, the permanent loss of auditory nerve fiber synapses connecting to inner hair cells (IHC) (Kujawa and Liberman, 2009), can be diagnosed reliably in humans using non-invasive measures. Human scalp electroencephalography (EEG) measures are commonly thought to dominantly reflect cortical and sub-cortical (brainstem) sources. However, frequency-following responses (FFRs) measured with low-frequency tones may be sensitive to neural deficits already at the level of the auditory nerve (AN). In a recent EEG and modeling study, we proposed that age-related reductions in the magnitude of the FFR to high-intensity low-frequency pure tones can be explained by age-related neural degeneration in the cochlear (Märcher-Rørsted et al., 2022). By measuring EEG in young and older listeners with normal audiometric sensitivity and comparing this to a model of the auditory nerve informed by human temporal bone histopathological data (Wu et al., 2020), it was possible to replicate pat-

terns obtained experimentally in relation to age-related auditory nerve fiber (ANF) loss. If phase-locked neural activity in the brainstem is limited by the integrity of the AN, the low-frequency FFR may have diagnostic potential. This, however, remains to be verified. Although this idea points towards a neural deficit in the periphery driving age-related reductions in FFR amplitudes, it is still possible that age-related central deficits (i.e. central de-synchronization) at least partly contribute to such reductions (Anderson et al., 2012; Clinard and Cotter, 2015; Walton, 2010). Examining the consequence of ANF loss on peripheral measures of neural phase locking as well as, simultaneously, the upstream consequence on temporal synchrony in the brainstem would allow disentangling of peripheral and central sources and their relative contribution to age-related FFR reductions. In the present study, we attempted to shed light on this by measuring both scalp EEG and electrocochleography in a chinchilla model of noise induced cochlear synaptopathy.

The chinchilla is a widely used model for a range of hearing related topics (Trevino et al., 2019). The hearing frequency range and sensitivity of the chinchilla, as well as its genetic heterogeneity, make it an ideal model for hearing research compared to other rodents (Miller, 1970). Additionally, the chinchilla has been documented to demonstrate similar age-related cochlear de-generation patterns as in humans (Bohne et al., 1990). Previous studies have demonstrated that a limited dose of noise for a sustained period of time can induce a temporary threshold shift (TTS), which leads to selective cochlear synaptopathy without damaging sensory cells in the cochlea (Henderson et al., 1983; Hickox et al., 2017). By selectively damaging inner hair cell (IHC) afferent transduction channels, it is possible to examine the influence of peripheral neural degeneration on candidate diagnostics.

Measures of peripheral function and neural phase locking have been studied in humans using both invasive and non-invasive measurement techniques (Gibson, 2017; Levine et al., 1992; Moser and Starr, 2016). Typically, transient evoked potentials are used since transient stimulation is ideal for isolating pre-synaptic activity from sensory cells (e.g. the summating potential, SP) from neural activity generated at the level of the AN (e.g. the compound action potential, CAP). The preservation of the SP component in combination with a decrease in the CAP amplitude has been related to peripheral neural degeneration in animals (Earl and Chertoff, 2010; Kujawa and Liberman, 2009) and has been suggested to be sensitive to cochlear synaptopathy in humans (Grant et al., 2020; Liberman

et al., 2016). Although these potentials have previously been studied, it is still unclear how a peripheral loss affects the phase-locking abilities in the auditory midbrain. The steady-state counterparts of the SP and the CAP components are usually defined as the cochlear microphonic (CM) and the auditory nerve neurophonic (ANN). Given that these responses are phase-locked to the stimulus frequency, they allow for the analysis of a longer period of sustained neural activity, which might be more sensitive to small neural changes at the level of the AN.

Using noise as an insult to target isolated AN loss is a common model for studying peripheral neural deficits. Although this is possible in animal studies, quantifying noise exposure over a lifetime in human subjects has proven to be notoriously difficult (Le Prell, 2019). Since aging is thought to be associated with progressive peripheral degeneration that supersede hearing loss (Wu et al., 2019), older human listener with clinically normal hearing can be expected to show signs of AN degeneration. However, there may be fundamental differences on the upstream consequences with these two paths to neural degeneration. While noise insults leave the periphery damaged, the central auditory system is assumed to be intact. In contrast, aging has been shown to introduce deficits in the central system, such as de-myelination (Tremblay et al., 2012) and decreases in the cardiovascular function causing a reduced endocochlear potential. Studying both aging and noise-induced cochlear synaptopathy in animal models is crucial for the validations of the development of robust human diagnostics.

Phase locking in the brainstem has been studied extensively since potentials from sub-cortical sources are more readily acquired with EEG than the peripheral counterparts. Reductions in the auditory brainstem function has been documented in aging humans (Konrad-Martin et al., 2012). However, noise-induced measures of brainstem temporal acuity have been shown to be *enhanced* in animals (Zhong et al., 2014). Although the interpretation of these enhancements has been generally attributed to outer hair cell (OHC) dysfunction (e.g., loss of cochlear compression, Kale and Heinz (2010)), the increase might also be driven by peripheral neural loss. If the periphery is damaged in isolation due to the noise insult, the enhancement observed in the brainstem could be a consequence of interaction between neural generators.

5.2 Materials and Methods

5.2.1 Participants & Experimental design

Data from ten male chinchillas weighing between 400 and 700 g were included in the study. Experiments were conducted to examine both within and across animal effects of noise exposure and aging. The animals were divided into three groups; a control group, an exposure group and an older group. Four unexposed (0-2 years of age) animals constituted the control group. Four awake and unrestrained chinchillas (0-1 years of age) were exposed to 100 dB sound pressure level (SPL) octave-band noise, centered around 1 kHz for 2 hours, to produce a temporary threshold shift (TTS). Previous studies have demonstrated that this noise dose leads to a significant amount of cochlear synaptopathy without damaging sensory cells (Hickox et al., 2017). Two of the exposure group animals

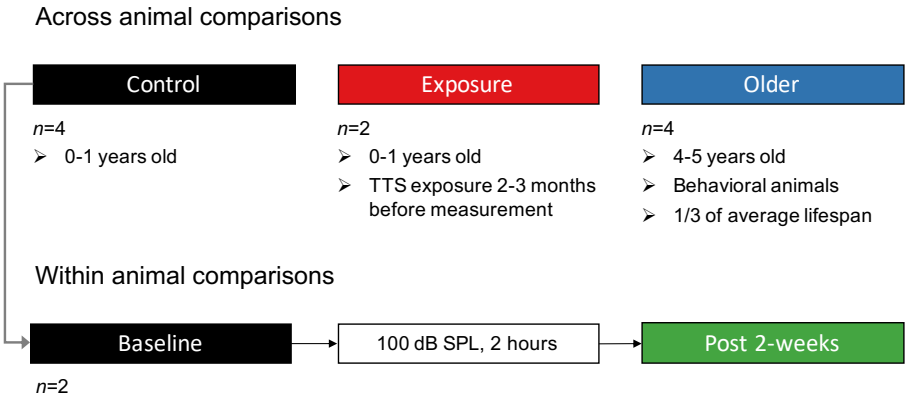

Figure 5.1: Overview of the animals used in this study. Top panel describes the across animal strategy, where as the bottom panel describes within animal strategy.

were exposed to the noise two months prior to the physiological measurements, and therefore had no baseline measurement in the present investigations. The two remaining animals in the exposure group were animals from the control group that were later exposed to the same TTS-inducing noise protocol. Four older chinchillas (4-5 years of age, 1/3 of average lifespan) were treated as the older group. The four older chinchillas were used in a behavioral experiment before participating in the current study, and were therefore not raised in quite.

Figure 5.1 shows the experimental design and an overview of the animals used in the experiment. All measurements took place in a double-walled, electrically shielded, sound-attenuating booth. All experiments were approved by

the Purdue Animal Care and Use Committee (PACUC Protocol No. 111000123).

5.2.2 Awake physiological measures

Prior to the electrophysiological evaluation, we recorded physiological measures in the awake animals. For these measurements, the animals were restrained in a cylindrical tube, terminated with a small hole of approximately the size of the animals' neck. This restricted axial movements of the animal during recording. Head rotation was restricted by a custom adjustable nose holder, which ensured that the animals' head was at a comfortable downwards angle ideal for positioning of the acoustic stimulation system. We used an ER10X measurement system coupled to an ER-2 transducer to deliver acoustic stimuli and record the ear-canal pressure. A custom-integrated system of hardware (Tucker-Davis Technologies and National Instruments) and software (MATLAB) was used for recording and sound delivery. The sample rate was 48 kHz. Prior to the measurements, the transfer function of the ear-canal was recorded. Sound delivery was compensated using an inverse filtering approach, ensuring a flat frequency response of the transducer (e.g., in-ear calibration). The animals were visually monitored during the measurements in real time using a digital camera to ensure that the animal was comfortable, and that airflow was not restricted.

To investigate the status of hearing and the health of OHCs, we measured DPOAEs from 0.5-8 kHz with fixed primary levels (F1 = 65, F2 = 75 dB SPL). Each DPOAE response (2F1 - F1) was estimated based on four presentations of a 1-s long stimulus for each set of primary frequencies. For the noise-exposed animals in the within animal group, DPOAEs were measured prior to the noise exposure, 24 hours after the noise exposure and at two weeks after the noise exposure. This allowed for a quantification of the TTS induced by the insult. Responses were collected for the right ear only in all animals.

The middle-ear muscle reflex (MEMR) has been demonstrated to be sensitive to noise induced as well as age-related cochlear synaptopathy in animals (Bharadwaj et al., 2021; Valero et al., 2016). We measured wideband MEMRs in response to broadband (0.5 -8 kHz) noise elicitors, as described in Bharadwaj et al. (2021). A 90 dB peak equivalent SPL (peSPL) click with a flat power spectrum from 0 to 10 kHz served as the probe. MEMRs were recorded in response to noise elicitors of various levels, ranging from 34 to 94 dB SPL in steps of 6 dB. Each trial consisted of click-noise-click sequences, adapted from Keefe et al. (2017),

with approximately 28 ms of silence between the first probe click and the onset of the elicitor (120 ms), followed by 14 ms of silence before another click was presented. For each elicitor level, we measured a series of 7 clicks, interleaved by noise elicitors. In total, 32 trials of this structure were collected for each elicitor level. A MEMR metric was extracted for each level by comparing the measured frequency transfer function of the middle-ear immittance measured at the first click to the average of clicks 2 through 7. A single MEMR value was then computed for each elicitor level by averaging the absolute value of the change of the ear-canal pressure from 0.5 - 0.2 kHz compared to the first click in the sequence. Offline artefact rejection was performed after the measurement, rejecting trials exceeding ± 2.5 standard deviations from the mean.

5.2.3 Anesthetized electro-physiological recordings

Electrophysiological measures were performed on anesthetized animals. To induce anesthesia, we first injected animals with xylazine (1 mg/kg, subcutaneous (SC)) followed by ketamine (50-65 mg/kg, SC), similar to previous studies in chinchillas (Henry et al., 2011). The animals were monitored continuously after the first injection to ensure uncompromised respiratory function. After full anesthesia, the animals were transported to the recording booth and placed on a thermally-regulated heating pad. The core temperature of the animal was monitored and maintained at 37 °C using a rectal probe. Additionally, we monitored the heart rate and oxygen saturation of the animal using a pulse oximeter system. Eye ointment was used during anesthesia to keep the eyes lubricated. Oxygen was provided through a tube placed near the animals nostrils. During the experiments, the animals were checked for vital signs and stability every 30 minutes. We provided lactated Ringer's solution both before and after the procedure (6 cc, 12 cc in total). After completion of the procedure, we used a xylazine reversal agent atipamezole (0.4 to 0.5 mg/kg intramuscular) to ensure fast recovery from anesthesia. The animals were closely monitored after the procedure until full recovery.

EEG data acquisition

The positioning and referencing strategy of electrophysiological recordings can dictate which neural sources are represented in the acquired response. In order to disentangle activity from peripheral neural generators from more

central generators in the auditory system, we measured non-invasive EEG using two different electrode configurations; a vertical montage, designed to pick up sources up until the auditory brainstem, and a horizontal montage which enhances contributions from peripheral (AN) sources (King et al., 2016).

For the vertical montage, we used three sub-dermal needle electrodes, positioned at the bridge of the nose (common ground), the dorsal mid-line between the eyes (non-inverting, vertex) and posterior to the right pinna (inverting, mastoid), typically used for ABR measurements. The responses were amplified 20.000 times (World Precision Instruments model ISO-80). For the horizontal setup, we used two gold-foil tiptrodes to capture electrical activity in the ear-canals of the animals positioned in the left ear (inverting) and the right ear (non-inverting), also commonly referred to as electrocochleography (ECochG). Common ground was positioned at the bridge of the nose using a sub-dermal needle electrode. Signals in this recording montage were amplified 50.000 times. Figure 5.4 A) and B) illustrates the two recording setups. The signals from both recording setups were filtered in real-time between 0.3 Hz and 3 kHz by analog filters (Stanford Research Systems model SR560). The electrical responses from the two measurement setup were recorded simultaneously and were digitized by a Tucker-Davis Technologies (TDT) system at a sample rate of 48 kHz. Online artefact rejection was performed, rejecting trials exceeding either 0.6 V for the vertical montage, or 3.6 V for the ECochG montage. Online running average waveforms were displayed during the recording to verify correct electrode placement and acceptable noise levels in all recording channels.

Sound delivery was calibrated using a custom insert-earphone tip with an ER7C microphone system. First, ear-canal transfer-functions were measured in the anesthetized animals. We used an inverse filtering approach to account for resonances in the ear canal, ensuring a flat frequency response. Sound was delivered using magnetically and grounded ER-2 insert-earphones.

ABR thresholds and supra-threshold click responses

To ensure that the animals had a normal hearing status, we measured a series of click-evoked ABRs. The animals were presented with 400 trials of clicks (100 μs) of each polarity of levels from 0 to 50 dB SPL, in steps of 10 dB. The presentation rate was 22 Hz. To estimate the hearing threshold of each animal, we used a template cross-correlation approach similar to Henry and Lucas (2010). In short, we used the highest level response waveform (50 dB SPL, 0 to 9 ms) from

the vertical-montage recording as a template of the auditory activity where clear responses to the sound were present. We then cross-correlated this template with the average responses for each of the remaining levels, providing a measure of similarity to the template. Cross-correlation coefficients were then z-scored and normalized between 0 and 1. A cubic spline function was fit to discrete data points, producing a cross-correlation growth function. This was then used to determine the electrophsyiological threshold to the auditory stimulus for each animal. The threshold was defined as the first value of the normalized z-scored cross-correlation coefficient function that exceeded 0.15 (15 %). Estimates were only conducted using data from the vertical EEG montage. Additionally, we measured a series of supra-threshold click responses. Here, the animals were presented with 1000 trials of clicks of each polarity of levels from 40 to 80 dB SPL, in steps of 20 dB. Presentation rate was reduced to 12.5 Hz to minimize neural adaptation. Responses from both montages were collected simultaneously.

The collected responses were further analyzed off-line. Responses were first filtered between 0.2 and 3 kHz using fourth-order butterworth filters, weighted by their inverse variance and averaged (John et al., 2001). The average responses were then demeaned and baseline corrected, by subtracting the mean of the response from -3 to 0 ms before the stimulus onset. To quantify potential deficits in peripheral neural activity, we identified both waves I and II in the ECochG response for the supra-threshold click responses. Peak amplitudes and latencies were visually identified and compared within and across animals.

Frequency-following responses

We collected FFRs to 10 ms tone bursts of low (516 Hz), mid (1032 Hz) and high (4128 Hz) frequencies. The tones were presented at levels from 40 to 80 dB SPL, in steps of 20 dB. For each condition, the animals listened to 1000 trials of each polarity (alternating). The stimulus presentation rate was 12.5 Hz. A 1-ms ramp was applied to the onset and the offset of the tone burst stimuli. Online artefact rejection was performed, rejecting trials exceeding either 0.6 V for the vertical montage, or 3.6 V for the ECochG montage. Online running average waveforms were displayed during the recording to verify the correct electrode placement and acceptable noise levels in all recording channels.

The recorded FFRs were filtered from 0.2 to 10 kHz using fourth-order butterworth filters, weighted by their inverse variance, averaged and demeaned. Average phase dependent ((C-2)/2) and phase-independent ((C+R)/2) responses

were then subjected to a frequency analysis by taking the FFT of the average response of each level and frequency. The spectral amplitude of the phase-dependent response to the stimulus frequency was used as a measure of the stimulus-driven neural phase-locking. For the phase-independent responses, we extracted the spectral amplitude of the second harmonic ($2f_c$) as an estimate of neural phase-locking, since this component has been shown to be minimally contaminated by pre-synaptic responses (Fontenot et al., 2017)). The responses from both vertical and ECochG montage were analyzed separately, and compared to each other.

5.3 Results

5.3.1 Hearing thresholds and OAEs

Extensive damage to OHCs can reduce auditory sensitivity. To ensure that noise exposed and older animals did not show signs of substantial OHC damage, we measured both DPOAEs and ABR thresholds. Figure 5.2 A) shows group-averaged DPOAE results from 0.5 to 8 kHz. We found no apparent differences between the groups for low frequency DPOAEs (0.5 to 1 kHz). In the high-frequency range (6-8 kHz), we observed a slight decrease of the DPOAE amplitude both for the TTS and the older animals, possibly reflecting a small degree of OHC loss in the basal region of the cochlea. For the within animal comparison, we measured DPOAEs at baseline, 24 hours after exposure and two weeks after exposure. Figure 5.2 B) shows DPOAE responses for the two animals used for the within animal comparison. We observed decreased DPOAE amplitudes in the post 24 hour measurement, consistent with results from previous studies (Bharadwaj et al., 2021; Henderson et al., 1983; Hickox et al., 2017). The greatest amplitude reductions were observed above the frequency of the noise band (1 kHz), consistent with previous studies on noise-induced cochlear synaptopathy in other mammals (Kujawa and Liberman, 2009; Kujawa and Liberman, 2015; Liberman and Liberman, 2015; Valero et al., 2016). After two weeks, DPOAE amplitudes recovered to baseline levels, demonstrating that the threshold elevation was temporary (i.e., TTS). Given these results, it was assumed that the animals in the study did not suffer from significant OHC loss.

Auditory thresholds were estimated using click-evoked ABRs. The click ABR relies on broadband synchronization of the neural population response to a

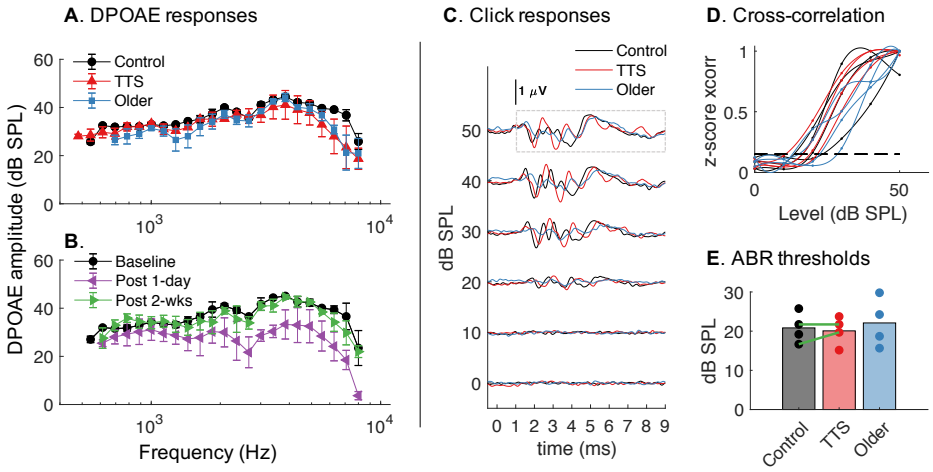

Figure 5.2: **A**) Group average DPOAEs for the control group (black, $n = 4$), TTS exposure group (red, $n = 2$) and older group (blue, $n = 4$). **B**) Within animal average DPOAEs ($n = 2$) for baseline (black), post 1-day exposure (purple) and post-2 week exposure (green) measurements. DPOAE amplitudes are seen to reduced after 1 day, but recover after 2 weeks, demonstrating the TTS effect. **C**) Click responses for clicks ranging from 0 to 50 dB SPL in steps of 10 dB for the control group (black), TTS group (red) and older group (blue). Dashed box indicates the template used for cross-correlation analysis. **D**) Normalized cross-correlation coefficients relative to the template (50 dB SPL) fitted with a cubic spline function. The dashed line shows the cut-off for the ABR threshold (0.15). **E**) ABR thresholds for the three animal groups. Green lines mark the animals used for within animal experiments pre- and post TTS exposure. Error bars show ± SEM.

transient stimulus and thus reflects broadband auditory sensitivity. Figure 5.2 C) shows group averaged ABRs for levels between 0 and 50 dB SPL for the control, TTS and older animals groups. At higher levels, a decrease in latency and an increase in the overall response amplitude were observed. ABR thresholds were estimated using a cross-correlation approach. Figure 5.2 D) shows normalized cross-correlation coefficients between the template (50 dB SPL from 0 to 9 ms) and the remaining levels. Fitted cubic spline functions are illustrated as solid lines for control (black), TTS (red), and older (blue) animals. The dashed line indicates the chosen cut-off value for significant ABR activity (0.15). Figure 5.2 E) shows the estimated threshold for each individual animal, along with group means. The results show that all animals had a click-evoked ABR threshold between 15 and 30 dB SPL. For one of the older animals, the estimated threshold was slightly elevated compared to the other animals (29 dB SPL). The results suggest that both noise exposure and aging did not damage OHCs sufficiently to manifest a substantial sensitivity loss. The green lines in figure 5.2 E) connect the results collected at baseline and two weeks after noise exposure for the two

control animals. Here, minimal threshold elevations were observed for one animal, but were not assumed to indicate OHC-driven effects across animals and groups.

5.3.2 MEMRs

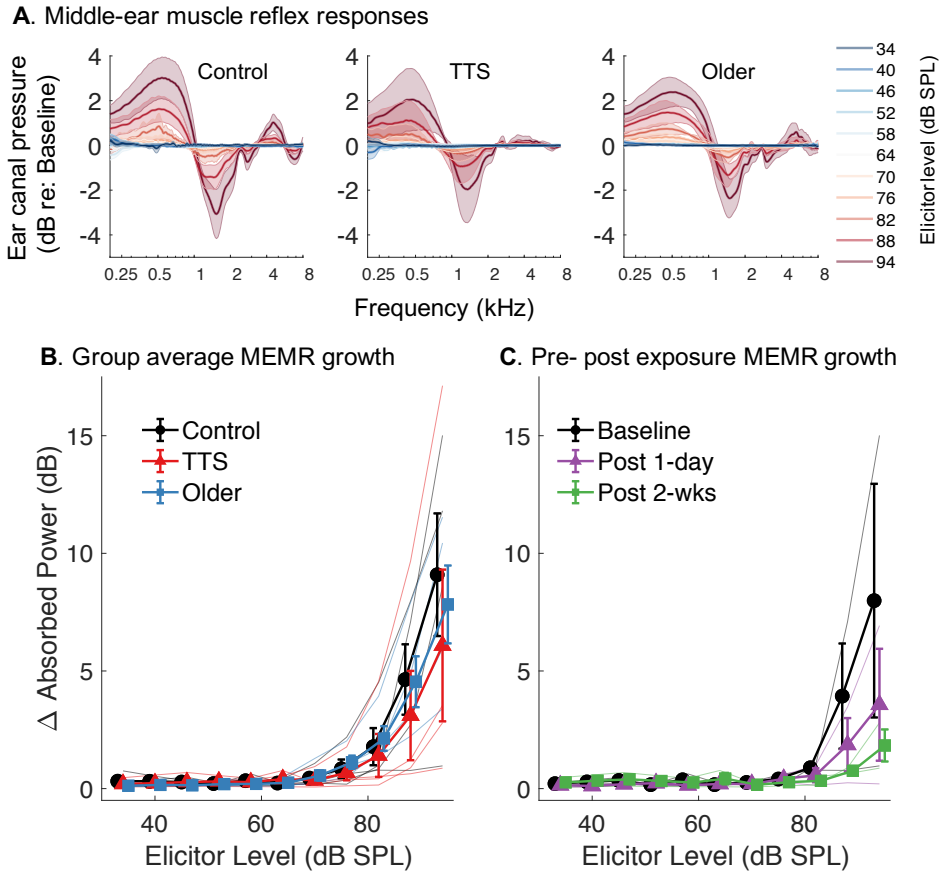

Figure 5.3: **A**) MEMR responses for the control (left), TTS (middle) and older (right) animals. The curves show the measured ear-canal pressure to the probe click, relative to the first click for eleven elicitor levels. **B**) Group average MEMR growth as a function of elicitor level for across animal comparison. Individual responses are indicated by thin solid lines for control (black), TTS (red) and older (blue) animals. **C**) Average pre- and post exposure MEMR for the two within-animal chinchillas. Error bars show ± SEM.

Figure 5.3 A) shows the group-averaged MEMR responses to wideband noise elicitors of various levels ranging from 34 to 94 dB SPL for control (left), TTS (middle) and older (right) animals.

To quantify differences across animals, we computed a MEMR metric by averaging the absolute value of change in ear-canal pressure from 0.5 - 0.2 kHz

at each elicitor level. Figure 5.3 B) and C) show the averaged MEMR growth as a function of the elicitor level for across-animal comparisons and within-animal comparisons, respectively. For the group-averaged measures, we observed a slight decrease of the MEMR growth both for the TTS and the older animals compared to controls. For the within-animal analysis, we observed a greater decrease of the MEMR strength, suggesting that across-animal variability may be a stronger effect than the effect of cochlear synaptopathy on the MEMR. Regarding the within-animal comparisons, we observed a decrease of the MEMR growth after noise exposure both at the post 1-day measurement and after two weeks, confirming previous observations in noise-exposed animal models (Valero et al., 2016).

5.3.3 Vertical and ECochG responses

We sought to disentangle peripheral activity from more central (brainstem) activity by using different electrode montages. Figure 5.4 A) shows an illustration of the horizontal ECochG montage. By utilizing the fact that peripheral activity is highly lateralized with monaural stimulation, the peripheral activity can be isolated by subtracting the potential observed at the contralateral ear. In this way, any activity that is the same at the two recording electrode positions (e.g., the brainstem) will be canceled out. Figure 5.4 B) shows an illustration of the classical vertical montage with electrodes positioned at the ipsilateral mastoid and the vertex, a montage more prone to to pick up both peripheral and central activity.

Figure 5.4 C) shows the grand-average response evoked by a 40 dB SPL click across all animals ($n = 10$) for both recording montages. For the vertical montage, distinct responses are observed representing both early peripheral activity (i.e., ABR wave-I from the AN), and later central sources (i.e., ABR wave-V from the inferior colliculus). The morphology and latency of the response were found to be comparable to previous studies in this species (Henry et al., 2011). As expected, the ECochG montage only shows distinct deflections at latencies closer to the onset of the stimulus (i.e., ABR waves-I and -II), demonstrating that the montage is optimized for peripheral activity. Based on these observations, it is assumed that the two montages will reflect peripheral and central activity differentially, allowing for the disentanglement of peripheral activity from central activity.

Figure 5.4 D) shows the grand-average click responses for levels between 0

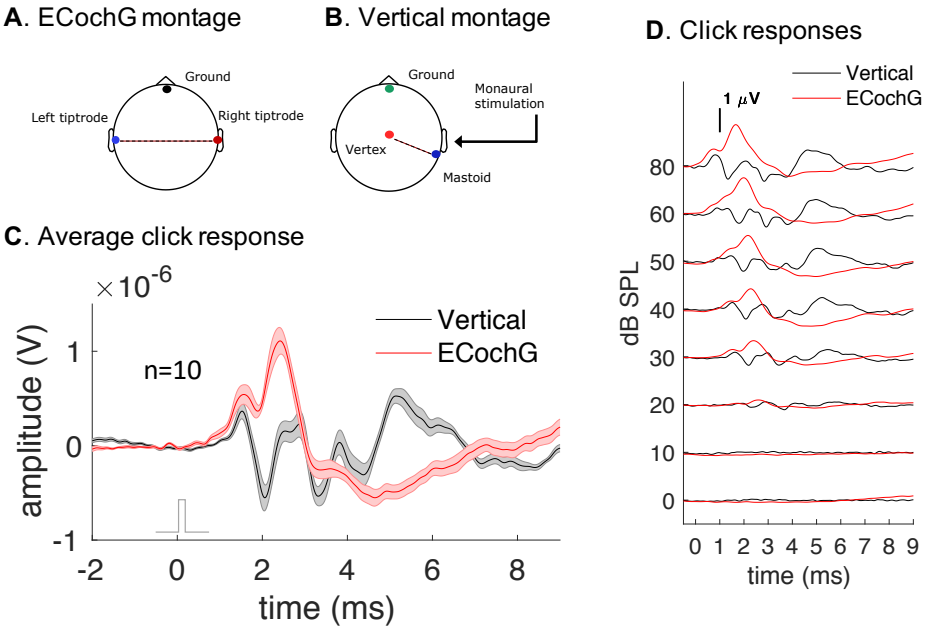

Figure 5.4: **A**) Illustration of the horizontal montage (ECochG) using a subdermal needle electrode at the bridge of the noise (common ground), and two gold-foil tiptrodes in left (inverting) and right (non-inverting) ear canals. **B**) vertical montage with using subdermal needle electrodes at the bridge of the noise (common ground), at the dorsal mid-line between the eyes (vertex, non-inverting) and at posterior to the ipsi-lateral pinna (mastoid, inverting). Sound was always presented monaurally to the right ear. **C**) Grand average click response at 40 dB SPL for the vertical montage (black) and the ECochG montage (red) averaged over all animals ($n = 10$). Error bars show ± SEM. **D**) Click responses for two different montages from 0 to 60 dB in steps of 10 dB SPL and at 80 dB SPL. Traces show grand average responses averaged over all animals.

and 80 dB SPL. As expected, the responses to higher levels show shorter latencies and increased amplitude for both montages.

Effects of TTS and aging on peripheral transient evoked potentials

The first components of the click-evoked ABR have been shown to correlate with the amount of synaptic loss in the cochlea in various animal models. Here, we extracted ABR wave-I and II amplitudes and latencies for each animal for supra-threshold click responses (40-80 dB in steps of 20 dB SPL) for the ECochG montage. Figure 5.5 shows ABR wave-I and II amplitudes and latencies for across- and within-animal comparisons. Figure 5.5 A) shows wave-I amplitude at three levels (40, 60 and 80 dB SPL) for the three animal groups. We observed a slight trend towards higher amplitudes at higher levels, as expected for the peripheral component. Surprisingly, we did not see any clear differences

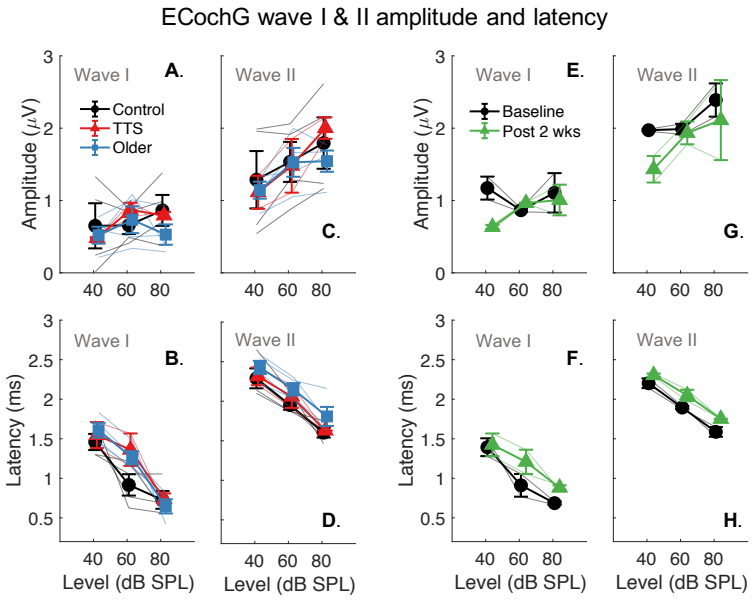

Figure 5.5: Identified wave-I and II amplitude and latency for across group comparison (**A** - **D**) and within animal comparisons (**E** - **H**). Individual animals are plotted as thin solid lines. Error bars show ± SEM.

between the groups. Figure 5.5 B) shows latency estimates of the first wave, demonstrating a decreasing latency with increasing level. Here, we observed that the control group, on average, showed smaller latencies than both the TTS and the older animals. Figure 5.5 C) shows the amplitude growth of wave-II in the ECochG montage. We did not find any clear differences between groups. We noted a substantial amount of variance in the control group (the two highest and the two lowest responses), which might suggest that this metric is inherently noisy across animals. Latency estimates for wave-II can be seen in figure 5.5 D).

Figure 5.5 E-H) show ABR wave-I and II amplitudes and latencies for within-animal comparisons. Here, we observed a general trend towards lower amplitudes and larger latencies for the post 2-week measurement compared to the baseline condition. However, the differences were smaller than what has been reported in previous studies. These results may suggest that evaluating the click-evoked response may exhibit low test-retest reliability.

5.3.4 Pure-tone FFRs

Transient evoked potentials are optimal for approximating latency differences between neural generators in the auditory system, but may not be as sensitive

to neural damage compared to responses evoked by periodic stimuli. To investigate whether sustained responses might be more sensitive to neural pathologies in the periphery, we measured FFRs to short, high-level tone bursts.

Effects of age and TTS across animals

Figure 5.6 A) shows group-averaged phase-dependent ((C-R)/2) FFR responses to a 10 ms, 516 Hz and 80 dB SPL tone burst for the ECochG electrode configuration. A clear response was observed for all three animal groups. However, a decrease in the response amplitude was found for both TTS animals and the older animals, possibly suggesting reduced neural phase locking at the level of the periphery.

To quantify these changes further, we transformed the measured response to the frequency domain, as shown in in figure 5.6 B). Spectral amplitudes at the stimulus frequency were extracted for each animal, and are shown as a function of stimulus level in figure 5.6 C). Consistent with the temporal and spectral analysis at the highest level (80 dB SPL), we observed a decrease of the spectral amplitude for the TTS and the older animals compared to the control animals. The differences were most pronounced at high levels. The corresponding temporal response for the vertical montage is shown in figure 5.6 D). Compared to the ECochG response, we observed a response which showed patterns of phase interaction, possibly suggesting multiple neural generators and non-linear effects (e.g., from harmonic content). Here, we observed differential effects for the two experimental groups. For the TTS animals, an increase in amplitude and a change in the morphology of the response waveform were found compared to the control animals. For the older animals, the overall morphology of the response was preserved, but with decreased amplitude. A spectral analysis confirmed these observations (figure 5.6 E)). Figure 5.6 F) shows the spectral amplitude of the FFR as a function of stimulation level. Again, the differences between groups were most pronounced at the higher presentation level.

Responses that are phase-locked to the frequency of the stimulus may be contaminated by non-neural pre-synaptic responses arising from the sensory cells in the cochlea (i.e., the cochlea microphonic, CM). However, recent modeling suggests that the phase-independent second harmonic of such a response is primarily driven by neural activity, and less contaminated by the CM (Fontenot et al., 2017). To investigate whether the differences observed in the peripheral response (horizontal ECochG montage) were driven by a possible basal hair-cell

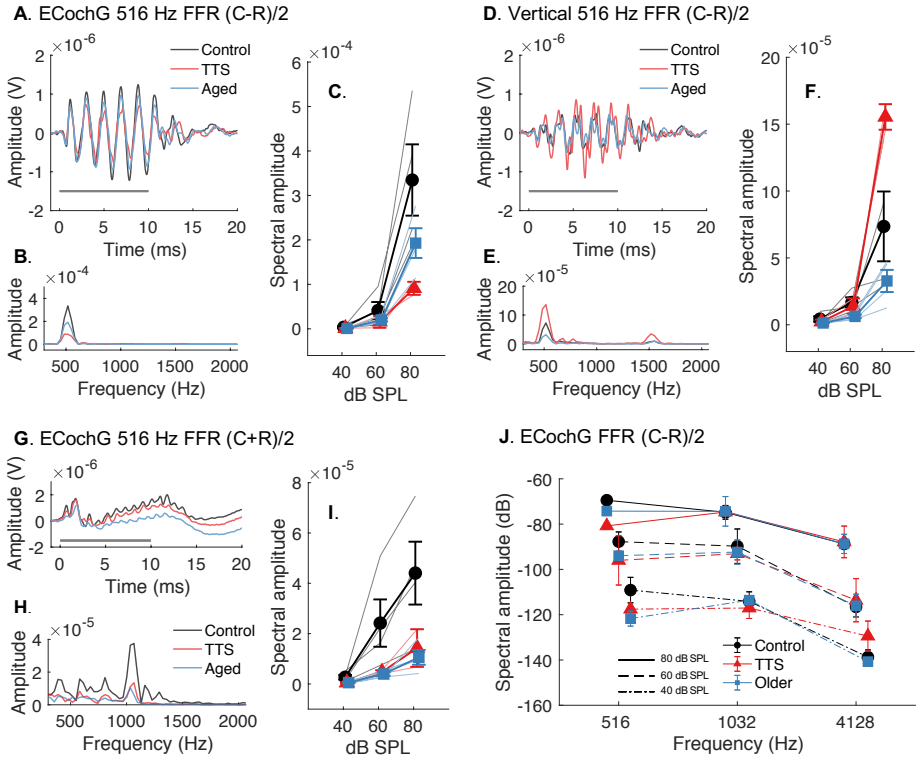

Figure 5.6: Group-average phase-dependent ((C-R)/2) FFR to a 10-ms 516 Hz tone at 80 dB SPL for the ECochG montage (**A**) and vertical montage (**D**). Solid grey line indicates the stimulation period. **B**) and **E**) show the FFT of the temporal waveforms shown in **A**) and **D**). **C**) and **F**) show the spectral amplitude at the frequency of the stimulus as a function of level for the two montages. **G**) Group average phase independent ((C+R)/2) FFR and corresponding frequency spectrum in **H**). **I**) shows the spectral amplitude of the second harmonic ($2f_c$) at a function of level for each group. Individual animal responses are shown in thin solid lines for control (black), TTS (red) and older (blue) chinchillas. **J**) FFR amplitude as a function of frequency for phase-dependent FFR for 40 dB SPL (dotted lines), 60 dB SPL (dashed lines) and 80 dB SPL (solid lines). Error bars show ± SEM.

loss, we computed the phase-independent response to the tone ((C+R)/2). The temporal response waveform obtained with the ECochG montage can be seen in figure 5.6 G), along with its corresponding frequency spectrum (figure 5.6 H)). A dramatic reduction in the second harmonic (1032 Hz) was found in both the TTS and the older group, suggesting that the differences in the phase-dependent analysis are primarily driven by neural deficits. The spectral amplitude of the second harmonic as a function of stimulation level can be seen in figure 5.6 I).

Apart from 516 Hz, we also measured FFRs to mid (1032 Hz) and high (4128 Hz) frequency tones. Figure 5.6 J) shows the spectral amplitude across the three frequencies for 40 (dot-dashed lines), 60 (dashed lines) and 80 (solid lines) dB

SPL for the three animal groups in the phase-dependent ECochG montage configuration. The results suggest that the low-frequency tone is most sensitive to neural deficits associated with TTS and aging, since we did not observe differences for higher frequencies between animal groups.

Effects of TTS within animals

Figure 5.7 shows FFR responses for within-animal comparisons. The peripheral FFR elicited by the 516 Hz tone for the baseline condition, and for the 2-weeks after the noise exposure is shown in figure 5.7 A). We observed consistent re-

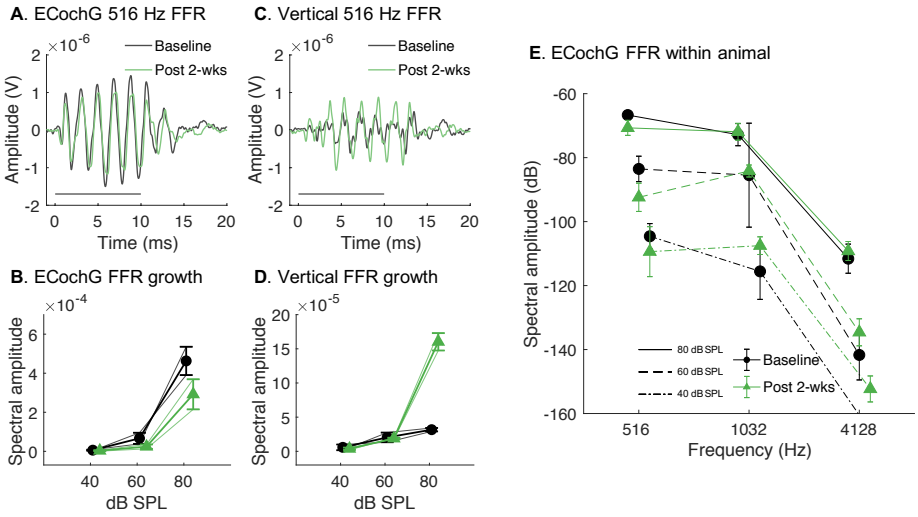

Figure 5.7: Time-domain FFR to the 516 Hz tone for the ECochG (**A**) and vertical (**C**) recording montage for baseline (black) and post 2-weeks noise exposure (green) ($n = 2$). FFR spectral amplitude at the FFR frequency as a function of level for baseline and post 2-weeks measurements for ECochG (**B**) and vertical (**D**) recording montages. **E**) Measured FFR amplitudes as a function of frequency (516, 1032 and 4128 Hz) and level (40, 60 and 80 dB SPL). Error bars show ± SEM.

ductions in the amplitude of the FFR time waveform at 2-weeks post-exposure for both animals. Figure 5.7 B) shows the spectral amplitude of the FFR as a function of level before and after the noise exposure. Individual animals are illustrated by thin solid lines. Figure 5.7 C) shows the FFR recorded from the vertical montage. Here, we see increases in amplitudes and changed FFR waveform morphology, consistent with the across-animal results. The effects of TTS were largest at higher levels. Consistent with the across-animal analysis, we computed the phase-independent response in the ECochG montage and extracted the spectral amplitude of the second harmonic (not shown here). Here,

we also found consistent reductions with TTS, suggesting a neural origin of the reduction. Figure 5.7 E) shows the obtained FFR as a function of frequency and level. Again, the low-frequency and high-level tone produces the most pronounced and consistent effects, also for within-animal comparisons.

5.4 Discussion

It is known that FFRs recorded at the scalp are reduced in older normal-hearing humans. However, it remains unclear whether peripheral neural degeneration at the level of the cochlea could be driving such age-related reductions. The current study investigated this by examining the effect of noise-induced and age-related cochlear synaptopathy on the peripheral- and central FFR in a chinchilla animal model. Peripheral and central responses were isolated using different electrode montages. Click-evoked responses confirmed that peripheral responses, measured with ear-canal tiptrodes (horizontal montage), were primarily driven by more peripheral sources such as the ABR wave-I and II. Central responses recorded from the vertex-to-mastoid (vertical) montage showed more complex morphology. These responses contained peaks (or waves) at later latencies, consistent with more central neural generators in the auditory mid-brain and brainstem.

We found decreased FFR amplitudes to low-frequency tones (516 Hz) in the peripheral ECochG montage for both the exposed and aged animals compared to controls. The effects were primarily observed at high levels (80 dB SPL). These results are consistent with the idea that neural loss is reflected by the peripheral FFR (Märcher-Rørsted et al., 2022). It has been argued that the peripheral response may be contaminated by the pre-synaptic CM response, especially in the chinchilla (Gardi et al., 1979; Hou and Lipscomb, 1977). Although we confirmed normal hearing among exposed and older animal groups, slight differences in high-frequency DPOAE amplitudes might suggest OHC loss and/or dysfunction in basal parts of the cochlea, which could lead to decreased CM responses. Assuming that the CM is superimposed on neural responses generated by the AN, declines in CM amplitude could be misinterpreted as reduced neural activity. To clarify whether the seen reduction was primarily due to a neural or a presynaptic decline, we computed the phase-independent response from the two stimulus polarities. The second harmonic of the phase-independent response has been proposed to primarily be generated by neural elements (Fontenot

et al., 2017). We found strong and consistent reductions of the second harmonic in both the exposed and the aged animals compared to control animals. This may further argue, that the reductions seen in the peripheral FFR are indeed due to a loss of ANF in the cochlea, and not due to the loss of basal OHCs. Although this points towards a neural component driving the reduction, it is still unclear to what extent the CM is contributing to the response. This may be reflected in higher frequency responses where AN phase-locking is minimal and should be dominated by the CM. For high-frequency (4128 Hz) tones, we found no considerable difference between groups, further adding to the interpretation of a neural component driven the differences seen at lower frequencies.

Assuming that the peripheral FFR is affected by neural loss at the level of the cochlea, we sought to investigate causal effects on more centrally-generated responses. If the periphery is driving a central response, we should see reductions at the level of the brainstem, even in young noise-exposed animals where the central auditory system is assumed to be intact. We therefore hypothesized that the central FFR should decrease, similar to results obtained for the peripheral measurements. In line with this hypothesis, we found convincing age-related reductions in the central FFR, consistent with age-related reductions found in previous studies in normal-hearing humans (Anderson et al., 2012; Märcher-Rørsted et al., 2022; Walton, 2010). In contrast to this result, we found enhanced FFRs and higher spectral amplitudes for vertical montage recordings in noise-exposed animals. As the central FFR is thought to be a composite and complex responses from multiple neural generators in the auditory system, the results are not straight-forward to interpret.

Several possible interpretations could explain such findings. Changes in the central auditory system have been documented as a result of severe peripheral intervention (Chambers et al., 2016). This study demonstrated restored brainstem responses, and enhanced cortical responses in cochlear deafferentated mice, which might suggest central plasticity already in sub-cortical structures. Other studies have confirmed similar results in hearing-impaired humans, especially at the level of the auditory cortex (List of studies with central gain).

Another explanation could be in relation to pre-synaptic OHC damage (Zhong et al., 2014). Mid-brain responses to the envelope of amplitude-modulated tones were found to be enhanced in noise, over-exposed chinchillas with threshold elevations (i.e. sensorineural hearing loss). The enhanced coding was considered to be consistent with an increase in the slope of the basilar membrane

growth with level input-output function, associated with OHC dysfunction and a loss of cochlear compression (Kale and Heinz, 2010). This may suggest that OHC loss and/or dysfunction could potentially be responsible for the enhancement seen here. Although the animals were considered to be normal hearing in the present study, it is unknown how subtle OHC dysfunction could influence the central FFR. Assuming that a substantial amount of OHC loss is needed to produce these results might argue against this interpretation.

Lastly, it may be possible that interactions between generators could explain these findings. It is known that the central FFR is composed of multiple, superimposed neural generators. The presence of multiple generators has been argued to produce waxing and waning of the FFR response over frequency, which has been demonstrated in cats (Gardi et al., 1979). In light of this, assuming that the central FFR is composed of both peripheral and central contributions, a reduction of one of these components could lead to a changed balance between the superimposed responses. Selectively reducing one of such generators could lead to altered destructive or constructive interference patterns, possibly leading to an enhanced response at the scalp. Although plausible, isolated responses from OHC, AN and brainstem are needed to confirm this hypothesis, and therefore remains unclear.

The MEMR has been established as a proxy for peripheral neural loss both in noise-exposure models (Bharadwaj et al., 2021; Valero et al., 2016), with age in humans (Bharadwaj et al., 2021; Märcher-Rørsted et al., 2022) and with tinnitus in humans (Wojtczak et al., 2017). In the present study, we found convincing reductions for within-animal comparisons. The MEMR response was reduced after noise-exposure, and was not recovered after 2-weeks, consistent with the TTS found in DPOAE amplitudes, and normal click-evoked ABR thresholds. For across-animal comparisons, we found, on average, reductions in both the aged animals and the noise-exposed animals. However, we noticed a high degree of variability between the animals. This suggests that the MEMR measure is highly influenced by individual differences, which may indicate that this measure is not reliable for across-animal studies unless the number of subjects in sufficiently high. The amplitude of the ABR wave-I has been established as a measure for ANF loss in animal models (Kujawa and Liberman, 2009; Sergeyenko et al., 2013). However, in the present study we did not find convincing differences on the amplitude of wave-I or II across groups or within animals. This may be explained by the presentation level (80 dB SPL), as differences are more readily seen at

higher levels where more fibers in the AN are firing. This may also indicate that sustained responses, such as the FFR measured here, are more robust to individual differences, and are more readily acquired electrophysiological correlates of neural loss in the cochlea. Further experimental data should be collected to confirm these findings. Histopathological analysis of the animals used in this study could be used to confirm the hypothesized loss of AN fibers.

Limitations and future work

The present work consists of exploratory measurements in a small number of animals. To further confirm these findings, a sufficient amount of animals should be measured to provide foundation for proper statistical analysis. Hypotheses concerning the origin of the reduction seen in the peripheral FFR should be further investigated. This could involve more isolated measurements of the population AN response, where the contribution of the CM is assumed to be negligible. Furthermore, effects seen at the level of the brainstem are difficult to interpret. If the enhancement seen in the central FFR is due to interaction between peripheral and central generators, the frequency of the stimulus should in theory influence the destructive or constructive interference pattern. The results here should be reproduced for a larger number of stimulus frequencies, which may readily be modeled to produce either destructive or constructive interference between neural generator sites (e.g., the AN and the brainstem). It still remains unclear whether the peripheral loss is driving the changes seen at the level of the brainstem. Here, more invasive measurements of isolated auditory nuclei should be recorded. Finally, the status of the AN should be confirmed in aged and nose-exposed animals by cochlear histopathology.

5.5 Conclusion

The present study investigated the influence of TTS and aging on measures of peripheral and central phase-locking. We hypothesized that peripheral loss in part could be responsible for changes seen in central temporal processing. We confirmed reduced peripheral and central activity in older animals, in line with previous work in aging humans. However, noise-exposed animals showed enhanced coding of low-frequency tones. Our interpretation implies interactions between peripheral and central generators, not seen in aging individuals, and

my imply that peripheral loss does not influence central processing in a causal manner. These results should be verified with more data.

Acknowledgements

This work was supported by the Novo Nordisk Foundation synergy grant NNF-17OC0027872 (UHeal), Augustinus fonden, William Demant fonden, and Knud Højgaards fond.

6

Overall discussion

This thesis examined the frequency-following response (FFR) to low-frequency pure tones and its potential relation to age-related cochlear neural degeneration. Through a series of electrophysiological experiments, and supported by computational modeling, the results obtained in this thesis suggest a potential value of the FFR as a diagnostic tool. The findings may also provide a valuable basis for further investigations of the relationship between peripheral and central auditory representations of the incoming sound as well as their relationship to perceptual outcome measures.

6.1 Summary of main results

In Chapter 2, the effect of age on the FFR recorded at the scalp was examined in a group of near-normal hearing ($\leq$ 20 dB HL from .125 to 6 kHz) older listeners and a group of young normal-hearing listeners. By stimulating with tonal frequency sweeps between .2 and 1.2 kHz, we confirmed age-related reductions in the phase-locked neural response to the frequency of the tone across a broad frequency range. We confirmed these findings using single-frequency pure tones at low- (326 Hz) and mid-frequency (706 Hz) tones. Although similar results have been reported in previous studies, the interpretation of these age-related reductions has primarily been focused on central effects (Clinard and Cotter, 2015; Clinard and Tremblay, 2013; Clinard et al., 2010; Mamo et al., 2016; Presacco et al., 2019; Roque et al., 2019). We challenged this hypothesis based on simulations obtained with a computation model of the auditory nerve (AN) (Bruce et al., 2018). We informed the model using recent histopathological data from human temporal bones (Wu et al., 2020) and simulated the consequences of different pathologies on the phase-locked AN response. Specifically, we investigated consequences of auditory nerve-fiber (ANF) loss, basal inner hair-cell (IHC) loss and outer hair-cell (OHC) loss. We found that typical age-related ANF loss reduced the simulated AN neurophonic response across frequency,

consistent with the experimental findings from the scalp-recorded EEG. Basal IHC loss also contributed to reduced AN responses, albeit by a smaller amount. Importantly, within the framework of the model, basal OHC loss and loss of sensitivity, which are associated with normal aging, showed only a very small effect on the sustained AN response phase-locked to the pure-tone stimuli. Our interpretation of these results suggested that a peripheral contribution of the age-related reductions observed experimentally in the scalp-recorded FFR is plausible. Given that the AN is a prerequisite for central (i.e. retro-cochlear) phase locking, we argued that the FFR could be sensitive to ANF loss, even if the primary neural generator is in the auditory brainstem. These results contrasted previous interpretations of the reduced FFR in normal or near-normal aging listeners.

Even though our experimental and simulated data from Chapter 2 were consistent, further investigations were undertaken in Chapter 3 to further evaluate the source(s) of an age-related decline in the brainstem FFR. If the FFR is sensitive to cochlear neural degeneration, the FFR should correlate with other measures of AN health. Compared to steady-state responses, the click-evoked auditory brainstem response (ABR) allows time-locked responses from the auditory periphery to be better isolated. In Chapter 3, we therefore compared ABR wave-I and FFR that were recorded in a large cohort of human listeners spanning a large age range (18-76 yrs). The participants had normal or near-normal hearing ($\leq$ 20 dB HL from .250 to 2 kHz). For these listeners, we found a strong age-related reduction of the action potential (AP) component of the ABR (corresponding to wave-I), consistent with previous studies of cochlear synaptopathy (CS) in animal models (Kujawa and Liberman, 2009; Parthasarathy and Kujawa, 2018; Sergeyenko et al., 2013; Shaheen et al., 2015; Valero et al., 2017; Valero et al., 2016) and consistent with the hypothesized neural degeneration in older human listeners (Wu et al., 2020). Importantly, transient evoked otoacoustic emission (TEAOE) amplitudes and summating potential (SP) amplitudes were not correlated with age, suggesting a relatively intact OHC function at lower frequencies in the older normal-hearing listeners. Consistent with the results from Chapter 2, we found an age-related reduction of the signal-to-noise ratio (SNR) of the scalp FFR to a low-frequency tone (326 Hz). To investigate whether the reduction of the FFR_{SNR} could be accounted for by peripheral neural loss, we examined the relationship between the FFR and the AP amplitudes. Here we found that the variance in the AP could explain the variance observed in the

FFR data. However, it is possible that deficits of more central origin co-exist and also contribute to the age-related reduction observed in the FFR. To investigate this, we added age as a factor to the linear model between the FFR and the AP amplitude. Interestingly, age improved the fit of the model, i.e., AP and age both contributed to explaining the variance in the FFR across subjects. This could imply that age-related changes in the FFR reflect both peripheral and central age effects. However, due to the strong covariation between the two measures and age, it was not possible to disentangle their relative contributions based on these results. To further investigate the connection between peripheral and central processing, we considered more direct measures of AN responses to tonal stimuli.

In Chapter 4, we used electrocochleography (ECochG) to measure potentials from the cochlea. By using electrodes positioned on the tympanic membrane (TM, i.e. closer to the cochlea), it was possible to isolate the peripheral AN neurophonic (ANN) to tonal stimuli. We recruited both young and older listeners, all with near-normal hearing ($\leq$ 25 dB HL from .125 to 6 kHz). We sought to disentangle peripheral activity from more central activity by utilizing electrode configurations, where recordings from both a classical montage (mastoid-to-vertex) and an ECochG montage (TM-to-mastoid) were obtained simultaneously, i.e. in response to the same stimulation. Transient evoked responses showed early time-locked components consistent with a cochlear source. Specifically, the compound action potential (CAP) was reduced in amplitude in the older normal-hearing listeners, consistent with age-related cochlear neural degeneration. Transient evoked responses from the auditory brainstem (e.g. wave V of the click ABR) were not significantly reduced with age. We confirmed the findings from Chapters 2 and 3 by investigating FFR responses to longer-duration (250-ms), lower-level tones (80 dB SPL). The older listeners showed a decreased FFR amplitude using the central montage (mastoid-to-vertex), consistent with the results from Chapters 2 and 3. Importantly, FFR amplitudes recorded with the peripheral montage (TM-to-mastoid), where AN activity was isolated, were similarly reduced. This provided further evidence that the reduced scalp FFR in the older listeners may reflect peripheral neural loss. Lastly, we collected responses to short (10-ms) high-intensity (100 dB SPL) tone pulses. This allowed us to isolate phase-locked responses to periodic stimuli at the level of the AN (i.e. the ANN). Here, the older listeners showed a decreased ANN amplitude compared to younger listeners when presenting

a tone at 1032 Hz. Additionally, we controlled for pre-synaptic contributions in the ANN by presenting frequencies above the limit of AN phase locking (i.e. 3096 Hz). Here we found strong age-effects on the cochlear microphonic (CM), yet with a much smaller amplitude than the age-related reductions observed at the lower frequencies (i.e. 1032 Hz) where we expected neural contributions from the AN. Assuming that the amplitude of the CM does not vary significantly with frequency, we concluded that the ANN reductions seen at the lower stimulation frequencies (516 Hz and 1032 Hz) were primarily driven by neural loss and minimally affected by a reduced superimposed CM response.

Although the different experiments reported in Chapters 2-4 consistently demonstrated age-related reductions of the FFR in aging humans, it is not possible to conclude that these reductions are causally related to cochlear neural degeneration. Age-related changes in the central auditory system may still contribute to these reductions. To further investigate the causal influence of AN loss on the scalp FFR, we turned to an animal model of CS. The results of this work were presented in Chapter 5. We used a chinchilla model of temporary threshold shift (TTS) in which a specific prolonged dose of noise exposure induces CS and selective ANF loss without affecting other cochlear structures (i.e. IHCs and OHCs). We found consistent reductions of the FFR in noise-exposed and aged animals for responses at the level of the AN using a horizontal tiptrode montage. Responses collected from a vertical montage (i.e. mastoid to vertex) reflecting more central (brainstem) neural components, were found to be enhanced in the noise-exposed animals, but not in the aged animals. This result, however, could relate to a complex interaction between neural generators in the central FFR response recorded in the chinchilla. If the central FFR is differentially sensitive to age and noise-exposure, this would make diagnosis of noise-induced ANF loss in humans particularly difficult. The results obtained in aged animals, however, confirmed that the FFR is sensitive to age-related ANF loss. Yet, the experiments reported in Chapter 5 were conducted on a small study sample and larger samples would be needed to draw more firm conclusions.

6.2 The FFR as a measure of cochlear neural degeneration

The results from the present studies may suggest the FFR to low-frequency tones as a potential diagnostic measure of age-related ANF loss in humans. The FFR

demonstrates properties that seem attractive in clinical settings. Although ABR wave-I is considered to reflect a direct measure of AN health, it is still not used in the clinical evaluation of ANF loss in clinics. Possible reasons could be due to the large variability within- and across-subjects due to the low test/retest reliability (Beattie, 1988; Lauter and Loomis, 1988). Reduced ABR wave-I amplitudes due to cochlear neural loss may be superimposed by variations due to sex, head size (Mitchell et al., 1989) as well as variations of physiological background noise. Additionally, the identification of the ABR wave peaks and their amplitudes typically requires a subjective inspection of the data.

In contrast, the FFR is relatively easy to analyze and the frequency-based FFT analysis used throughout this thesis allowed for noise-floor corrected readouts, the SNR, that may be more robust to individual differences in physiological noise and may be more robust in test-retest evaluations. Although plausible, this remains to be evaluated in more detail. Additionally, due to the periodic nature of the stimuli used here, it is possible to obtain responses over longer stimulation periods, in contrast to responses to transient sounds where the response to single pulses is usually considered as the outcome measure. With longer stimulation periods, it is possible to record the FFR at lower SPLs (80-90dB) compared to the ABR that typically requires levels well above 100 dB peak-to-peak equivalent SPL. Furthermore, pure tone stimulation may be especially suited for clinical settings, since it is relatively simple to account for loss of audibility in hearing-impaired patients which is difficult when stimulating with broadband stimuli like noises and transients. These aspects may suggest that the FFR could be an interesting complimentary measure to the ABR wave-I in clinical settings.

Chapter 3 suggested that the variation in the FFR across subjects in a large aging group cannot be explained exclusively by the AP amplitude. We observed that the variance in the FFR_{SNR} was better explained when age was included in the linear model. Several possibilities could explain this finding. While it may be possible that age-related changes in the central auditory system (i.e. central desynchronization) represent a separate source of the reduced response, it may also be possible that an age-related peripheral effect, not captured by the AP, is responsible. Indeed, transient and sustained responses of subcortical origin have been suggested to result from different mechanisms of temporal processing (Johnson and Brown, 2005). Thus, responses to transient stimuli and sustained stimuli may not capture processing deficits in a similar manner,

also at the level of the AN. The FFR may therefore capture aspects of ANF loss that the transient evoked response like the ABR wave-I does not.

Non-electrophysiological measures have also been proposed as proxies for ANF loss, in particular the middle-ear muscle reflex (MEMR). Chapters 2, 3 and 5 demonstrated reduced MEMR growth functions in older individuals. However, we observed a considerable amount of variability in the MEMR measures, and conclusions could only be drawn on a listener group level. Although this variability may reflect relevant effects of noise exposure, especially in young normal-hearing listeners, the results from the investigations presented here did not find such relations (i.e. NESI and TTS scores did not correlate with MEMR growth in younger ($\leq$ 30 years of age) listeners in Chapter 3. Our results indicate that the MEMR is not a robust metric of ANF loss on an *individual* level, at least with the equipment used in our investigations.

In all of the human-listener experiments performed in this thesis, we measured elevated extended high-frequency (EHF) audiometric thresholds in the older listeners with relatively normal low-frequency thresholds. The results from Chapter 3 demonstrated a strong correlation between the age of the participants and their pure-tone average (PTA) at EHFs (8 to 16 kHz). Histopathological data suggest that a combination of IHC, OHC and AN damage is likely to co-exists in the cochlear base in older humans. An important question is therefore whether a basal loss of hair cells drives the observed age-related reductions in the electrophysiological measures, even when presenting stimuli at lower frequencies. Efforts have been made to mask the effect of basal loss and the results of Carcagno and Plack (2020) suggest that high-frequency masking noise might eliminate age-related effects on the supra-threshold ABR and FFR. However, our simulations reported in Chapter 2 suggested that OHC damage does not affect the phase-locked response at the level of the AN. Other simulation studies have also indicated that isolated OHC loss/dysfunction does not influence the amplitude of the supra-threshold ABR wave-I (Buran et al., 2022; Verhulst et al., 2018). These modelling results suggest, that OHC loss is unlikely to account for the reductions observed in the obtained evoked responses. Histopathological data suggest that IHC loss is most pronounced at basal areas of the cochlea, and that ANF loss tends to be of broadband character. While OHC loss may not affect the FFR or ABR response, the masking of basal IHC and ANF activity may be sufficient to eliminate age-related reductions. Although OHC loss in itself may not influence the AN response at high intensities, it is possible that

a reduced presynaptic response (i.e. the CM), superimposed on an intact AN response, reflects age-related reductions, at least for the FFR. However, the results from Chapter 4 suggested that the reduction of the CM amplitude, which is superimposed on the ANN, is negligible compared to the ANN. Based on this, we argue that the age-related reductions observed throughout this work are not driven by basal OHC loss and reduced CM responses. Despite these results, the consistent elevation of EHF thresholds seen in older listeners may suggest that basal loss of OHC could be correlated with a more apical ANF loss (i.e. at lower frequencies), and EHF thresholds may be indicative of ANF loss at mid-frequency regions, as has been suggested by others (Liberman et al., 2016). While this point remains to be verified, the work presented here may argue for this relation.

6.3 The connection between FFR and EFR studies

We have considered responses to sustained tonal stimuli as potential measures of neural loss at the level of the cochlea. Historically, many studies have investigated the envelope following response (EFR) to amplitude modulated (AM) pure-tones instead of FFRs to the carrier of tonal stimuli (with a flat temporal envelope). The choice of AM EFRs originated from investigations of CS in animal models. Experiments by Shaheen et al. (2015) investigated the effect of CS on peripheral temporal processing using EFRs in cochlear synaptopathic mice. Due to the high-frequency hearing range of the mouse and the fact that ANF loss was primarily observed in basal cochlear regions (i.e. between 16 and 64 kHz), high-frequency tone carriers were employed. Since the AN cannot phase-lock to such high-frequency carriers, lower-frequency (0.4 to 1.4 kHz) amplitude modulations (AMs) were imposed. The study found significantly reduced EFR responses across a broad range of AM frequencies (from .8 to 1.4 kHz) for high carrier frequencies (32 kHz) where a significant amount of ANF loss was observed.

Similar EFR measures of modulation processing and their relation to perception were afterwards pursued in electrophysiological studies in humans. Bharadwaj et al. (2015) adapted the EFR metric and argued that temporal processing reflected in EFR measures may be related to behavioral outcome measures, such as spatial hearing performance. Although the study found a relationship between spatial attention performance and EFR amplitudes, the connection

to peripheral neural loss remained unclear. Other studies used EFRs imposing different modulation depths on a tonal or noise carriers (Encina-Llamas et al., 2019; Garrett and Verhulst, 2019). The rationale behind using different modulation depths arose due to data from guinea pigs (Furman et al., 2013), where low-spontaneous rate (LSR) ANFs were found to be selectively damaged by noise exposure while mid- and high-spontaneous rate fibers where left intact. Given that LSR fibers are responsible for the coding of high intensities, it was proposed that shallow modulation depths EFRs at high intensities would be especially sensitive to the loss of low-spontaneous rate fibers. However, the findings from these studies did not provide clear evidence that low modulation depths are particularly sensitive to peripheral neural loss. More recent data from mice indicated that low-SR fibers may, in fact, not be selectively damaged by noise exposure as previously argued (Suthakar and Liberman, 2021). Vasilkov et al. (2021) optimized the use of EFRs to ramped noise pulses, based on computational modeling, and showed consistent age-related reductions. It remains to be explored to what extent the results obtained with tonal FFR vs (high-frequency) carriers containing modulations at similar frequencies as the FFR tones reflect similar mechanisms sensitive to cochlear degeneration. In the data reported in Chapter 3, we observed greater age-related FFR reductions compared to EFR reductions, but with the caveat that the EFRs were recorded with fewer repetitions, using a single polarity and employing lower stimulation levels. Simulations using both stimulus types may also contribute to a better understanding here.

While controlled noise exposure and aging lead to frequency-specific basal CS and ANF loss in animal models, histopathology in humans has suggested a broadband ANF loss (Wu et al., 2020). Higher-frequency EFRs (above 100 Hz), which are considered to be of brainstem origin, usually require high frequency carriers (e.g. a 4 kHz pure tone Bharadwaj et al. (2015), Garrett and Verhulst (2019), and Vasilkov et al. (2021)) to avoid resolved modulation sidebands. When using relatively high-frequency carriers, stimulation occurs at basal areas of the cochlear (i.e. at and above 4 kHz) and upward spread of excitation, particularly at high stimulus intensities, dominates in the basal part of the cochlea. However, if it is assumed that ANF loss extends towards apical cochlear areas, the low-frequency FFR may be a more sensitive measure of population ANF loss across frequency. Since it is possible to stimulate more apically, high-intensity low-frequency pure-tones arguably excite a larger population of ANFs than EFRs

obtained with high carrier frequencies (Dau, 2003). EFRs can also be obtained with broadband carriers, such as broadband noise. However, such carriers contain random intrinsic envelope fluctuations (e.g., Dau et al. (1997, 1999)) that are superimposed with the applied envelope frequency of interest (e.g. 100 Hz). This, in turn, can be expected to mask the EFR SNR, particularly at those high envelope frequencies commonly considered to investigate correlates of CS. The FFR elicited by a high-level low-frequency tone, on the other hand, is dominated by the sinusoidal activation across cochlear frequency. Given these considerations, the low-frequency FFR may be more sensitive to the relatively broad band ANF loss, assumed to occur in humans.

6.4 Limitations of the study

This series of studies undertaken in this work provided evidence that age-related reductions in the FFR are related to neural deficits already at the level of the cochlea. However, this conclusion is based on different assumptions that could be challenged. In particular, in the presented studies we assumed that ANF loss is directly linked to the age of the subject. For humans, this assumption is based on reasonably sparse histopathological data from human temporal bones. The AN status of the individual listeners is likely to display a considerable variability, also within similarly aged subjects. Even if the FFR reductions should be dominated by age-related ANF loss, the underlying ground truth of AN health remains unknown. In animal models, it is possible to confirm ANF loss and verify findings, but this is impossible in human subjects. A solid direct *in vivo* measure of AN health in individual subjects is needed to evaluate the proposed correlates of ANF loss. Emerging cochlear imaging may present possibilities in this direction. However, until convincing correlations between cochlear neural health and electrophysiological measures are made, all measures of ANF loss in humans, such as the far-field gross potentials considered here (even with closely placed electrodes), remain indirect.

Regarding electrophysiological measures, it is commonly assumed that differences between the electrical potentials recorded from the ear-canal vs. the scalp mainly reflect differences resulting from the different generators 'seen' by the sensors (i.e. electrodes) and outweigh differences due to confounding factors. However, it has been shown that electrophysiological recordings are highly variable due to various factors, like sex and head size (Mitchell et al., 1989).

Although this is known, these factors are often assumed to be negligible. The degree to which individual differences due to small differences in physiology or anatomy affect the outcomes of this work is unclear and should be carefully addressed in future investigations. Furthermore, we assumed throughout our studies that the state of attention, relaxation and vigilance is the same for all participants. It has been suggested that neural responses already at the level of the brainstem are affected by attention (Forte et al., 2017) and have been shown to be enhanced in musically trained individuals (Wong et al., 2007). These aspects contribute to the uncertainty when interpreting the experimental results collected in this work.

The present study focused on age as a reliable marker of ANF loss. However, there may be other confounding effects that are related to age that may have contributed to the observed reduced electrophysiological responses. Aging is a complex process and arguably causes multiple aspects of sensory neural circuits to change their function (Tremblay et al., 2012). Age-related neural degeneration in the cochlea is likely to co-occur with the degeneration of the stria vascularis, cardiovascular effects, as well as degeneration processes in the central auditory system. One should thus be cautious to make strong conclusions about connections between electrophysiological measures and years of age.

6.5 Perspectives and outlook

The perspectives of diagnosing cochlear neural loss are exciting and promising. Although it has been shown that peripheral axons of ANFs are detached from cochlear ribbon synapses due to acoustic over exposure, therapeutic intervention may be possible (Suzuki et al., 2016). The fact that the central axon of the AN does not deteriorate as quickly as the peripheral axon may open for therapeutics that promote reattachment of the disconnected nerve fibers. Recent evidence in animal models suggested the use of neurotrophins (NT-3) to keep the peripheral axon alive (Cassinotti et al., 2022; Stankovic, 2004; Wan et al., 2014) and demonstrated that it is possible to re-attach synapses to the IHCs. In connection to potential corresponding interventions in humans, robust and non-invasive assessments of the status of the AN would be crucial. Furthermore, it has been shown that early-age noise exposure and associated ANF damage can lead to accelerated clinical hearing loss (i.e. loss of OHCs and IHCs) in

animal models. To prevent further damage in young individuals, the early diagnosis of such loss could be used to advise against further noise exposure and/or treatment possibilities. The FFR measure presented in this series of studies may further advance our understanding of the consequence of ANF loss and, in turn, may push investigations further to find reliable robust diagnostics of ANF loss in people.

6.6 Conclusion

This thesis presented a series of experiments examining age-related changes in FFR to low-frequency pure tones and its potential relation to cochlear neural degeneration. We consistently observed age-related reductions of the FFR to low-frequency pure tones through a number of electrophysiological investigations. Our experimental findings were consistent with computational simulations of AN activity, which were argued to be able to account for the reductions of phase-locked neural activity at the level of the auditory brainstem. Electrocochleographic recordings obtained from the tympanic membrane provided further evidence that population-level neurophonic responses are reduced at the level of the AN in aging humans. If the AN is a prerequisite for intact brainstem phase locking, tonal stimuli might provide diagnostic value beyond what can be measured using transient evoked responses. Although the evidence presented here is consistent, there may be other age-related factors responsible for reduced FFR responses in humans. The degree to which the FFR captures ANF loss in aging humans still needs to be validated by structural measures of AN health.

Bibliography

Abdala, C. and R. C. Folsom (1995). "Frequency contribution to the click-evoked auditory brain-stem response in human adults and infants". In: *J. Acoust. Soc. Am.* 97.4, pp. 2394–2404.

Aiken, S. J. and T. W. Picton (2008). "Envelope and spectral frequency-following responses to vowel sounds". In: *Hear. Res.* 245.1-2, pp. 35–47.

Anderson, S., A. Parbery-Clark, T. White-Schwoch, and N. Kraus (2012). "Aging Affects Neural Precision of Speech Encoding". In: *J. Neurosci.* 32.41, pp. 14156–14164.

Beattie, R. C. (1988). "Interaction of Click Polarity, Stimulus Level, and Repetition Rate on the Auditory Brainstem Response". In: *Scand. Audiol.* 17.2, pp. 99–109.

Benjamini, Y and Y Hochberg (1995). "Controlling the False Discovery Rate : A Practical and Powerful Approach to Multiple Testing". In: *Society* 57.1, pp. 289–300.

Bharadwaj, H. M., S. Masud, G. Mehraei, S. Verhulst, and B. G. Shinn-Cunningham (2015). "Individual Differences Reveal Correlates of Hidden Hearing Deficits". In: *J. Neurosci.* 35.5, pp. 2161–2172.

Bharadwaj, H. M., A. R. Mai, J. M. Simpson, I. Choi, M. G. Heinz, and B. G. Shinn-Cunningham (2019). "Non-Invasive Assays of Cochlear Synaptopathy – Candidates and Considerations". In: *Neuroscience* 407, pp. 53–66.

Bharadwaj, H. M., S. Verhulst, L. Shaheen, M. C. Liberman, and B. G. Shinn-Cunningham (2014). "Cochlear neuropathy and the coding of supra-threshold sound". In: *Front. Syst. Neurosci.* 8.February, pp. 1–18.

Bharadwaj, H. M. et al. (2021). "Cross-Species Experiments Reveal Widespread Cochlear Neural Damage in Normal Hearing". In: *bioRxiv*.

Bidelman, G. M. (2015). "Multichannel recordings of the human brainstem frequency-following response: Scalp topography, source generators, and distinctions from the transient ABR". In: *Hear. Res.* 323, pp. 68–80.

Bidelman, G. M. (2018). “Subcortical sources dominate the neuroelectric auditory frequency-following response to speech”. In: *Neuroimage* 175.March, pp. 56–69.

Bidelman, G. M., J. W. Villafuerte, S. Moreno, and C. Alain (2014). “Age-related changes in the subcortical-cortical encoding and categorical perception of speech”. In: *Neurobiol. Aging* 35.11, pp. 2526–2540.

Blackburn, H. L. and A. L. Benton (1957). “Revised administration and scoring of the Digit Span Test.” In: *J. Consult. Psychol.* 21.2, pp. 139–143.

Bohne, B. A., M. M. Gruner, and G. W. Harding (1990). “Morphological correlates of aging in the chinchilla cochlea”. In: *Hear. Res.* 48.1-2, pp. 79–91.

Bramhall, N. F., G. P. McMillan, and S. D. Kampel (2021). “Envelope following response measurements in young veterans are consistent with noise-induced cochlear synaptopathy”. In: *Hear. Res.* 408, p. 108310.

Bramhall, N. et al. (2019). “The search for noise-induced cochlear synaptopathy in humans: Mission impossible?” In: *Hear. Res.* 377, pp. 88–103.

Brand, T. and V. Hohmann (2002). “An adaptive procedure for categorical loudness scaling”. In: *J. Acoust. Soc. Am.* 112.4, pp. 1597–1604.

Bruce, I. C., Y. Erfani, and M. S. Zilany (2018). “A phenomenological model of the synapse between the inner hair cell and auditory nerve: Implications of limited neurotransmitter release sites”. In: *Hear. Res.* 360, pp. 40–54.

Bruce, I. C., M. B. Sachs, and E. D. Young (2003). “An auditory-periphery model of the effects of acoustic trauma on auditory nerve responses”. In: *J. Acoust. Soc. Am.* 113.1, pp. 369–388.

Brungart, D. S. et al. (2019). “Relationship Between Subjective Reports of Temporary Threshold Shift and the Prevalence of Hearing Problems in Military Personnel”. In: *Trends Hear.* 23, p. 233121651987260.

Buran, B. N., G. P. McMillan, S. Keshishzadeh, S. Verhulst, and N. F. Bramhall (2022). “Predicting synapse counts in living humans by combining computational models with auditory physiology”. In: *J. Acoust. Soc. Am.* 151.1, pp. 561–576.

Carcagno, S. and C. J. Plack (2020). “Effects of age on electrophysiological measures of cochlear synaptopathy in humans”. In: *Hear. Res.* 396, p. 108068.

Caspary, D. M., L. Ling, J. G. Turner, and L. F. Hughes (2008). “Inhibitory neurotransmission, plasticity and aging in the mammalian central auditory system”. In: *J. Exp. Biol.* 211.11, pp. 1781–1791.

Cassinotti, L. R. et al. (2022). “Cochlear Neurotrophin-3 overexpression at mid-life prevents age-related cochlear synaptopathy and slows age-related hearing loss”. In: *bioRxiv*.

Chambers, A. R. et al. (2016). “Central Gain Restores Auditory Processing following Near-Complete Cochlear Denervation”. In: *Neuron* 89.4, pp. 867–879.

Chanda, S. and M. A. Xu-Friedman (2010). “A Low-Affinity Antagonist Reveals Saturation and Desensitization in Mature Synapses in the Auditory Brain Stem”. In: *J. Neurophysiol.* 103.4, pp. 1915–1926.

Choudhury, B. et al. (2012). “Intraoperative Round Window Recordings to Acoustic Stimuli From Cochlear Implant Patients”. In: *Otol. Neurotol.* 33.9, pp. 1507–1515.

Clinard, C. G. and C. M. Cotter (2015). “Neural representation of dynamic frequency is degraded in older adults”. In: *Hear. Res.* 323, pp. 91–98.

Clinard, C. G. and K. L. Tremblay (2013). “Aging Degrades the Neural Encoding of Simple and Complex Sounds in the Human Brainstem”. In: *J. Am. Acad. Audiol.* 24.7, pp. 590–599.

Clinard, C. G., K. L. Tremblay, and A. R. Krishnan (2010). “Aging alters the perception and physiological representation of frequency: Evidence from human frequency-following response recordings”. In: *Hear. Res.* 264.1-2, pp. 48–55.

Dau, T. (2003). “The importance of cochlear processing for the formation of auditory brainstem and frequency following responses”. In: *J. Acoust. Soc. Am.* 113.2, pp. 936–950.

Dau, T., B. Kollmeier, and A. Kohlrausch (1997). “Modeling auditory processing of amplitude modulation. I. Detection and masking with narrow-band carriers”. In: *J. Acoust. Soc. Am.* 102.5, pp. 2892–2905.

Dau, T., J. Verhey, and A. Kohlrausch (1999). “Intrinsic envelope fluctuations and modulation-detection thresholds for narrow-band noise carriers”. In: *J. Acoust. Soc. Am.* 106.5, pp. 2752–2760.

Dau, T., O. Wegner, V. Mellert, and B. Kollmeier (2000). “Auditory brainstem responses with optimized chirp signals compensating basilar-membrane dispersion”. In: *J. Acoust. Soc. Am.* 107.3, pp. 1530–1540.

Delorme, A. and S. Makeig (2004). “EEGLAB: an open source toolbox for analysis of single-trial EEG dynamics including independent component analysis”. In: *J. Neurosci. Methods* 134.1, pp. 9–21.

Dobie, R. A. and M. J. Wilson (1996). " A comparison of t test, F test, and coherence methods of detecting steady-state auditory-evoked potentials, distortion-product otoacoustic emissions, or other sinusoids ". In: *J. Acoust. Soc. Am.* 100.4, pp. 2236–2246.

Don, M., C. W. Ponton, J. J. Eggermont, and A. Masuda (1993). "Gender differences in cochlear response time: An explanation for gender amplitude differences in the unmasked auditory brain-stem response". In: *J. Acoust. Soc. Am.* 94.4, pp. 2135–2148.

Don, M., C. W. Ponton, J. J. Eggermont, and A. Masuda (1994). "Auditory brainstem response (ABR) peak amplitude variability reflects individual differences in cochlear response times". In: *J. Acoust. Soc. Am.* 96.6, pp. 3476–3491.

Dynes, S. B. and B. Delgutte (1992). "Phase-locking of auditory-nerve discharges to sinusoidal electric stimulation of the cochlea". In: *Hear. Res.* 58.1, pp. 79–90.

Earl, B. R. and M. E. Chertoff (2010). "Predicting Auditory Nerve Survival Using the Compound Action Potential". In: *Ear Hear.* 31.1, pp. 7–21.

Encina-Llamas, G., T. Dau, and B. Epp (2021). "On the use of envelope following responses to estimate peripheral level compression in the auditory system". In: *Sci. Rep.* 11.1, p. 6962.

Encina-Llamas, G., J. M. Harte, T. Dau, B. Shinn-Cunningham, and B. Epp (2019). "Investigating the Effect of Cochlear Synaptopathy on Envelope Following Responses Using a Model of the Auditory Nerve". In: *JARO - J. Assoc. Res. Otolaryngol.* 20.4, pp. 363–382.

Fernandez, K. A., P. W. C. Jeffers, K. Lall, M. C. Liberman, and S. G. Kujawa (2015). "Aging after Noise Exposure: Acceleration of Cochlear Synaptopathy in "Recovered" Ears". In: *J. Neurosci.* 35.19, pp. 7509–7520.

Ferraro, J. (1998). *Electrocochleography.Current Opinion in Otolaryngology & Head and Neck Surgery*. Volume 6, pp. 338–341.

Fontenot, T. E., C. K. Giardina, and D. C. Fitzpatrick (2017). "A model-based approach for separating the cochlear microphonic from the auditory nerve neurophonic in the ongoing response using electrocochleography". In: *Front. Neurosci.* 11.OCT, pp. 1–18.

Forte, A. E., O. Etard, and T. Reichenbach (2017). "The human auditory brainstem response to running speech reveals a subcortical mechanism for selective attention". In: *bioRxiv*, pp. 1–12.

Frisina, R. D. (2001). “Subcortical neural coding mechanisms for auditory temporal processing”. In: *Hear. Res.* 158.1-2, pp. 1–27.

Frisina, R. D. and R. D. Frisina (1997). “Speech recognition in noise and presbycusis: Relations to possible neural mechanisms”. In: *Hear. Res.* 106.1-2, pp. 95–104.

Fu, Z., H. Yang, F. Chen, X. Wu, and J. Chen (2019). “Brainstem encoding of frequency-modulated sweeps is relevant to Mandarin concurrent-vowels identification for normal-hearing and hearing-impaired listeners”. In: *Hear. Res.* 380, pp. 123–136.

Fuglsang, S. A., J. Märcher-Rørsted, T. Dau, and J. Hjortkjær (2020). “Effects of Sensorineural Hearing Loss on Cortical Synchronization to Competing Speech during Selective Attention”. In: *J. Neurosci.* 40.12, pp. 2562–2572.

Furman, A. C., S. G. Kujawa, and M. C. Liberman (2013). “Noise-induced cochlear neuropathy is selective for fibers with low spontaneous rates”. In: *J. Neurophysiol.* 110.3, pp. 577–586.

Gardi, J., M. Merzenich, and C. McKean (1979). “Origins of the Scalp-Recorded Frequency-Following Response in the Cat”. In: *Int. J. Audiol.* 18.5, pp. 353–380.

Garrett, M. and S. Verhulst (2019). “Applicability of subcortical EEG metrics of synaptopathy to older listeners with impaired audiograms”. In: *Hear. Res.* 380, pp. 150–165.

Gatehouse, S. and W. Noble (2004). “The Speech, Spatial and Qualities of Hearing Scale (SSQ)”. In: *Int. J. Audiol.* 43.2, pp. 85–99.

Gibson, W. P. (2017). “The Clinical Uses of Electrocochleography”. In: *Front. Neurosci.* 11.

Gleich, O., P. Semmler, and J. Strutz (2016). “Behavioral auditory thresholds and loss of ribbon synapses at inner hair cells in aged gerbils”. In: *Exp. Gerontol.* 84, pp. 61–70.

Goossens, T., C. Vercammen, J. Wouters, and A. van Wieringen (2016). “Aging affects neural synchronization to speech-related acoustic modulations”. In: *Front. Aging Neurosci.* 8.JUN, pp. 1–16.

Goossens, T., C. Vercammen, J. Wouters, and A. van Wieringen (2018). “Neural envelope encoding predicts speech perception performance for normal-hearing and hearing-impaired adults”. In: *Hear. Res.* 370, pp. 189–200.

Grant, K. J. et al. (2020). “Electrophysiological markers of cochlear function correlate with hearing-in-noise performance among audiometrically normal subjects”. In: *J. Neurophysiol.* 124.2, pp. 418–431.

Grinn, S. K., K. B. Wiseman, J. A. Baker, and C. G. Le Prell (2017). “Hidden Hearing Loss? No Effect of Common Recreational Noise Exposure on Cochlear Nerve Response Amplitude in Humans”. In: *Front. Neurosci.* 11.

Grose, J. H., E. Buss, and J. W. Hall (2017). “Loud Music Exposure and Cochlear Synaptopathy in Young Adults: Isolated Auditory Brainstem Response Effects but No Perceptual Consequences”. In: *Trends Hear.*

Grose, J. H., S. K. Mamo, and J. W. Hall (2009). “Age effects in temporal envelope processing: Speech unmasking and auditory steady state responses”. In: *Ear Hear.* 30.5, pp. 568–575.

Guest, H., K. J. Munro, and C. J. Plack (2017a). “Tinnitus with a normal audiogram: Role of high-frequency sensitivity and reanalysis of brainstem-response measures to avoid audiometric over-matching”. In: *Hear. Res.* 356.October, pp. 116–117.

Guest, H., K. J. Munro, and C. J. Plack (2019). “Acoustic middle-ear-muscle-reflex thresholds in humans with normal audiograms: No relations to tinnitus, speech perception in noise, or noise exposure”. In: *Neuroscience*, pp. 1–8.

Guest, H., K. J. Munro, G. Prendergast, S. Howe, and C. J. Plack (2017b). “Tinnitus with a normal audiogram: Relation to noise exposure but no evidence for cochlear synaptopathy”. In: *Hear. Res.* 344.September 2017, pp. 265–274.

Harris, K. C., K. I. Vaden, C. M. McClaskey, J. W. Dias, and J. R. Dubno (2018). “Complementary metrics of human auditory nerve function derived from compound action potentials”. In: *J. Neurophysiol.* 119.3, pp. 1019–1028.

Harris, K. C. et al. (2021). “Neural Presbyacusis in Humans Inferred from Age-Related Differences in Auditory Nerve Function and Structure”. In: *J. Neurosci.* 41.50, pp. 10293–10304.

Hecox, K. and R. Galambos (1974). “Brain Stem Auditory Evoked Responses in Human Infants and Adults”. In: *Arch. Otolaryngol. - Head Neck Surg.* 99.1, pp. 30–33.

Heeringa, A. N., L. Zhang, G. Ashida, R. Beutelmann, F. Steenken, and C. Köppl (2020). “Temporal coding of single auditory nerve fibers is not degraded in aging gerbils”. In: *J. Neurosci.* 40.2, pp. 343–354.

Henderson, D., R. P. Hamernik, R. J. Salvi, and W. A. Ahroon (1983). "Comparison of Auditory-Evoked Potentials and Behavioral Thresholds in the Normal and Noise-Exposed Chinchilla". In: *Int. J. Audiol.* 22.2, pp. 172–180.

Henry, K. R. (1995). "Auditory nerve neurophonic recorded from the round window of the Mongolian gerbil". In: *Hear. Res.* 90.1-2, pp. 176–184.

Henry, K. S., S. Kale, R. E. Scheidt, and M. G. Heinz (2011). "Auditory brainstem responses predict auditory nerve fiber thresholds and frequency selectivity in hearing impaired chinchillas". In: *Hear. Res.* 280.1-2, pp. 236–244.

Henry, K. S. and J. R. Lucas (2010). "Auditory sensitivity and the frequency selectivity of auditory filters in the Carolina chickadee, Poecile carolinensis". In: *Anim. Behav.* 80.3, pp. 497–507.

Herdman, A. T., O. Lins, P. Van Roon, D. R. Stapells, M. Scherg, and T. W. Picton (2002). "Intracerebral sources of human auditory steady-state responses". In: *Brain Topogr.* 15.2, pp. 69–86.

Herrmann, B., A. Parthasarathy, and E. L. Bartlett (2017). "Ageing affects dual encoding of periodicity and envelope shape in rat inferior colliculus neurons". In: *Eur. J. Neurosci.* 45.2, pp. 299–311.

Hickox, A. E., E. Larsen, M. G. Heinz, L. Shinobu, and J. P. Whitton (2017). "Translational issues in cochlear synaptopathy". In: *Hear. Res.* 349, pp. 164–171.

Hind, S. E., R. Haines-Bazrafshan, C. L. Benton, W. Brassington, B. Towle, and D. R. Moore (2011). "Prevalence of clinical referrals having hearing thresholds within normal limits". In: *Int. J. Audiol.* 50.10, pp. 708–716.

Hou, S. M. and D. M. Lipscomb (1977). "On the source of the scalp recorded auditory frequency-following response (FFR)". In: *J. Acoust. Soc. Am.* 61.S1, S27–S27.

Humes, L. E. (2005). "Do 'auditory processing' tests measure auditory processing in the elderly?" In: *Ear Hear.* 26.2, pp. 109–119.

ISO 389-6. 2007, D. S. E. N. (n.d.). "Acoustics—Reference Zero for the Calibration of Audiometric Equipment—Part 6: Reference Threshold of Hearing for Test Signals of Short Duration." In: ().

Jensen, J. B., A. C. Lysaght, M. C. Liberman, K. Qvortrup, and K. M. Stankovic (2015). "Immediate and Delayed Cochlear Neuropathy after Noise Exposure in Pubescent Mice". In: *PLoS One* 10.5. Ed. by F.-G. Zeng, e0125160.

Jerger, J. and K. Johnson (1988). "Interactions of Age, Gender, and Sensorineural Hearing Loss on ABR Latency". In: *Ear Hear.* 9.4, pp. 168–176.

John, M. S., A. Dimitrijevic, and T. W. Picton (2001). “Weighted averaging of steady-state responses”. In: *Clin. Neurophysiol.* 112.3, pp. 555–562.

Johnson, D. H. (1980). “The relationship between spike rate and synchrony in responses of auditory-nerve fibers to single tones”. In: *J. Acoust. Soc. Am.* 68.4, pp. 1115–1122.

Johnson, T. and C. Brown (2005). “Threshold prediction using the auditory steady-state response and the tone burst auditory brain stem response: A within-subject comparison”. In: *Ear Hear.* 26.6, pp. 559–576.

Joris, P. X., L. H. Carney, P. H. Smith, and T. C. Yin (1994a). “Enhancement of neural synchronization in the anteroventral cochlear nucleus. I. Responses to tones at the characteristic frequency”. In: *J. Neurophysiol.* 71.3, pp. 1022–1036.

Joris, P. X., C. Schreiner, and A. Rees (2004). “Neural Processing of Amplitude-Modulated Sounds”. In: *Physiol. Rev.* 84.2, pp. 541–577.

Joris, P. X. and P. H. Smith (2008). “The volley theory and the spherical cell puzzle”. In: *Neuroscience* 154.1, pp. 65–76.

Joris, P. X., P. H. Smith, and T. C. Yin (1994b). “Enhancement of neural synchronization in the anteroventral cochlear nucleus. II. Responses in the tuning curve tail”. In: *J. Neurophysiol.* 71.3, pp. 1037–1051.

Kale, S. and M. G. Heinz (2010). “Envelope coding in auditory nerve fibers following noise-induced hearing loss”. In: *JARO - J. Assoc. Res. Otolaryngol.* 11.4, pp. 657–673.

Keefe, D. H., M. P. Feeney, L. L. Hunter, and D. F. Fitzpatrick (2017). “Aural Acoustic Stapedius-Muscle Reflex Threshold Procedures to Test Human Infants and Adults”. In: *J. Assoc. Res. Otolaryngol.* 18.1, pp. 65–88.

Keithley, E. M., A. F. Ryan, and N. K. Woolf (1989). “Spiral ganglion cell density in young and old gerbils”. In: *Hear. Res.* 38.1-2, pp. 125–133.

Kiang, N. Y.-S. (1965). “Dischange Patterens of Single Fibers in the Cats Auditory Nerve”. In: *M.I.T. Press* 35.

King, A., K. Hopkins, and C. J. Plack (2016). “Differential Group Delay of the Frequency Following Response Measured Vertically and Horizontally”. In: *JARO - J. Assoc. Res. Otolaryngol.* 17.2, pp. 133–143.

Konrad-Martin, D. et al. (2012). “Age-Related Changes in the Auditory Brainstem Response”. In: *J. Am. Acad. Audiol.* 23.01, pp. 018–035.

Kowalski, N., D. A. Depireux, and S. A. Shamma (1996). “Analysis of dynamic spectra in ferret primary auditory cortex. II. Prediction of unit responses to arbitrary dynamic spectra”. In: *J. Neurophysiol.* 76.5, pp. 3524–3534.

Kraus, N. and E. Skoe (2010). “Auditory brainstem response to complex sounds: a tutorial”. In: *Ear Hear.* 31.3, pp. 302–324.

Krishnan, A. (2006). “Human frequency following response”. In: *Audit. evoked potentials Basic Princ. Clin. Appl.*, pp. 313–315.

Kuhlmann, L., A. N. Burkitt, A. Paolini, and G. M. Clark (2002). “Summation of spatiotemporal input patterns in leaky integrate-and-fire neurons: Application to neurons in the cochlear nucleus receiving converging auditory nerve fiber input”. In: *J. Comput. Neurosci.* 12.1, pp. 55–73.

Kujawa, S. G. (2006). “Acceleration of Age-Related Hearing Loss by Early Noise Exposure: Evidence of a Misspent Youth”. In: *J. Neurosci.* 26.7, pp. 2115–2123.

Kujawa, S. G. and M. C. Liberman (2009). “Adding Insult to Injury: cochlear nerve degeneration after”. In: 29.45, pp. 14077–14085.

Kujawa, S. G. and M. C. Liberman (2015). “Synaptopathy in the noise-exposed and aging cochlea: Primary neural degeneration in acquired sensorineural hearing loss”. In: *Hear. Res.* 330, pp. 191–199.

Lai, J., A. L. Sommer, and E. L. Bartlett (2017). “Age-related changes in envelope-following responses at equalized peripheral or central activation”. In: *Neurobiol. Aging* 58, pp. 191–200.

Lauter, J. L. and R. L. Loomis (1988). “Individual Differences in Auditory Electric Responses: Comparisons of Between-Subject and Within-Subject Variability II. Amplitude of Brainstem Vertex-positive Peaks”. In: *Scand. Audiol.* 17.2, pp. 87–92.

Le Prell, C. G. (2019). “Effects of noise exposure on auditory brainstem response and speech-in-noise tasks: a review of the literature”. In: *Int. J. Audiol.* 58.sup1, S3–S32.

Levine, S. C., R. H. Margolis, E. M. Fournier, and S. M. Winzenburg (1992). “Tympanic Electrocochleography for Evaluation of Endolymphatic Hydrops”. In: *Laryngoscope* 102.6, pp. 614–622.

Liberman, L. D. and M. C. Liberman (2015). “Dynamics of cochlear synaptopathy after acoustic overexposure”. In: *JARO - J. Assoc. Res. Otolaryngol.* 16.2, pp. 205–219.

Liberman, M. C. (1978). “Auditory-nerve response from cats raised in a low-noise chamber”. In: *J. Acoust. Soc. Am.* 63.2, pp. 442–455.

Liberman, M. C., M. J. Epstein, S. S. Cleveland, H. Wang, and S. F. Maison (2016). "Toward a Differential Diagnosis of Hidden Hearing Loss in Humans". In: *PLoS One* 11.9. Ed. by M. S. Malmierca, e0162726.

Lightfoot, G. R. (1993). "Correcting for factors affecting ABR wave V latency". In: *Br. J. Audiol.* 27.3, pp. 211–220.

Lin, F. R., R. Thorpe, S. Gordon-Salant, and L. Ferrucci (2011a). "Hearing Loss Prevalence and Risk Factors Among Older Adults in the United States". In: *Journals Gerontol. Ser. A Biol. Sci. Med. Sci.* 66A.5, pp. 582–590.

Lin, H. W., A. C. Furman, S. G. Kujawa, and M. C. Liberman (2011b). "Primary neural degeneration in the guinea pig cochlea after reversible noise-induced threshold shift". In: *JARO - J. Assoc. Res. Otolaryngol.* 12.5, pp. 605–616.

Liu, L.-F., A. R. Palmer, and M. N. Wallace (2006). "Phase-Locked Responses to Pure Tones in the Inferior Colliculus". In: *J. Neurophysiol.* 95.3, pp. 1926–1935.

Lobarinas, E., R. Salvi, and D. Ding (2013). "Insensitivity of the audiogram to carboplatin induced inner hair cell loss in chinchillas". In: *Hear. Res.* 302, pp. 113–120.

Lopez-Calderon, J. and S. J. Luck (2014). "ERPLAB: an open-source toolbox for the analysis of event-related potentials". In: *Front. Hum. Neurosci.* 8.

Mamo, S. K., J. H. Grose, and E. Buss (2016). "Speech-evoked ABR: Effects of age and simulated neural temporal jitter". In: *Hear. Res.* 333, pp. 201–209.

Märcher-Rørsted, J., G. Encina-Llamas, T. Dau, M. C. Liberman, P.-z. Wu, and J. Hjortkjær (2022). "Age-related reduction in frequency-following responses as a potential marker of cochlear neural degeneration". In: *Hear. Res.* 414, p. 108411.

Marmel, F., D. Linley, R. P. Carlyon, H. E. Gockel, K. Hopkins, and C. J. Plack (2013). "Subcortical neural synchrony and absolute thresholds predict frequency discrimination independently". In: *JARO - J. Assoc. Res. Otolaryngol.* 14.5, pp. 757–766.

Marsh, J. T., W. S. Brown, and J. C. Smith (1974). "Differential brainstem pathways for the conduction of auditory frequency-following responses". In: *Electroencephalogr. Clin. Neurophysiol.* 36.C, pp. 415–424.

Matthews, L. J., F.-S. Lee, J. H. Mills, and J. R. Dubno (1997). "Extended High-Frequency Thresholds in Older Adults". In: *J. Speech, Lang. Hear. Res.* 40.1, pp. 208–214.

Mepani, A. M. et al. (2019). “Middle Ear Muscle Reflex and Word Recognition in “Normal-Hearing” Adults”. In: *Ear Hear.*, p. 1.

Miller, J. D. (1970). “Audibility Curve of the Chinchilla”. In: *J. Acoust. Soc. Am.* 48.2B, pp. 513–523.

Miller, L. M., M. A. Escabí, H. L. Read, and C. E. Schreiner (2002). “Spectrotemporal Receptive Fields in the Lemniscal Auditory Thalamus and Cortex”. In: *J. Neurophysiol.* 87.1, pp. 516–527.

Mitchell, C., D. S. Phillips, and D. R. Trune (1989). “Variables affecting the auditory brainstem response: Audiogram, age, gender and head size”. In: *Hear. Res.* 40.1-2, pp. 75–85.

Møller, A. R. and P. J. Jannetta (1982). “Evoked potentials from the inferior colliculus in man”. In: *Electroencephalogr. Clin. Neurophysiol.* 53.6, pp. 612–620.

Møller, A. R., P. J. Jannetta, and L. N. Sekhar (1988). “Contributions from the auditory nerve to the brain-stem auditory evoked potentials (BAEPs): results of intracranial recording in man”. In: *Electroencephalogr. Clin. Neurophysiol. Potentials Sect.* 71.3, pp. 198–211.

Moser, T. and A. Starr (2016). “Auditory neuropathy-neural and synaptic mechanisms”. In: *Nat. Rev. Neurol.* 12.3, pp. 135–149.

Noble, W., N. S. Jensen, G. Naylor, N. Bhullar, and M. A. Akeroyd (2013). “A short form of the Speech, Spatial and Qualities of Hearing scale suitable for clinical use: The SSQ12”. In: *Int. J. Audiol.* 52.6, pp. 409–412.

Oetting, D., T. Brand, and S. D. Ewert (2014). “Optimized loudness-function estimation for categorical loudness scaling data”. In: *Hear. Res.* 316, pp. 16–27.

Oostenveld, R., P. Fries, E. Maris, and J.-M. Schoffelen (2011). “FieldTrip: Open Source Software for Advanced Analysis of MEG, EEG, and Invasive Electrophysiological Data”. In: *Comput. Intell. Neurosci.* 2011, pp. 1–9.

Parthasarathy, A. and E. Bartlett (2012). “Two-channel recording of auditory-evoked potentials to detect age-related deficits in temporal processing”. In: *Hear. Res.* 289.1-2, pp. 52–62.

Parthasarathy, A., P. A. Cunningham, and E. L. Bartlett (2010). “Age-related differences in auditory processing as assessed by amplitude-modulation following responses in quiet and in noise”. In: *Front. Aging Neurosci.* 2.DEC, pp. 1–10.

Parthasarathy, A., J. Datta, J. A. L. Torres, C. Hopkins, and E. L. Bartlett (2014). "Age-related changes in the relationship between auditory brainstem responses and envelope-following responses". In: *JARO - J. Assoc. Res. Otolaryngol.* 15.4, pp. 649–661.

Parthasarathy, A., K. E. Hancock, K. Bennett, V. DeGruttola, and D. B. Polley (2019). "Neural signatures of disordered multi-talker speech perception in adults with normal hearing". In: *bioRxiv*, pp. 1–22.

Parthasarathy, A., B. Herrmann, and E. L. Bartlett (2018). "Aging alters envelope representations of speech-like sounds in the inferior colliculus". In: *bioRxiv*, p. 266650.

Parthasarathy, A. and S. G. Kujawa (2018). "Synaptopathy in the aging cochlea: Characterizing early-neural deficits in auditory temporal envelope processing". In: *J. Neurosci.* 38.32, pp. 7108–7119.

Parthasarathy, A., J. Lai, and E. L. Bartlett (2016). "Age-Related Changes in Processing Simultaneous Amplitude Modulated Sounds Assessed Using Envelope Following Responses". In: *JARO - J. Assoc. Res. Otolaryngol.* 17.2, pp. 119–132.

Paul, B. T., I. C. Bruce, and L. E. Roberts (2017). "Evidence that hidden hearing loss underlies amplitude modulation encoding deficits in individuals with and without tinnitus". In: *Hear. Res.* 344, pp. 170–182.

Pérez-González, D. and M. S. Malmierca (2014). "Adaptation in the auditory system: an overview". In: *Front. Integr. Neurosci.* 8.

Pichora-Fuller, M. K., B. A. Schneider, E. MacDonald, H. E. Pass, and S. Brown (2007). "Temporal jitter disrupts speech intelligibility: A simulation of auditory aging". In: *Hear. Res.* 223.1-2, pp. 114–121.

Picton, T., S. Hillyard, H. Krausz, and R. Galambos (1974). "Human auditory evoked potentials. I: Evaluation of components". In: *Electroencephalogr. Clin. Neurophysiol.* 36, pp. 179–190.

Plack, C. J., D. Barker, and G. Prendergast (2014). "Perceptual consequences of "hidden" hearing loss". In: *Trends Hear.* 18, pp. 1–11.

Prendergast, G. et al. (2019). "Effects of Age and Noise Exposure on Proxy Measures of Cochlear Synaptopathy". In: *Trends Hear.* 23, p. 233121651987730.

Presacco, A., J. Z. Simon, and S. Anderson (2016a). "Effect of informational content of noise on speech representation in the aging midbrain and cortex". In: *J. Neurophysiol.* 116.5, pp. 2356–2367.

Presacco, A., J. Z. Simon, and S. Anderson (2016b). "Evidence of degraded representation of speech in noise, in the aging midbrain and cortex". In: *J. Neurophysiol.* 116.5, pp. 2346–2355.

Presacco, A., J. Z. Simon, and S. Anderson (2019). "Speech-in-noise representation in the aging midbrain and cortex: Effects of hearing loss". In: *PLoS One* 14.3, pp. 1–26.

Probst, R., B. L. Lonsbury-Martin, and G. K. Martin (1991). "A review of otoacoustic emissions". In: *J. Acoust. Soc. Am.* 89.5, pp. 2027–2067.

RStudio Team (2020). *RStudio: Integrated Development Environment for R*.

Reale, R. A. and C. D. Geisler (1980). "Auditory-nerve fiber encoding of two-tone approximations to steady-state vowels". In: *J. Acoust. Soc. Am.* 67.3, pp. 891–902.

Rodríguez Valiente, A., A. Trinidad, J. R. García Berrocal, C. Górriz, and R. Ramírez Camacho (2014). "Extended high-frequency (9-20 kHz) audiometry reference thresholds in 645 healthy subjects". In: *Int. J. Audiol.* 53.8, pp. 531–545.

Rønne, F. M., T. Dau, J. Harte, and C. Elberling (2012). "Modeling auditory evoked brainstem responses to transient stimuli". In: *J. Acoust. Soc. Am.* 131.5, pp. 3903–3913.

Roque, L., C. Gaskins, S. Gordon-Salant, M. J. Goupell, and S. Andersona (2019). "Age effects on neural representation and perception of silence duration cues in speech". In: *J. Speech, Lang. Hear. Res.* 62.4, pp. 1099–1116.

Rothman, J. S. and E. D. Young (1996). "Enhancement of neural synchronization in computational models of ventral cochlear nucleus bushy cells". In: *Audit. Neurosci.* 2.1, pp. 47–62.

Rumschlag, J. A. et al. (2022). "Age-related central gain with degraded neural synchrony in the auditory brainstem of mice and humans". In: *Neurobiol. Aging* 115, pp. 50–59.

Ryan, A. and P. Dallos (1975). "Effect of absence of cochlear outer hair cells on behavioural auditory threshold". In: *Nature* 253.5486, pp. 44–46.

Sachs, M. B., H. F. Voigt, and E. D. Young (1983). "Auditory nerve representation of vowels in background noise". In: *J. Neurophysiol.* 50.1, pp. 27–45.

Saeed, S. and R. Ramsden (1994). "Hearing loss." In: *Practitioner* 238.1539, pp. 454–460.

Schaette, R. and D. McAlpine (2011). “Tinnitus with a Normal Audiogram: Physiological Evidence for Hidden Hearing Loss and Computational Model”. In: *J. Neurosci.* 31.38, pp. 13452–13457.

Schneider, B., F. Speranza, and M. K. Pichora-Fuller (1998). “Age-related changes in temporal resolution: Envelope and intensity effects.” In: *Can. J. Exp. Psychol. Can. Psychol. expérimentale* 52.4, pp. 184–191.

Schuknecht, H. F. and R. C. Woellner (1955a). “Laryngology and Otology AN EXPERIMENTAL AND CLINICAL STUDY”. In: *J. Laryngol. Otol.* 69(02).February 1955, pp. 75–97.

Schuknecht, H. F. and R. C. Woellner (1955b). “An Experimental and Clinical Study of Deafness from Lesions of the Cochlear Nerve”. In: *J. Laryngol. Otol.* 69.2, pp. 75–97.

Sergeyenko, Y., K. Lall, M. C. Liberman, and S. G. Kujawa (2013). “Age-Related Cochlear Synaptopathy: An Early-Onset Contributor to Auditory Functional Decline”. In: *J. Neurosci.* 33.34, pp. 13686–13694.

Shaheen, L. A., M. D. Valero, and M. C. Liberman (2015). “Towards a Diagnosis of Cochlear Neuropathy with Envelope Following Responses”. In: *JARO - J. Assoc. Res. Otolaryngol.* 16.6, pp. 727–745.

Shehabi, A. M., G. Prendergast, and C. J. Plack (2022). “The Relative and Combined Effects of Noise Exposure and Aging on Auditory Peripheral Neural Deafferentation: A Narrative Review”. In: *Front. Aging Neurosci.* 14.

Shera, C. A. and J. J. Guinan (1999). “Evoked otoacoustic emissions arise by two fundamentally different mechanisms: A taxonomy for mammalian OAEs”. In: *J. Acoust. Soc. Am.* 105.2, pp. 782–798.

Simpson, M. J., S. G. Jennings, and R. H. Margolis (2020). “Techniques for Obtaining High-quality Recordings in Electrocochleography”. In: *Front. Syst. Neurosci.* 14.

Skoe, E., J. Krizman, S. Anderson, and N. Kraus (2015). “Stability and plasticity of auditory brainstem function across the lifespan”. In: *Cereb. Cortex* 25.6, pp. 1415–1426.

Smith, J. C., J. T. Marsh, and W. S. Brown (1975). “Far-field recorded frequency-following responses: Evidence for the locus of brainstem sources”. In: *Electroencephalogr. Clin. Neurophysiol.* 39.5, pp. 465–472.

Snyder, R. L. and C. E. Schreiner (1984). “The auditory neurophonic: Basic properties”. In: *Hear. Res.* 15.3, pp. 261–280.

Snyder, R. and C. Schreiner (1985). “Forward masking of the auditory nerve neurophonic (ANN) and the frequency following response (FFR)”. In: *Hear. Res.* 20.1, pp. 45–62.

Sohmer, H, H Pratt, and R Kinarti (1977). “Sources of frequency following responses (FFR) in man”. In: *Electroencephalogr. Clin. Neurophysiol.* 42.5, pp. 656–664.

Stamper, G. C. and T. A. Johnson (2015). “Auditory Function in Normal-Hearing, Noise-Exposed Human Ears”. In: *Ear Hear.* 36.2, pp. 172–184.

Stankovic, K. (2004). “Survival of Adult Spiral Ganglion Neurons Requires erbB Receptor Signaling in the Inner Ear”. In: *J. Neurosci.* 24.40, pp. 8651–8661.

Steinhoff, H. J., F. Böhnke, and T. Janssen (1988). “Click ABR intensity-latency characteristics in diagnosing conductive and cochlear hearing losses”. In: *Arch. Otorhinolaryngol.* 245.5, pp. 259–265.

Stevens, J, R Booth, S Brennan, R Feirn, and R Meredith (2013). “Guidance for Auditory Brainstem Response testing in babies. Version 2.1”. In: *Newborn Hear. Screen. Assess.* March, pp. 344–354.

Sumner, C. J. and A. R. Palmer (2012). “Auditory nerve fibre responses in the ferret”. In: *Eur. J. Neurosci.* 36.4, pp. 2428–2439.

Sun, X.-M. (2012). “Ear Canal Pressure Variations Versus Negative Middle Ear Pressure: Comparison Using Distortion Product Otoacoustic Emission Measurement in Humans”. In: *Ear Hear.* 33.1, pp. 69–78.

Suthakar, K. and M. C. Liberman (2021). “Auditory-Nerve Responses in Mice with Noise-Induced Cochlear Synaptopathy”. In: *J. Neurophysiol.*

Sutton, G. (2008). “Guidelines for the early audiological assessment and management of babies referred from the newborn hearing screening programme.” In: July, p. 2008.

Suzuki, J., G. Corfas, and M. C. Liberman (2016). “Round-window delivery of neurotrophin 3 regenerates cochlear synapses after acoustic overexposure”. In: *Sci. Rep.* 6.April, pp. 1–11.

Thompson, D. J., J. A. Sills, K. S. Recke, and D. M. Bui (1980). “Acoustic Reflex Growth in the Aging Adult”. In: *J. Speech, Lang. Hear. Res.* 23.2, pp. 405–418.

Tremblay, M.-È., M. L. Zettel, J. R. Ison, P. D. Allen, and A. K. Majewska (2012). “Effects of aging and sensory loss on glial cells in mouse visual and auditory cortices”. In: *Glia* 60.4, pp. 541–558.

Trevino, M., E. Lobarinas, A. C. Maulden, and M. G. Heinz (2019). "The chinchilla animal model for hearing science and noise-induced hearing loss". In: *J. Acoust. Soc. Am.* 146.5, pp. 3710–3732.

Valero, M. D., J. A. Burton, S. N. Hauser, T. A. Hackett, R. Ramachandran, and M. C. Liberman (2017). "Noise-induced cochlear synaptopathy in rhesus monkeys (Macaca mulatta)". In: *Hear. Res.* 353, pp. 213–223.

Valero, M. D., K. E. Hancock, and M. C. Liberman (2016). "The middle ear muscle reflex in the diagnosis of cochlear neuropathy". In: *Hear. Res.* 332, pp. 29–38.

Vasilkov, V., M. Garrett, M. Mauermann, and S. Verhulst (2021). "Enhancing the sensitivity of the envelope-following response for cochlear synaptopathy screening in humans: The role of stimulus envelope". In: *Hear. Res.* 400, p. 108132.

Verhulst, S., A. Altoè, and V. Vasilkov (2018). "Computational modeling of the human auditory periphery: Auditory-nerve responses, evoked potentials and hearing loss". In: *Hear. Res.* 360, pp. 55–75.

Verschooten, E. and P. X. Joris (2014). "Estimation of neural phase locking from stimulus-evoked potentials". In: *JARO - J. Assoc. Res. Otolaryngol.* 15.5, pp. 767–787.

Viana, L. M. et al. (2015). "Cochlear neuropathy in human presbycusis: Confocal analysis of hidden hearing loss in post-mortem tissue". In: *Hear. Res.* 327, pp. 78–88.

Walton, J. P. (2010). "Timing is everything: Temporal processing deficits in the aged auditory brainstem". In: *Hear. Res.* 264.1-2, pp. 63–69.

Wan, G., M. E. Gómez-Casati, A. R. Gigliello, M. Charles Liberman, and G. Corfas (2014). "Neurotrophin-3 regulates ribbon synapse density in the cochlea and induces synapse regeneration after acoustic trauma". In: *Elife* 2014-Octob, pp. 1–35.

Werff, K. R. V. and K. S. Burns (2011). "Brain stem responses to speech in younger a". In: pp. 168–180.

Wojtczak, M., J. A. Beim, and A. J. Oxenham (2017). "Weak Middle-Ear-Muscle Reflex in Humans with Noise-Induced Tinnitus and Normal Hearing May Reflect Cochlear Synaptopathy". In: *Eneuro* 4.6, ENEURO.0363–17.2017.

Wong, P. C. M., E. Skoe, N. M. Russo, T. Dees, and N. Kraus (2007). "Musical experience shapes human brainstem encoding of linguistic pitch patterns". In: *Nat. Neurosci.* 10.4, pp. 420–422.

Worden, F. G. and J. T. Marsh (1968). “Frequency-following (microphonic-like) neural responses evoked by sound”. In: *Electroencephalogr. Clin. Neurophysiol.* 25.1, pp. 42–52.

Wu, P. Z., L. D. Liberman, K. Bennett, V. de Gruttola, J. T. O’Malley, and M. C. Liberman (2019). “Primary Neural Degeneration in the Human Cochlea: Evidence for Hidden Hearing Loss in the Aging Ear”. In: *Neuroscience* 407, pp. 8–20.

Wu, P. Z., J. T. O’Malley, V. de Gruttola, and M. Charles Liberman (2020). “Age-related hearing loss is dominated by damage to inner ear sensory cells, not the cellular battery that powers them”. In: *J. Neurosci.* 40.33, pp. 6357–6366.

Xu-Friedman, M. A. and W. G. Regehr (2005). “Dynamic-clamp analysis of the effects of convergence on spike timing. II. Few synaptic inputs”. In: *J. Neurophysiol.* 94.4, pp. 2526–2534.

Young, E. D. and M. B. Sachs (1979). “Representation of steady-state vowels in the temporal aspects of the discharge patterns of populations of auditory-nerve fibers”. In: *J. Acoust. Soc. Am.* 66.5, pp. 1381–1403.

Zheng, X.-Y., D.-L. Ding, S. L. McFadden, and D. Henderson (1997). “Evidence that inner hair cells are the major source of cochlear summating potentials”. In: *Hear. Res.* 113.1-2, pp. 76–88.

Zhong, Z., K. S. Henry, and M. G. Heinz (2014). “Sensorineural hearing loss amplifies neural coding of envelope information in the central auditory system of chinchillas”. In: *Hear. Res.* 309, pp. 55–62.

Zilany, M. S. A., I. C. Bruce, P. C. Nelson, and L. H. Carney (2009). “A phenomenological model of the synapse between the inner hair cell and auditory nerve: Long-term adaptation with power-law dynamics”. In: *J. Acoust. Soc. Am.* 126.5, pp. 2390–2412.

Contributions to Hearing Research

Vol. 1: *Gilles Pigasse*, Deriving cochlear delays in humans using otoacoustic emissions and auditory evoked potentials, 2008.
External examiners: Mark Lutman, Stefan Stenfeld

Vol. 2: *Olaf Strelcyk*, Peripheral auditory processing and speech reception in impaired hearing, 2009.
External examiners: Brian Moore, Kathrin Krumbholz

Vol. 3: *Eric R. Thompson*, Characterizing binaural processing of amplitude-modulated sounds, 2009.
External examiners: Michael Akeroyd, Armin Kohlrausch

Vol. 4: *Tobias Piechowiak*, Spectro-temporal analysis of complex sounds in the human auditory system, 2009.
External examiners: Jesko Verhey, Steven van de Par

Vol. 5: *Jens Bo Nielsen*, Assessment of speech intelligibility in background noise and reverberation, 2009.
External examiners: Björn Hagerman, Ejnar Laukli

Vol. 6: *Helen Connor*, Hearing aid amplification at soft input levels, 2010.
External examiners: Inga Holube, Birgitta Larsby

Vol. 7: *Morten Løve Jepsen*, Modeling auditory processing and speech perception in hearing-impaired listeners, 2010.
External examiners: Birger Kollmeier, Ray Meddis

Vol. 8: *Sarah Verhulst*, Characterizing and modeling dynamic processes in the cochlea using otoacoustic emissions, 2010.
External examiners: David Kemp, Stephen Neely

Vol. 9: *Sylvain Favrot*, A loudspeaker-based room auralization system for auditory research, 2010.
External examiners: Bernhard Seeber, Michael Vorländer

Vol. 10: *Sébastien Santurette*, Neural coding and perception of pitch in the normal and impaired human auditory system, 2011.
External examiners: Christopher Plack, Christian Lorenzi

Vol. 11: *Iris Arweiler*, Processing of spatial sounds in the impaired auditory system, 2011.
External examiners: Joost Festen, Jürgen Tchorz

Vol. 12: *Filip Munch Rønne*, Modeling auditory evoked potentials to complex stimuli, 2012.
External examiners: Bob Burkard, Stephen Neely

Vol. 13: *Claus Forup Corlin Jespersgaard*, Listening in adverse conditions: Masking release and effects of hearing loss, 2012.
External examiners: Stuart Rosen, Christian Lorenzi

Vol. 14: *Rémi Decorsière*, Spectrogram inversion and potential applications for hearing research, 2013.
External examiners: Michael Stone, Oded Ghitza

Vol. 15: *Søren Jørgensen*, Modeling speech intelligibility based on the signal-to-noise envelope power ration, 2014.
External examiners: John Culling, Martin Cooke

Vol. 16: *Kasper Eskelund*, Electrophysiological assessment of audiovisual integration in speech perception, 2014.
External examiners: Lawrence Rosenblum, Matthias Gondan

Vol. 17: *Simon Krogholt Christiansen*, The role of temporal coherence in auditory stream segregation, 2014.
External examiners: Shihab Shamma, Guy Brown

Vol. 18: *Márton Marschall*, Capturing and reproducing realistic acoustic scenes for hearing research, 2014.
External examiners: Sascha Spors, Ville Pulkki

Vol. 19: *Jasmina Catic*, Human sound externalization in reverberant environments, 2014.
External examiners: Bernhard Seeber, Steven van de Par

Vol. 20: *Michał Fereczkowski*, Design and evaluation of individualized hearing-aid signal processing and fitting, 2015.
External examiners: Christopher Plack, Enrique Lopez-Poveda

Vol. 21: *Alexandre Chabot-Leclerc*, Computational modeling of speech intelligibility in adverse conditions, 2015.
External examiners: Steven van de Par, John Culling

Vol. 22: *Federica Bianchi*, Pitch representations in the impaired auditory system and implications for music perception, 2016.
External examiners: Ingrid Johnsrude, Christian Lorenzi

Vol. 23: *Johannes Zaar*, Measures and computational models of microscopic speech perception, 2016.
External examiners: Judy Dubno, Martin Cooke

Vol. 24: *Johannes Käsbach*, Characterizing apparent source width perception, 2016.
External examiners: William Whitmer, Jürgen Tchorz

Vol. 25: *Gusztáv Löcsei*, Lateralized speech perception with normal and impaired hearing, 2016.
External examiners: Thomas Brand, Armin Kohlrausch

Vol. 26: *Suyash Narendra Joshi*, Modelling auditory nerve responses to electrical stimulation, 2017.
External examiners: Laurel Carney, Bob Carlyon

Vol. 27: *Henrik Gerd Hassager*, Characterizing perceptual externalization in listeners with normal, impaired and aided-impaired hearing, 2017.
External examiners: Volker Hohmann, Piotr Majdak

Vol. 28: *Richard Ian McWalter*, Analysis of the auditory system via synthesis of natural sounds, speech and music, 2017.
External examiners: Maria Chait, Christian Lorenzi

Vol. 29: *Jens Cubick*, Characterizing the auditory cues for the processing and perception of spatial sounds, 2017.
External examiners: Ville Pulkki, Pavel Zahorik

Vol. 30: *Gerard Encina-Llamas*, Characterizing cochlear hearing impairment using advanced electrophysiological methods, 2017.
External examiners: Roland Schaette, Ian Bruce

Vol. 31: *Christoph Scheidiger*, Assessing speech intelligibility in hearing-impaired listeners, 2018.
External examiners: Enrique Lopez-Poveda, Tim Jürgens

Vol. 32: *Alan Wiinberg*, Perceptual effects of non-linear hearing aid amplification strategies, 2018.
External examiners: Armin Kohlrausch, James Kates

Vol. 33: *Thomas Bentsen*, Computational speech segregation inspired by principles of auditory processing, 2018.
External examiners: Stefan Bleeck, Jürgen Tchorz

Vol. 34: *François Guérit*, Temporal charge interactions in cochlear implant listeners, 2018.
External examiners: Julie Arenberg, Olivier Macherey

Vol. 35: *Andreu Paredes Gallardo*, Behavioral and objective measures of stream segregation in cochlear implant users, 2018.
External examiners: Christophe Micheyl, Monita Chatterjee

Vol. 36: *Søren Fuglsang*, Characterizing neural mechanisms of attention-driven speech processing, 2019.
External examiners: Shihab Shamma, Maarten de Vos

Vol. 37: *Borys Kowalewski*, Assessing the effects of hearing-aid dynamic-range compression on auditory signal processing and perception, 2019.
External examiners: Brian Moore, Graham Naylor

Vol. 38: *Helia Relaño Iborra*, Predicting speech perception of normal-hearing and hearing-impaired listeners, 2019.
External examiners: Ian Bruce, Armin Kohlrausch

Vol. 39: *Axel Ahrens*, Characterizing auditory and audio-visual perception in virtual environments, 2019.
External examiners: Pavel Zahorik, Piotr Majdak

Vol. 40: *Niclas A. Janssen*, Binaural streaming in cochlear implant patients, 2019.
External examiners: Tim Jürgens, Hamish Innes-Brown

Vol. 41: *Wiebke Lamping*, Improving cochlear implant performance through psychophysical measures, 2019.
External examiners: Can Gnasia, David Landsberger

Vol. 42: *Antoine Favre-Félix*, Controlling a hearing aid with electrically assessed eye gaze, 2020.
External examiners: Jürgen Tchorz, Graham Naylor

Vol. 43: *Raul Sanchez Lopez*, Clinical auditory profiling and profile-based hearing-aid fitting, 2020.
External examiners: Judy R. Dubno, Pamela E. Souza

Vol. 44: *Juan Camilo Gil Garvajal*, Modeling audiovisual speech perception, 2020.
External examiners: Salvador Soto-Faraco, Kaisa Maria Tippana

Vol. 45: *Charlotte Amalie Emdal Navntoft*, Improving cochlear implant performance with new pulse shapes: a multidisciplinary approach, 2020.
External examiners: Andrew Kral, Johannes Frijns

Vol. 46: *Naim Mansour*, Assessing hearing device benefit using virtual sound environments, 2021.
External examiners: Virginia Best, Pavel Zahorik

Vol. 47: *Anna Josefine Munch Sørensen*, The effects of noise and hearing loss on conversational dynamics, 2021.
External examiners: William McAllister Whitmer, Martin Cooke

Vol. 48: *Thirsa Huisman*, The influence of vision on spatial localization in normal-hearing and hearing-imparied listeners, 2021.
External examiners: Steven van de Par, Christopher Stecker

Vol. 49: *Florine Lena Bachmann*, Subcortical electrophysiological measures of running speech, 2021.
External examiners: Samira Anderson, Tobias Reichenbach

Vol. 50: *Nicolai Pedersen*, Audiovisual speech analysis with deep learning, 2021.
External examiners: Zheng-Hua Tan, Hani Camille Yehia

Vol. 51: *Aleksandra Koprowska*, Auditory Training Strategies to Improve Speech Intelligibility in Hearing-Impaired Listeners, 2022.
External examiners: Ulrich Hoppe, David Jackson Morris

Vol. 52: *Hyojin Kim*, Physiological correlates of the audibility of masked signals at supra-threshold levels, 2022.
External examiners: Laurel Carney, Jesko L. Verhey

Vol. 53: *Chiara Casolani*, Electrophysiological characterization of tinnitus in listeners with normal audiogram and supra-threshold hearing deficits, 2022.
External examiners: Pim van Dijk, Holger Schulze

Vol. 54: *Mie Lærkegård Jørgensen*, Exploring innovative Hearing-Aid Techniques for Tinnitus Treatment, 2022.
External examiners: Pim van Dijk, Tobias Kleinjung

Vol. 55: *Mihaela-Beatice Neagu*, Evaluation of pupillometry as a diagnostic tool, 2022.
External examiners: Adrianna Zekveld, William McAllister Whitmer

Vol. 56: *Paolo Mesiano*, Assessing the effects of fundamental-frequency dynamics on the intelligibility of competing voices, 2022.
External examiners: Stuart Rosen, Emily Buss

The end.

To be continued...

Our communication in social settings relies on our ability to accurately capture the acoustic environment through our sense of hearing. Hearing loss affects this ability, with detrimental consequences for many aspects of social life. Clinical hearing loss is in its most common age-related form defined as a loss of sensitivity, but not all hearing difficulties are necessarily captured by traditional clinical audiological assessment of sensitivity. Recent evidence suggests that neural losses at the level of the inner ear, the cochlea, can be caused by aging and noise exposure without affecting threshold sensitivity. Specifically, it has been shown that the amount of functional auditory nerve fibers (ANF) in the cochlea declines progressively throughout life. Such neural loss is argued to precede the loss of sensory cells in the cochlea and may exist before hearing loss is detected in the hearing clinic. Yet, the consequence of ANF loss on our ability to communicate in everyday life is still debated and robust in-vivo diagnostic measures are missing.

Frequency-following responses (FFR) are neurophonic potentials that track the periodicity of an acoustic stimulus and can be recorded in humans using scalp electroencephalography. FFRs to relatively low frequency tones reflect phase-locked neural activity at the level of the auditory brainstem, but may reflect, at least in part, neural deficits already at the level of the cochlea. The work presented here constitutes a series of investigations exploring the potential relationship between cochlear neural degeneration and the low-frequency pure tone FFR. Together, the work presented in this thesis supports a relationship between age-related ANF loss and the brainstem FFR to low-frequency pure tones. As a result, the FFR might constitute valuable potential tool for diagnosing cochlear neural degeneration in humans.

DTU Health Tech
Department of Health Technology

Ørsteds Plads
Building 352
DK-2800 Kgs. Lyngby
Denmark
Tel: (+45) 45 25 39 50
www.dtu.dk